



University of Kentucky
UKnowledge

University of Kentucky Master's Theses

Graduate School

2008

PROCESS FOR FORMATION OF CATIONIC POLY (LACTIC-CO-GLYCOLIC ACID) NANOPARTICLES USING STATIC MIXERS

Yamuna Reddy Charabudla
University of Kentucky

[Right click to open a feedback form in a new tab to let us know how this document benefits you.](#)

Recommended Citation

Charabudla, Yamuna Reddy, "PROCESS FOR FORMATION OF CATIONIC POLY (LACTIC-CO-GLYCOLIC ACID) NANOPARTICLES USING STATIC MIXERS" (2008). *University of Kentucky Master's Theses*. 580. https://uknowledge.uky.edu/gradschool_theses/580

This Thesis is brought to you for free and open access by the Graduate School at UKnowledge. It has been accepted for inclusion in University of Kentucky Master's Theses by an authorized administrator of UKnowledge. For more information, please contact UKnowledge@lsv.uky.edu.

ABSTRACT OF THESIS

PROCESS FOR FORMATION OF CATIONIC POLY (LACTIC-CO-GLYCOLIC ACID) NANOPARTICLES USING STATIC MIXERS

Nanoparticles have received special attention over past few years as potential drug carriers for proteins/peptides and genes. Biodegradable polymeric poly (lactic-co-glycolic acid) (PLGA) nanoparticles are being employed as non-viral gene delivery systems for DNA. This work demonstrates a scalable technology for synthesis of nanoparticles capable of gene delivery. Cationic PLGA nanoparticles are produced by emulsion-diffusion-evaporation technique employing polyvinyl alcohol (PVA) as stabilizer and chitosan chloride for surface modification. A sonicator is used for the emulsion step and a static mixer is used for dilution in the diffusion step of the synthesis. A static mixer is considered ideal for the synthesis of PLGA nanoparticles as it is easily scalable to industrial production. The resulting nanoparticles are spherical in shape with size in the range of 100–250 nm and possess a zeta potential above +30 mV, indicating good stability of the colloid with a positive charge to bind to anionic DNA. The mechanism of nanoparticle formation was analyzed using multimodal size distributions (MSD), zeta potential data, and transmission electron microscopy (TEM) images. Several emulsion techniques and dilution effect were analyzed in this work. PVA acts as a compatibilizer for chitosan chloride and dilution of primary emulsion has little effect over the particle size of the PLGA nanoparticles.

Key Words: Emulsion solvent diffusion technique, Nanoparticles, PLGA, Static mixer, Chitosan.

Yamuna Reddy Charabudla

08-14-2008

PROCESS FOR FORMATION OF CATIONIC POLY (LACTIC-CO-GLYCOLIC
ACID) NANOPARTICLES USING STATIC MIXERS

By

YAMUNA REDDY CHARABUDLA

Dr. Eric A. Grulke
Director of Thesis

Dr. Douglass S. Kalika
Director of Graduate Studies

01-05-2008
Date

RULES FOR THE USE OF THESES

Unpublished theses submitted for the Master's degree and deposited in the University of Kentucky Library are as a rule open for inspection, but are to be used only with due regard to the rights of the authors. Bibliographical references may be noted, but quotations or summaries of parts may be published only with the permission of the author, and with the usual scholarly acknowledgments.

Extensive copying or publication of the thesis in whole or in part also requires the consent of the Dean of the Graduate School of the University of Kentucky.

THESIS

Yamuna Reddy Charabudla

The Graduate School

University of Kentucky

2009

PROCESS FOR FORMATION OF CATIONIC POLY (LACTIC-CO-GLYCOLIC
ACID) NANOPARTICLES USING STATIC MIXERS

THESIS

A thesis submitted in partial fulfillment of the
requirements for the degree of Master of Science in
Chemical Engineering in the College of Engineering
at the University of Kentucky

By

Yamuna Reddy Charabudla

Lexington, Kentucky

Director: Dr. Eric A. Grulke, Professor of Chemical and Materials Engineering

Lexington, Kentucky

2009

ACKNOWLEDGEMENTS

I would like to thank my adviser, Dr. Eric A. Grulke for giving me the opportunity to work on such wonderful project. This work would not have been possible without his constant support and guidance.

I would like to thank my thesis committee members: Dr. Tate T.H. Tsang and Dr. Stephen E. Rankin for their valuable inputs that helped me deliver a better finished product.

I am thankful to my friends and family for believing in me and for extending their constant support.

TABLE OF CONTENTS

Acknowledgements.....	iii
List of Tables	vi
List of Figures.....	vii
List of Files	xiv
1. Introduction	1
2. Literature Review	2
Drug delivery and drug delivery systems.....	2
Gene delivery	3
Nanoparticles and physicochemical properties	4
Polymeric nanoparticles and polymer selection for synthesis	6
Synthesis of polymeric nanoparticles.....	9
PLGA, PVA and chitosan chloride	12
Static Mixers	14
3. Materials and methods.....	16
Materials.....	16
Sonication.....	16
Colloid Mixer	16
Static mixer	17
Characterization of nanoparticles.....	18
Light scattering particle size analysis	18
Zeta potential Measurements.....	19
Transmission electron microscope (TEM) analysis	19
4. Results and discussion.....	20
Mechanisms for formation of nanoparticles.....	20
Dissolution of polymers in their solvents	20
Different possible binary polymer emulsions.....	25

Emulsion formed by the ternary polymer system.....	36
Synthesis of cationic PLGA nanoparticles.....	40
Preliminary work.....	40
Effect of static mixer on size of nanoparticles	40
Sonication and Homogenization.....	46
Dilution effect on the size of the particles.....	51
Sonication and Static mixer.....	56
Transmission electron microscopy measurement	62
5. Conclusions	68
6. Appendices	69
Abbreviations	69
Polymers	69
Nomenclature.....	69
Number based multimodal size distributions of all secondary emulsions in this work .70	
Dissolution of polymers in their solvents (Table 4.1)	70
Effect of PVA on Chitosan chloride aqueous solution (Table 4.2).....	71
Different possible binary polymer emulsions (Table 4.3).....	74
Emulsion formed by the ternary polymer system (Table 4.4).....	76
Effect of Static mixer (Table 4.5).....	77
Sonication - homogenization (Table 4.6)	78
Effect of dilution ratio on the PLGA nanoparticle size (Table 4.7)	80
Sonication - static mixer (Table 4.8)	97
References.....	99
Vita.....	103

LIST OF TABLES

Table 2.1. Size-related retention or elimination mechanisms.....	5
Table 2.2. Summary of polymers with different topology that are used in drug delivery. 7	
Table 4.1. Summary of particles found in individual polymer solutions used.	22
Table 4.2. Effect of PVA on MSD of chitosan chloride particles in DIUF H ₂ O.	28
Table 4.3. Summary of particle formation with different possible binary combinations of polymers used.	33
Table 4.4. Summary of particle formation in the ternary polymer system used.....	37
Table 4.5. Nanoparticle size obtained by using homogenizer for primary emulsion and subsequent use of static mixer for particle size reduction.	43
Table 4.6. Particle sizes obtained by using sonication for primary emulsion and homogenization for secondary emulsion generation.	48
Table 4.7. Summary of dilution ratio effect on the PLGA nanoparticle particle size.	53
Table 4.8. Particle sizes obtained by using sonication for primary emulsion and static mixer for secondary emulsion generation.....	58
Table 4.9. MSD summary of secondary emulsion from the static mixer for TEM measurement.....	64

LIST OF FIGURES

Figure 3.1. Series of helical mixing elements in a KM static mixer.....	17
Figure 3.2. Process flow diagram of Static mixer.....	18
Figure 4.1. Volume based MSD of 0.3wt% chitosan chloride in DIUF H2O [Table 4.1, row 3].....	24
Figure 4.2. Volume based MSD of 0.03wt% chitosan chloride in DIUF H2O. [Table 4.1, row 5].....	24
Figure 4.3. Volume based MSD of particles formed by emulsifying 1 ml EA in 5 ml solution of 0.3wt% chitosan chloride in DIUF H2O. [Table 4.1, row 6]	25
Figure 4.4. Volume based MSD of 0.3wt% chitosan chloride in DIUF H2O – batch-1. [Table 4.2, S.No.1].....	30
Figure 4.5. Volume based MSD of 1wt% PVA and 0.3wt% chitosan chloride in DIUF H2O – batch-1. [Table 4.2, S.No.2].....	30
Figure 4.6. Volume based MSD of 0.3wt% chitosan chloride in DIUF H2O – batch-2. [Table 4.2, S.No.3].....	31
Figure 4.7. Volume based MSD of 1wt% PVA and 0.3wt% chitosan chloride in DIUF H2O – batch -2. [Table 4.2, S.No.4].....	31
Figure 4.8. Volume based MSD of 0.3wt% chitosan chloride in DIUF H2O – batch-3. [Table 4.2, S.No.5].....	32
Figure 4.9. Volume based MSD of 1wt% PVA and 0.3wt% chitosan chloride in DIUF H2O – batch -3. [Table 4.2, S.No.6].....	32
Figure 4.10. Volume based MSD of 1wt% PVA and 0.3wt% chitosan chloride in DIUF H2O. [Table 4.3, row 2].....	35
Figure 4.11. Volume based MSD of nanoparticles formed by 1 ml 1wt% PLGA in EA emulsified in 5 ml aqueous solution of 1wt% PVA. [Table 4.3, row 3].....	35
Figure 4.12. Volume based MSD of nanoparticles formed by 1 ml solution of 1wt% PLGA in EA emulsified in 5 ml aqueous solution of 0.3wt% chitosan chloride. [Table 4.3, row 4].....	36
Figure 4.13. Volume based MSD of nanoparticles formed by 1 ml 1wt% PLGA in EA emulsified in 5 ml of 1wt% PVA and 0.3wt% chitosan chloride in DIUF H2O. [Table 4.4, row 2].....	39
Figure 4.14. Volume based MSD of 2nd batch of nanoparticles formed by 1 ml 1wt% PLGA in EA emulsified in 5 ml aqueous solution of 1wt% PVA and 0.3wt% chitosan chloride. [Table 4.4, row 3]	39

Figure 4.15. Correlation function of nanoparticles in 100 times dilute primary emulsion from homogenization of 10ml organic phase and 50ml of aqueous phase. [Table 4.5, S.No.1]	41
Figure 4.16. Correlation function of 0.3wt% chitosan chloride in DIUF H ₂ O [Table 4.1, row 3]	41
Figure 4.17. Volume based MSD of nanoparticles in 100 times dilute primary emulsion from homogenization of 10ml organic phase and 50ml of aqueous phase. [Table 4.5, S.No.1]	45
Figure 4.18. Volume based MSD in 100 times diluted emulsion from homogenization of 10ml of organic and 50ml of aqueous phase and subsequently processing 3 times through static mixer at 135ml/min. [Table 4.5, S.No.2]	45
Figure 4.19. Volume based MSD in 100 times diluted emulsion from homogenization of 10ml of organic and 50ml of aqueous phase and subsequently processing 6 times through static mixer at 135ml/min. [Table 4.5, S.No.3]	46
Figure 4.20. Volume based MSD in secondary emulsion generated by homogenization at dilution rate 1:100 of primary emulsion formed by sonication of 1ml 1wt% PLGA in EA and 5ml of 1wt% PVA and 0.3wt% chitosan chloride aqueous solution. [Table 4.6, S.No.1]	50
Figure 4.21. Volume based MSD in secondary emulsion generated by homogenization at dilution rate 1:100 of primary emulsion formed by sonication of 1ml 1wt% PLGA in EA and 5ml of 1wt% PVA and 0.3wt% chitosan chloride aqueous solution. [Table 4.6, S.No.2]	50
Figure 4.22. Volume based MSD in secondary emulsion generated by homogenization at dilution rate 1:10 of primary emulsion formed by sonication of 1ml 1wt% PLGA in EA and 5ml of 1wt% PVA and 0.3wt% chitosan chloride aqueous solution. [Table 4.6, S.No.3]	51
Figure 4.23. Effect of dilution ratio on volume based particle size distribution of PLGA nanoparticles.	55
Figure 4.24. Effect of dilution ratio on number based particle size distribution of PLGA nanoparticles.	55
Figure 4.25. Volume based MSD of nanoparticles generated by sonication of 1ml organic solution and 5ml aqueous solution resulting in primary emulsion followed by using static mixer at 180ml/min and dilution ratio 1:10 to generate secondary emulsion. [Table 4.8, S.No.1]	60
Figure 4.26. Volume based MSD of nanoparticles generated by sonication of 1ml organic solution and 5ml aqueous solution resulting in primary emulsion followed by using static mixer at 200ml/min and dilution ratio 1:10 to generate secondary emulsion. [Table 4.8, S.No.2]	60

Figure 4.27. Volume based MSD of nanoparticles generated by sonication of 1ml organic solution and 5ml aqueous solution resulting in primary emulsion followed by using static mixer at 260ml/min and dilution ratio 1:10 to generate secondary emulsion. [Table 4.8, S.No.3]	61
Figure 4.28. Volume based MSD of secondary emulsion, after removing EA, generated by sonication of 1ml organic and 5ml aqueous phase resulting in primary emulsion followed by use of static mixer at 260ml/min and dilution ratio 1:10. [Table 4.8, S.No.4]	61
Figure 4.29. Volume based MSD of PLGA nanoparticles in TEM sample.	63
Figure 4.30. Number based MSD of PLGA nanoparticles in TEM sample.	63
Figure 4.31. TEM images of the PLGA nanoparticles with size around 100nm in the secondary emulsion processed through the static mixer at 390ml/min.	65
Figure 4.32. TEM images of the PLGA nanoparticles with size around 100nm in the secondary emulsion processed through the static mixer at 390ml/min.	65
Figure 4.33. TEM images of the nanoparticles with diameter around 300nm in the secondary emulsion processed through the static mixer at 390ml/min.	66
Figure 4.34. TEM images of the nanoparticles with diameter around 300nm in the secondary emulsion processed through the static mixer at 390ml/min.	66
Figure 4.35. TEM images of spherical nanoparticles with sizes in the range of 100-1000nm in the secondary emulsion processed through the static mixer at 390ml/min. ...	67
Figure 6.1. Number based MSD of 0.3wt% chitosan chloride in DIUF H2O [Table 4.1, row 3]	70
Figure 6.2. Number based MSD of 0.03wt% chitosan chloride in DIUF H2O. [Table 4.1, row 5]	70
Figure 6.3. Number based MSD of particles formed by emulsifying 1 ml EA in 5 ml solution of 0.3wt% chitosan chloride in DIUF H2O. [Table 4.1, row 6]	71
Figure 6.4. Number based MSD of 0.3wt% chitosan chloride in DIUF H2O – batch-1. [Table 4.2, S.No.1].....	71
Figure 6.5. Number based MSD of 1wt% PVA and 0.3wt% chitosan chloride in DIUF H2O – batch -1. [Table 4.2, S.No.2].....	72
Figure 6.6. Number based MSD of 0.3wt% chitosan chloride in DIUF H2O – batch-2. [Table 4.2, S.No.3].....	72
Figure 6.7. Number based MSD of 1wt% PVA and 0.3wt% chitosan chloride in DIUF H2O – batch -2. [Table 4.2, S.No.4].....	73

Figure 6.8. Number based MSD of 0.3wt% chitosan chloride in DIUF H2O – batch-3. [Table 4.2, S.No.5].....	73
Figure 6.9. Number based MSD of 1wt% PVA and 0.3wt% chitosan chloride in DIUF H2O – batch -3. [Table 4.2, S.No.6].....	74
Figure 6.10. Number based MSD of 1wt% PVA and 0.3wt% chitosan chloride in DIUF H2O. [Table 4.3, row 2].....	74
Figure 6.11. Number based MSD of nanoparticles formed by 1 ml 1wt% PLGA in EA emulsified in 5 ml aqueous solution of 1wt% PVA. [Table 4.3, row 3].....	75
Figure 6.12. Number based MSD of nanoparticles formed by 1 ml solution of 1wt% PLGA in EA emulsified in 5 ml aqueous solution of 0.3wt% chitosan chloride. [Table 4.3, row 4].....	75
Figure 6.13. Number based MSD of nanoparticles formed by 1 ml 1wt% PLGA in EA emulsified in 5 ml of 1wt% PVA and 0.3wt% chitosan chloride in DIUF H2O. [Table 4.4, row 2].....	76
Figure 6.14. Number based MSD of 2nd batch of nanoparticles formed by 1 ml 1wt% PLGA in EA emulsified in 5 ml aqueous solution of 1wt% PVA and 0.3wt% chitosan chloride. [Table 4.4, row 3]	76
Figure 6.15. Number based MSD of nanoparticles in 100 times dilute primary emulsion from homogenization of 10ml organic phase and 50ml of aqueous phase. [Table 4.5, S.No.1].....	77
Figure 6.16. Number based MSD in 100 times diluted emulsion from homogenization of 10ml of organic and 50ml of aqueous phase and subsequently processing 3 times through static mixer at 135ml/min. [Table 4.5, S.No.2]	77
Figure 6.17. Number based MSD in 100 times diluted emulsion from homogenization of 10ml of organic and 50ml of aqueous phase and subsequently processing 6 times through static mixer at 135ml/min. [Table 4.5, S.No.3]	78
Figure 6.18. Number based MSD in secondary emulsion generated by homogenization at dilution rate 1:100 of primary emulsion formed by sonication of 1ml 1wt% PLGA in EA and 5ml of 1wt% PVA and 0.3wt% chitosan chloride aqueous solution. [Table 4.6, S.No.1].....	78
Figure 6.19. Number based MSD in secondary emulsion generated by homogenization at dilution rate 1:100 of primary emulsion formed by sonication of 1ml 1wt% PLGA in EA and 5ml of 1wt% PVA and 0.3wt% chitosan chloride aqueous solution. [Table 4.6, S.No.2].....	79
Figure 6.20. Number based MSD in secondary emulsion generated by homogenization at dilution rate 1:10 of primary emulsion formed by sonication of 1ml 1wt% PLGA in EA and 5ml of 1wt% PVA and 0.3wt% chitosan chloride aqueous solution. [Table 4.6, S.No.3].....	79

Figure 6.21. Volume based MSD of first batch of secondary emulsion with dilution ratio 1:10. [Table 4.7, row 2]	80
Figure 6.22. Number based MSD of first batch of secondary emulsion with dilution ratio 1:10. [Table 4.7, row 2]	80
Figure 6.23. Volume based MSD of second batch of secondary emulsion with dilution ratio 1:10. [Table 4.7, row 3]	81
Figure 6.24. Number based MSD of second batch of secondary emulsion with dilution ratio 1:10. [Table 4.7, row 3]	81
Figure 6.25. Volume based MSD of third batch of secondary emulsion with dilution ratio 1:10. [Table 4.7, row 4]	82
Figure 6.26. Number based MSD of third batch of secondary emulsion with dilution ratio 1:10. [Table 4.7, row 4]	82
Figure 6.27. Volume based MSD of fourth batch of secondary emulsion with dilution ratio 1:10. [Table 4.7, row 5]	83
Figure 6.28. Number based MSD of fourth batch of secondary emulsion with dilution ratio 1:10. [Table 4.7, row 5]	83
Figure 6.29. Volume based MSD of first batch of secondary emulsion with dilution ratio 1:30. [Table 4.7, row 6]	84
Figure 6.30. Number based MSD of first batch of secondary emulsion with dilution ratio 1:30. [Table 4.7, row 6]	84
Figure 6.31. Volume based MSD of second batch of secondary emulsion with dilution ratio 1:30. [Table 4.7, row 7]	85
Figure 6.32. Number based MSD of second batch of secondary emulsion with dilution ratio 1:30. [Table 4.7, row 7]	85
Figure 6.33. Volume based MSD of third batch of secondary emulsion with dilution ratio 1:30. [Table 4.7, row 8]	86
Figure 6.34. Number based MSD of third batch of secondary emulsion with dilution ratio 1:30. [Table 4.7, row 8]	86
Figure 6.35. Volume based MSD of first batch of secondary emulsion with dilution ratio 1:60. [Table 4.7, row 9]	87
Figure 6.36. Number based MSD of first batch of secondary emulsion with dilution ratio 1:60. [Table 4.7, row 9]	87
Figure 6.37. Volume based MSD of second batch of secondary emulsion with dilution ratio 1:60. [Table 4.7, row 10]	88

Figure 6.38. Number based MSD of second batch of secondary emulsion with dilution ratio 1:60. [Table 4.7, row 10]	88
Figure 6.39. Volume based MSD of third batch of secondary emulsion with dilution ratio 1:60. [Table 4.7, row 11]	89
Figure 6.40. Number based MSD of third batch of secondary emulsion with dilution ratio 1:60. [Table 4.7, row 11]	89
Figure 6.41. Volume based MSD of first batch of secondary emulsion with dilution ratio 1:80. [Table 4.7, row 12]	90
Figure 6.42. Number based MSD of first batch of secondary emulsion with dilution ratio 1:80. [Table 4.7, row 12]	90
Figure 6.43. Volume based MSD of second batch of secondary emulsion with dilution ratio 1:80. [Table 4.7, row 13]	91
Figure 6.44. Number based MSD of second batch of secondary emulsion with dilution ratio 1:80. [Table 4.7, row 13]	91
Figure 6.45. Volume based MSD of third batch of secondary emulsion with dilution ratio 1:80. [Table 4.7, row 14]	92
Figure 6.46. Number based MSD of third batch of secondary emulsion with dilution ratio 1:80. [Table 4.7, row 14]	92
Figure 6.47. Volume based MSD of fourth batch of secondary emulsion with dilution ratio 1:80. [Table 4.7, row 15]	93
Figure 6.48. Number based MSD of fourth batch of secondary emulsion with dilution ratio 1:80. [Table 4.7, row 15]	93
Figure 6.49. Volume based MSD of first batch of secondary emulsion with dilution ratio 1:100. [Table 4.7, row 16]	94
Figure 6.50. Number based MSD of first batch of secondary emulsion with dilution ratio 1:100. [Table 4.7, row 16]	94
Figure 6.51. Volume based MSD of second batch of secondary emulsion with dilution ratio 1:100. [Table 4.7, row 17]	95
Figure 6.52. Number based MSD of second batch of secondary emulsion with dilution ratio 1:100. [Table 4.7, row 17]	95
Figure 6.53. Volume based MSD of third batch of secondary emulsion with dilution ratio 1:100. [Table 4.7, row 18]	96
Figure 6.54. Number based MSD of third batch of secondary emulsion with dilution ratio 1:100. [Table 4.7, row 18]	96

Figure 6.55. Number based MSD of nanoparticles generated by sonication of 1ml organic solution and 5ml aqueous solution resulting in primary emulsion followed by using static mixer at 180ml/min and dilution ratio 1:10 to generate secondary emulsion. [Table 4.8, S.No.1] 97

Figure 6.56. Number based MSD of nanoparticles generated by sonication of 1ml organic solution and 5ml aqueous solution resulting in primary emulsion followed by using static mixer at 200ml/min and dilution ratio 1:10 to generate secondary emulsion. [Table 4.8, S.No.2] 97

Figure 6.57. Number based MSD of nanoparticles generated by sonication of 1ml organic solution and 5ml aqueous solution resulting in primary emulsion followed by using static mixer at 260ml/min and dilution ratio 1:10 to generate secondary emulsion. [Table 4.8, S.No.3] 98

Figure 6.58. Number based MSD of secondary emulsion, after removing EA, generated by sonication of 1ml organic and 5ml aqueous phase resulting in primary emulsion followed by use of static mixer at 260ml/min and dilution ratio 1:10. [Table 4.8, S.No.4] 98

LIST OF FILES

1. Thesis-final.pdf

1. Introduction

Drug delivery is the process of supplying therapeutic agent in desired dosage to the targeted site of action in the body. Drug delivery improves the therapeutic effect of the drug over the traditional routes of drug administration by concentrating the dosage near the location at which it is needed. Gene delivery is the process in which external deoxyribonucleic acid (DNA) is introduced into the cell to restore its normal functioning. Gene therapy has become an important option considered for treating several genetic and acquired diseases. DNA fragments carry a negative charge, and are rod-like, and relatively stiff, creating suspensions with high viscosities at low loadings.

Complexation of DNA fragments with oppositely charged polymers tends to neutralize the DNA and promote the formation of globular structures with much smaller effective volumes and lower solution viscosities. Synthesis of polymeric nanoparticles with desired surface characteristics plays a vital role in achieving targeted gene delivery. Biodegradable polymeric nanoparticles like poly (lactic-co-glycolic acid) PLGA are being widely examined for their performance as gene carriers. There have been recent reports of sub-micron complexes of polymer/DNA that could provide safe and efficient delivery methods. In this work, PLGA nanoparticles are generated using polyvinyl alcohol (PVA) as stabilizer; chitosan chloride modifies the surface, conferring a positive charge on PLGA nanoparticles.

Various methods are available for the synthesis of polymeric nanoparticles. The emulsion – diffusion – evaporation method is chosen for the synthesis because of its ability to generate PLGA nanoparticles using less toxic and easily removable solvents, such as ethyl acetate. Development of scalable methods facilitates the production of polymeric nanoparticles on an industrial scale. It is presumed in this work that static mixers can generate good secondary emulsions, resulting in the formation of nanoparticles with uniform size. The formation of the nanoparticles should be rapid and it is likely that the diameters of the particles will be related to the flow rates in the static mixer. Initially a homogenizer followed by a static mixer is employed for synthesis and then the process is improved by using a sonicator instead of homogenizer for the primary emulsion generation to get more uniform particle size.

The objective of this work is to develop proof of concept data using a static mixer to generate uniform PLGA nanoparticles in aqueous media for gene therapy and other applications. Liquid-liquid interfacial generation can be done using baffled stirred tank agitation, rotor stator mixers, ultrasonic mixers, and static mixers (Quadros and Baptista 2003; Thakur, Vial et al. 2003; El-Jaby, McKenna et al. 2007). Static mixers seem particularly suited to solving the scale-up challenges from the bench to full scale production because they are low shear devices requiring small volumes, can readily be adapted for a variety of flow rates, and can be cleaned and sterilized easily. These characteristics will speed adaptation of processes to industrial scale production of PLGA nanoparticles for gene delivery. The key research will be to produce homogeneously sized nanoparticles highly efficient for gene delivery. The Particle size distribution based on volume and number of nanoparticles, zeta potential and TEM images of the product are analyzed.

2. Literature Review

Drug delivery and drug delivery systems

Discovery of highly potent and specific drugs poses complex problems for drug delivery. Many novel drugs have inherent drawbacks such as poor stability, high molecular weight, very short half-life in vivo, or highly toxicity (Wheatley and Langer 1987). Unconventional drugs, such as peptides, proteins, genes and oligonucleotides, increased the need for sophisticated and effective drug carriers. Drug delivery systems minimize the side effects of toxic drugs by supplying active compounds to the intended site in the body. Controlled release methods are usually required for these novel drugs to be maintained at relatively steady concentrations in the body. Depending on the requirement, the system may release the drug at uniform or programmed rates over time periods ranging from hours to months (Solaro 2002). Advantages of drug delivery systems over other conventional modes of drug dosage include improved efficiency, low toxicity, and decreased drug dosage frequency, resulting in better patient compliance. Therefore, some of the most desired characteristics of drug delivery systems are high drug entrapment efficiency, high in vivo stability, and ability to achieve controlled and targeted delivery (Solaro 2002).

Drug delivery systems. A drug delivery system is a formulation or a device that facilitates the introduction of the therapeutic agent to the desired site of action in the body (Jain and Editor 2008). Drug delivery systems can be classified into three generations based on their functional properties (Barratt 2003). First generation materials deliver the drug to the deserved site only if they are implanted close enough to desired site. Because of this, they are not considered as true drug carriers. Microcapsules and microspheres used for chemoembolization, protein and peptide delivery and drug delivery into the brain belong to this generation.

Second generation systems transport the drugs through the body, delivering them at the desired site. These systems are generally less than 1 μm in dimension so that they can move across membranes, such as the stomach lining, capillaries, etc. These are considered as true carriers of drugs. Colloidal drug carriers such as liposomes, nanospheres, nanocapsules comprise this group. For intravenous delivery, nanoparticles are used as the smallest capillaries in the body range from 5-6 μm in diameter (Hans and Lowman 2002). Polymeric nanoparticles are considered as good substitute for liposomes because of the technological limitations of liposomes. These include poor solubility, instability, poor drug encapsulation efficiency, rapid leakage of hydrophilic drugs, difficult surface functionalization and lack of control over their release profile (Barratt 2000; Hans and Lowman 2002; Solaro 2002; Barratt 2003; Goldberg, Langer et al. 2007).

Third generation systems are considered improved second generation systems. In addition to sustained drug delivery, they have the ability to recognize their targets. This is achieved by functionalizing the nanoparticles with biomolecules that can attach to specific sites in the body. These nanoparticles are guided to the intended site by the attached antibodies, peptides or sugar moieties (Barratt 2003; Yang, Wang et al. 2006). These sophisticated drug delivery carriers enable delivery of entirely new classes of drugs.

Depending on the physical form, drug delivery systems are classified as molecular and particulate carriers (Barratt 2003). A few examples of molecular carriers include- soluble polymer molecules with covalently attached drugs, targeting moieties along with drugs in some cases, drug-antibody complexes, antibody-natural macromolecule complexes, antibody-lipophilic prodrug conjugates, and cyclodextrins with a drug molecule in its central cavity. Molecular carriers can deliver a wide variety of associated drugs. The drawback with molecular carriers is the low payload per particle conveyed to the deserved site. Patient cells like erythrocytes or lymphocytes loaded ex vivo with drug, and synthetic drug delivery carriers like liposomes and nanoparticles are examples of particulate drug carriers. The size and shape of synthetic particulate carriers play a prominent role in deciding its efficacy as drug delivery system. These carriers can convey large number of drug molecules per particle. However the disadvantage is the complexity and regulatory aspect involved in the synthesis of these carriers.

Gene delivery

Gene therapy is an evolving technique for treating genetic disorders by inserting an extraneous gene or a portion of it into a targeted site. Altering with genetic materials like DNA or Ribonucleic acid (RNA) helps in restoring a missing function of cell or fixing a malfunctioning cell. Gene therapy is not yet approved by FDA for clinical application it is still in experimental stage. Gene delivery to the intended site can be done by means of viral or non-viral vectors. Initially viral vectors were considered efficient because of their capacity to penetrate and transfer the genetic material into the cells. However, the disadvantages associated with viral vectors like insertional mutagenesis, possibility of viral infection, induction of immune response, high cost of production and difficulty in scaling up to industrial level inhibit their usage (Yang, Wang et al. 2006; Kang, Lim et al. 2008).

Alternative non-viral vectors are more preferable over viral vectors as they are easy to produce, transport, store, reproduce in large quantities, have greater capacity to carry nucleic acids, can transfer larger transgenes and are less susceptible to immune response (Goldberg, Langer et al. 2007; Gwak and Kim 2008; Kang, Lim et al. 2008). Some of the commonly used non-viral vectors include cationic liposomes, cationic polymer nanoparticles, and inorganic particles produced either from natural or synthetic materials. Because of their inherent advantages like flexibility in synthesis methods to produce a desired product, cationic polymeric nanoparticles have received great attention. Condensed DNA is obtained by mixing both DNA and cationic polymer solutions together, forming a DNA-polymer complex in the nanometer size range (Yang, Wang et al. 2006; Goldberg, Langer et al. 2007). The three main components of nanoparticles required for targeted delivery of protein are: 1) a biocompatible polymer matrix that is compatible both with drug and stabilizer, 2) a stabilizing agent, and 3) a structurally defined component for guiding the nanoparticles to the intended site (Solaro 2002). One of the most commonly used cationic polymers for gene delivery is poly (ethylene imine) (PEI) (Yang, Wang et al. 2006; Goldberg, Langer et al. 2007). Using branched PEI, DNA can be condensed to generate 100 nm spherical polymeric molecules and these nanoparticles also offer high gene transfection efficiency. The main limitation of PEI usage is its high cytotoxicity (Goldberg, Langer et al. 2007; Gwak and Kim 2008; Kang, Lim et al. 2008).

Nanoparticles and physicochemical properties

Extensive research in the field of drug delivery led to application of nanoparticles as potential drug carriers. Solid colloidal particles in the range of 10 to 1000 nm are referred to as nanoparticles (Lee 2001). Colloidal particles have high surface areas, and flexible synthesis methods to obtain different internal structures and surface properties making them highly suitable for a wide range of drug delivery applications. Nanoparticles with different structures can be synthesized (spheres, rods or disks), but nanospheres are simplest to produce and are widely used. Other structures like nanocapsules, nanotubes, nanogels, and dendrimers are preferred for some specific applications (Goldberg, Langer et al. 2007).

Nanocapsules have lower polymeric content and large lipophilic drug payload capacity compared to that of nanospheres (Limayem Blouza, Charcosset et al. 2006). Nanotubes have large inner volumes facilitating the binding of particles with wide size range from small chemical molecules to large proteins (Martin and Kohli 2003; Gao and Xu 2009). Advantages of nanogels are that they can be synthesized in the absence of active compound and they also prevent payload aggregation (Goldberg, Langer et al. 2007). Dendrimers have low polydispersity and high functionality (Yang and Kao 2006).

Nanoparticles can be of two types depending upon the process followed in their synthesis (Lee 2001). Nanospheres have a matrix type structure with drug dispersed in it. Nanocapsules have a membrane-wall structure with the drug entrapped in its oily core (Lee 2001; Barratt 2003). Because of their high surface area, drugs can also be adsorbed on the nanoparticles.

Numerous methods are available for the synthesis of nanoparticles with controlled composition, shape, size and morphology. These methods also give an excellent opportunity to modulate the structure, composition and physicochemical properties of nanoparticles so that better solubility, immunocompatibility and cellular uptake can be achieved. Drug formulation needs precise definition of requirements and objectives so that appropriate method for synthesis can be chosen. The raw materials for synthesis of nanoparticles can either be synthetic or natural materials. The manufacturing process for particular nanoparticles will depend upon the physical and chemical properties of raw materials to be used in their synthesis and the solubility characteristics of active component involved (Lee 2001). Properties such as biocompatibility, degradation behavior, administration route, desired drug release profile, and biomedical application type need to be considered when selecting nanoparticles materials (Lee 2001).

Desired biodistribution of the therapeutics in the body can be obtained by controlled and targeted drug delivery using nanoparticles. Nanoparticles possess high surface area to volume ratios which results in higher dissolution rates and thereby result in better bioavailability (Goldberg, Langer et al. 2007). Nanoparticle-drug complexes protect orally administered drugs with lower half-life from harsh environments in the body, reduce chemical and enzymatic degradation in the body, and lengthen the circulation time of the drug/carrier pair (Mittal, Sahana et al. 2007). Controlled release kinetics of the drug and targeted delivery of active compound to the specific site via nanoparticles carriers reduces the toxic side effects and improves the efficacy and therapeutic index of

the drugs. Nanoparticles can also be successfully used to deliver lipophilic drugs with poor solubility as well as bioactive compounds.

Size and surface properties like surface charge, hydrophilic-hydrophobic balance, and site-specific components play an important role in selecting nanoparticles for specific drug delivery applications. The purpose of drug delivery is served only if the nanoparticles deliver the drug to the targeted site, but this requires overcoming of many hurdles in the path depending upon the route of administration.

Size-related effects. The size of the nanoparticle has direct impact on the stability, cellular uptake, biodistribution, and drug release (Mittal, Sahana et al. 2007). Drug delivery systems with sizes in nanometer range can easily cross cell membranes (Goldberg, Langer et al. 2007). In intravenous administration, nanoparticles with length scales of approximately 100 nm can escape through the discontinuous capillary endothelium. Nanoparticles of this length scale or smaller can enter solid tumors, infected sites, or inflamed sites through the defective endothelium capillary at these sites (Barratt 2000; Yang, Wang et al. 2006). These small particles can also escape through the gaps between endothelial cells of the organs like liver, spleen, and bone marrow (Barratt 2000). Nanoparticles with size below 10 nm are prevented to reach targeted site as they are eliminated through renal clearance (Goldberg, Langer et al. 2007). Good circulation times are observed in particles with sizes ranging in between 70 nm and 200 nm (Goldberg, Langer et al. 2007). The spleen and phagocytes both eliminate particles greater than 200 nm from circulation in body (Goldberg, Langer et al. 2007). In oral administration route, only particles having sizes below 200 nm can diffuse across enterocytes (Barratt 2003). Summarizing above information it can be concluded that particles in range 100 nm to 200 nm are better for drug delivery.

Table 2.1. Size-related retention or elimination mechanisms

Size, nm	Response	Reference
< 200	Elimination by spleen and phagocytes	(Goldberg, Langer et al. 2007)
< 200	Oral administration, diffusion across enterocytes	(Barratt 2003)
70 < D < 200	Good circulation times	(Goldberg, Langer et al. 2007)
<100	Permeation through the gaps of endothelial cells in organs (liver, spleen, bone marrow)	(Barratt 2000)
<10	Renal clearance	(Goldberg, Langer et al. 2007)

Surface-property related effects. Nanoparticle surface properties have large effects on their performance for drug delivery. Prolonged circulation times of drugs in the body as well as targeted delivery of drug to specific site can be achieved by altering the surface characteristics of the nanoparticles (Rolland and Sullivan 2003). Nanoparticles, especially those with hydrophilic surfaces, are very promising drug carriers as they can escape the undesired elimination from the body through mononuclear phagocytes, macrophages, and reticuloendothelial systems (RES) of blood and other organs (Yang, Wang et al. 2006). Coating an antigen with specific antibody to promote phagocytosis of the antigen is called opsonization (Clancy 1998). High surface concentrations of hydrated polymer chains on hydrophilic particles reduce protein adsorption and, consequently, opsonization (Ottenbrite and Editor 1999; Barratt 2000; Solaro 2002; Yang, Wang et al. 2006). One of the most commonly used polymers for surface modification of nanoparticles to prevent opsonization is PEG. The nanoparticles with hydrophilic surfaces thereby can experience longer circulation times in vivo. Nanoparticles with hydrophobic surface are more susceptible to elimination by spleen, liver and lungs as they are considered foreign by the body. Thus, if the liver is the desired site of action, then a hydrophobic drug delivery system is a good choice (Hans and Lowman 2002).

The surface charge of nanoparticles is another crucial parameter to be considered. Zeta potential quantifies the surface charge on the particle. Zeta potential is an indicator of the colloidal stability. The higher the absolute value of zeta potential the greater is the charge on the surface. The stability of the particles improves with high repulsive interactions, resulting in more uniform distribution of stable particles in colloids (Hans and Lowman 2002). Using cationic nanoparticles for gene delivery result in good gene binding capacity, high gene transfection efficiency, and relatively low toxicity (Yang, Wang et al. 2006). This is because most of the cells have negatively charged membranes and cationic nanoparticles are preferred as they have good cell binding capacity.

Polymeric nanoparticles and polymer selection for synthesis

Nanoparticles can be made from polymers, nonpolar lipids, inorganic compounds and also from natural macromolecules like proteins and polysaccharides (Barratt 2003; Yang, Wang et al. 2006). Polymeric nanoparticles are considered to be promising drug delivery carriers as they can be chemically modified to be biodegradable and biocompatible (Lee 2001; Solaro 2002; Yang, Wang et al. 2006; Mittal, Sahana et al. 2007). Polymeric nanoparticles are capable of delivering wide range of active compounds to different body parts over specific time period (Hans and Lowman 2002). Natural polymers are not much of interest as they may vary in purity and most often need to be cross linked to prevent dissolution during use. Cross linking methods often cause denaturation of the entrapped drug (Lee 2001; Hans and Lowman 2002). Synthetic polymers offer choice among wide variety of chemistry, structures, and dimensions so that appropriate polymer for particular application can be selected. Different structures available for polymer molecules include linear, branched, cross-linked, block, graft, multivalent, dendrimers, and star shaped polymers (Goldberg, Langer et al. 2007). Surface properties of the polymeric nanoparticles like functionality and charge can also be altered during their fabrication.

Table 2.2. Summary of polymers with different topology that are used in drug delivery.

S.No.	Shape	Subtype	Polymers	Drug delivered	Reference
1.	Linear		PHPMA	Doxorubicin	(Qiu and Bae 2006)
			PSMA	Neocarcinostatin	(Qiu and Bae 2006)
			PVP	Para-nitroaniline, Interleukin - 6	(Qiu and Bae 2006)
			Dextran	Protein	(Qiu and Bae 2006; Jin, Zhu et al. 2008)
			Alginate	Gatifloxacin	(Qiu and Bae 2006; Motwani, Chopra et al. 2008)
			Chitosan	Doxycycline	(Qiu and Bae 2006; Shanmuganathan, Shanumugasundaram et al. 2008)
			PEG	DNA	(Kainthan, Gnanamani et al. 2006; Qiu and Bae 2006)
2.	Branched	Hyperbranched polymer	Hyperbranched poly (aspartamide)s	Beclomethasone dipropionate	(Mather, Viswanathan et al. 2006; Pitarresi, Casadei et al. 2007)
		Graft copolymer	PEI-graft-PCL (PEC)	Doxorubicin, DNA	(Qiu and Bae 2007)
		Star-shaped polymer	PDMAPAAM–PNIPAM	DNA	(Zhou, Ishikawa et al. 2007)

Table 2.2(continued). Summary of polymers with different topology that are used in drug delivery.

			Chlorin-cored PCL -b- mPEG	Paclitaxel	(Peng, Shieh et al.)
3.	Cross linked	Polymer networks	(PVA) hydrogels	proxiphylline	(Wu and Brazel 2008)
			PEG-PLLA-PEG hydrogels	Dextran	(He, Kim et al. 2008)
		Interpenetrating polymer networks	poly (acrylic acid- <i>co</i> -acrylamide)/ <i>O</i> - carboxymethyl chitosan hydrogel	Insulin	(Yin, Ding et al. 2008)
		Semi- interpenetrating polymer networks	PEGDMA/PLA semi-IPN	Protein	(Lee and Yuk 2007)

Polymeric nanoparticles can be produced cheaply and easily in large scale by following any one of the numerous methods available for synthesis. Polymeric nanoparticles can be produced either starting directly from polymers or starting from monomers (Barratt 2000; Lee 2001; Barratt 2003). Polymeric nanoparticles are not only used for targeted and sustained delivery of drugs but also for better control over the drug release profile. Polymeric nanoparticles can deliver drugs to maintain steady plasma concentration over a period of time thereby decreasing frequency of doses and side effects (Mittal, Sahana et al. 2007). Enhanced bioavailability is achieved because of comparatively more stable and soluble polymer-drug complexes and also because of the small size of the particles. Defined particle size, three-dimensional structure, and composition can easily be obtained as formulation of the polymeric systems is more governable (Goldberg, Langer et al. 2007).

Chemical properties and structure of polymers play a vital role as they help control the interactions between the drug and its external environment, thus affecting their efficiency as drug carriers (Goldberg, Langer et al. 2007). Along with the physicochemical properties, drug loading efficiency, drug release rate and also biodistribution of drug in the body are highly affected by the structure of the polymer (Goldberg, Langer et al. 2007). Molecular weight and polydispersity of a polymer also play significant roles in characterizing its biological properties (Goldberg, Langer et al. 2007; Mittal, Sahana et al. 2007). The molecular weight of the polymer affects the nanoparticles size and encapsulation capacity (Lee 2001; Hans and Lowman 2002; Mittal, Sahana et al. 2007). Lower molecular weight polymer results in small sized nanoparticles with low encapsulation efficiency. Use of high molecular weight polymer or high concentration of polymer during synthesis method results in particles with larger size and higher drug loading efficiency.

Complexation mechanisms. Drugs can be attached to the polymer during the polymerization. Drugs can also be added to preformed polymeric nanoparticles, which adsorb them on the nanoparticle surface or by incorporating the drug into polymeric matrix (Lee 2001). In some cases, drugs are covalently bonded to the polymer forming a drug-polymer complex in which the drug is uniformly dispersed. It can also be physically entrapped in the polymer vesicles (Goldberg, Langer et al. 2007). Drug loading efficiency into the nanoparticles is highly affected by the pharmaceutical's properties, synthesis parameters and structural compatibility between the drug and the polymer (Yang, Wang et al. 2006). Based on the solubility of the drug, a process for loading of active components into polymeric nanoparticles is selected. Hydrophobic drugs are loaded using oil-in-water emulsion procedure whereas the water-in-oil-in-water double emulsion method is used for hydrophilic materials. Ionic complexation has also been used to load some specific drugs into nanoparticles.

Synthesis of polymeric nanoparticles

A very good reference for synthesis of polymeric nanoparticles is encyclopedia by Lee 2001. *In situ* polymerization of monomer for synthesis of nanoparticles encounters some major disadvantages. One of it is the multi-component nature of the polymerization medium, which results in unpredictable molecular weights of the polymerized nanoparticles (Lee 2001). The molecular weight of the polymer greatly influences the

degradation rate, drug release behavior of the nanoparticles and biodistribution of drug in the body. With *in-situ* polymerization of monomers, prediction of molecular weight is difficult and is considered a major disadvantage. Most of the polymers produced in this manner are not biodegradable. Drug activity may be hindered if its chemical groups interact either with reactive monomers and/or with H⁺ ions in anionic polymerizations (Lee 2001). Elimination of toxic residues such as initiator, unreacted monomer, and surfactant molecules are time consuming and inefficient procedures (Lee 2001). In order to overcome all these drawbacks, methods involving preformed polymers are developed so that biodegradable, well-characterized and non-toxic polymeric nanoparticles are generated.

Both natural and synthetic polymer molecules can be used to produce nanoparticles. Natural polymers that are widely used include proteins like albumin, gelatin, legumin, vicilin and polysaccharides like alginate, agarose, and Chitosan (Lee 2001). Because of their inherent properties like biodegradability and bioavailability, they are widely used as biomaterials. Nanoparticles with natural macromolecules are mainly produced by two main methods. One of them is emulsification-based method involving in the formation of a water-in-oil emulsion followed by chemical cross-linking or heat denaturation of the macromolecules (Lee 2001). In cases where heat sensitive drugs are used, heat denaturation for hardening of nanoparticles may be a disadvantage. If heat sensitive drugs are employed, a better alternative is to use chemical hardening agents. A second technique is a phase separation-based process in which phase separation in an aqueous medium is followed by chemical cross-linking. For the synthesis of nanoparticles using this method, it is necessary to use hardening agents like glutaraldehyde to crosslink the polymer in the three-dimensional nanoparticle. The use of a hardening agent is highly undesirable as it may interact with drug, or residual agent may leach from the nanoparticles during use, causing toxicity issues.

Most of the synthetic polymers are composed of big molecules with typical solution characteristics and easily form colloidal dispersion with well defined particle size. Numerous methods are reported in literature for the manufacture of the nanoparticles using synthetic materials. The common process in all the methods is coacervation (Solaro 2002). The generated colloidal dispersion is then eventually converted into nanoparticles by a process which involves externally induced separation of at least two phases for the production of nanoparticles. Aggregation of the colloidal particles in the dispersion can be prevented by the use of stabilizers. Stabilizers coat the outer surface of the particles with a metastable microphase which prevents coalescence of these particles. The manufacturing method is selected based upon the raw materials and their solubility characteristics. Some of the commonly used techniques include emulsification-solvent evaporation method, solvent displacement method, salting-out technique, emulsification-diffusion method. These emulsion based methods differ in solubility of organic phase in aqueous phase. The emulsification-evaporation method uses water and volatile, immiscible solvents which can be easily separated after nanoparticles are produced. The solvent displacement, salting-out, and emulsification-diffusion methods use partially or completely miscible organic solvents.

In emulsification-solvent evaporation method, a preformed polymer is dissolved in a volatile water-immiscible organic solvent to form a solution (Lee 2001; Hans and Lowman 2002). This solution is emulsified in an aqueous phase containing a surfactant or stabilizer resulting in oil-in-water emulsion. The coalescence of the organic droplets can be avoided by continuous stirring. Emulsification can also be enhanced by using sonication or microfluidization with a homogenizer. Nanoparticles are formed when organic solvent is removed from the droplets by evaporation under stirring at room temperature or by rotary evaporation under reduced pressure. Generally lipophilic compounds that are soluble in the polymer solution can be effectively entrapped using emulsification-solvent evaporation method. The main disadvantage with this method is that it generally uses toxic chlorinated solvents and surfactants. Slight modifications to this method are suggested in literature to allow for efficient entrapment of amphiphilic and hydrophilic into the nanoparticles.

Solvent displacement method uses semi-polar and completely water miscible liquids like ethanol, methanol or acetone (Solaro 2002). Lipophilic stabilizer if used, polymer, and drug are dissolved in the solvent. Under stirring, this organic solution is then added to aqueous phase containing stabilizer resulting in rapid solvent diffusion. This in turn results in instantaneous nanoparticle formation. The organic phase is separated under reduced pressure. This method is not preferred for hydrophilic drugs as they rapidly diffuse into the water phase resulting in extensive loss of drug. A major drawback to this technique is that it is not easy to select suitable solvent/nonsolvent systems for the polymer and drug employed such that high entrapment and production yield is obtained.

Salting-out techniques often employ water miscible acetone as solvent unlike emulsification-solvent evaporation method that employs toxic chlorinated solvents (Lee 2001; Hans and Lowman 2002; Solaro 2002). An aqueous solution of colloidal stabilizer and electrolyte that act as salting-out agent is used in this method. Saturation of the aqueous phase with the salting-out agent avoids the miscibility of both phases. An aqueous phase is added to an organic phase containing dissolved polymer and drug under continuous stirring to form an emulsion. Addition of aqueous phase is continued until phase inversion is observed and an oil-in-water emulsion is formed. This emulsion is further diluted by addition of pure water to break the equilibrium between the two phases. As a result, acetone completely diffuses into the water resulting in precipitation of polymeric spherical nanoparticles. Solvent and electrolytes are removed by cross-flow filtration technique. The scale-up of the salting-out technique is fairly easy (Solaro 2002). This method is relatively versatile as variety of polymers can be used with this technique and it can also use solvents other than acetone and also non-electrolyte salting-out agents (Allemann, Gurny et al. 1992). This method does not require use of surfactants. This technique allows for good loadings of lipophilic drugs. The recycle of salts and solvent used in the process is a major concern. The compatibility of salt with the drug should also be taken into consideration for this method.

The emulsion-diffusion process employs a partially miscible organic solvent such as benzyl alcohol for nanoparticles preparation (Hans and Lowman 2002; Solaro 2002). In this method, polymer dissolved in an organic phase is slowly added to an aqueous phase containing dissolved stabilizer under rigorous stirring. As the organic phase is just

slightly miscible in water, after the addition of aqueous phase is completed initially an oil-in-water emulsion is observed. This emulsion is diluted by adding sufficient quantity of pure water under stirring leading to the diffusion of organic phase into the water. This results in precipitation of the polymer and the consequent formation of nanoparticles. The mechanism of formation of nanoparticles in emulsion-diffusion technique is explained based on interfacial phenomenon.

This work is mainly based on a new method called emulsion-diffusion-evaporation developed by Ravi Kumar et al. This method is basically a combination of emulsion-evaporation and emulsion-diffusion techniques for nanoparticle preparation (Kumar, Bakowsky et al. 2004; Mittal, Sahana et al. 2007). In this method, a preformed polymer dissolved in a volatile and slightly miscible organic solvent like ethyl acetate (Kumar, Bakowsky et al. 2004). Then an emulsion of organic phase in aqueous phase containing is generated. Immediately after this, the emulsion is slowly diluted by sufficient pure water under continuous stirring resulting in nanoparticle formation. Organic solvent is removed by evaporation. This method involves usage of less toxic ethyl acetate solvent and the removal of organic solvent is fairly easy.

PLGA, PVA and chitosan chloride

Selection of polymer is done based upon the type of drug delivery application and the properties of the drug to be delivered. Some of the commonly used synthetic polymers include PLGA, PCL, PLA, PGA, PHB, etc (Lee 2001; Hans and Lowman 2002; Barratt 2003; Yang, Wang et al. 2006). Among these PLGA is one of the most popular polymers used because of its good biodegradability, biocompatibility and non-toxic nature (Lee 2001; Hans and Lowman 2002; Mittal, Sahana et al. 2007). FDA approval is an added advantage to this commercial polymer. PLGA has a high molecular weight and free carboxylate end-groups, which give it good drug loading capacity (Goldberg, Langer et al. 2007). Increased PLA content makes the copolymer more hydrophobic and increases PGA results in hydrophilic copolymer (Hans and Lowman 2002). Using low molecular weight PLGA in organic solution yields nanoparticles with smaller size (Lee 2001; Hans and Lowman 2002). Varying the molecular weight and the ratio of lactic and glycolic acid of the polymer, the rate of degradation and the consequent drug delivery rate of the PLGA nanoparticles can be controlled (Lee 2001; Hans and Lowman 2002; Mi, Shyu et al. 2003; Mittal, Sahana et al. 2007; Tahara, Sakai et al. 2008). As a result, controlled release of active compound over a desired period of time is possible using PLGA.

Biodegradation is defined as the biological cleavage of the polymer structure (Merkli, Tabatabay et al. 1998). Heller proposed three different mechanisms for polymer degradation based on the solubility of the polymer (Merkli, Tabatabay et al. 1998; Lee 2001). In case of hydrophobic polymers like PLGA, backbone cleavage of the polymer results in small non-toxic soluble molecules (Anderson and Shive 1997). Homogeneous erosion of polymer in the particle core is observed during degradation of PLGA (Anderson and Shive 1997). Hydrolytic cleavage followed by enzymatic cleavage of the polymer chains produce degradation products. Under physiological conditions, hydrolysis of PLGA results in glycolic acid and lactic acid that are easily removed from the body by Krebs cycle (Lee 2001). Various body cells can well sustain these PLGA degradation products.

In gene delivery applications, PLGA can be employed as a better substitute for PEI because it is biodegradable, it possesses high gene transfection efficiency and PLGA also has lower toxicity compared to that of PEI (Gwak and Kim 2008; Kang, Lim et al. 2008). Sustained gene expression can be obtained using PLGA nanoparticles, making it an efficient gene delivery vector (Gwak and Kim 2008; Kang, Lim et al. 2008). Coating of cationic polymer chitosan on PLGA nanoparticles has improved the nucleic acid loading into the polymer (Tahara, Sakai et al. 2008). Chitosan also reduces the initial burst of nucleic acid thereby more sustained release over a prolonged period is obtained (Tahara, Sakai et al. 2008). Thus PLGA nanoparticles modified by chitosan are considered very promising non-viral gene delivery vectors.

The ability of a chemical to cause an injury on reaching a susceptible site in or on the body is termed as toxicity (Lewis 1999). Most chemicals can adversely affect the human tissue if they come in direct contact with the tissue. Toxicity depends on depends on number of factors like nature of the chemical, dose of chemical, time period of exposure, state of dispersion, affinity for human tissue and sensitivity of tissue (Lewis 1999; Bennett 2005). Toxicity is measured in terms of threshold limits or lethal dose 50 (LD₅₀). Threshold limit is defined as the conditions under which all workers may be repeatedly exposed to the chemical without any harm. The values are expressed in terms of time-weighted average concentrations for a normal day. Lethal dose 50 is the amount of chemical which will kill one-half of the experimental animals tested. It is expressed per kilogram of body weight. Ethyl acetate is the solvent for PLGA in this work. The threshold limit value of ethyl acetate is 400ppm in air.

Stabilizer plays an important role in formation of nanoparticles. Appropriate stabilizer suitable for the drug delivery application has to be chosen from the wide variety of synthetic and natural polymeric stabilizers available. The concentration of stabilizer has a high impact on nanoparticle formation (Lee 2001; Hans and Lowman 2002). In general, increasing stabilizer concentration decreases the nanoparticle size formed. Low concentrations of stabilizer lead to the coalescence of the polymer droplets in the emulsion decreasing the nanoparticle productivity. Interaction between drug and stabilizer is of major concern to use high concentrations of stabilizer which leads to low drug entrapment into the polymer (Italia, Bhatt et al. 2007). So within certain limits, variation in particle size can be achieved by varying stabilizer amount used. Biodegradable PVA is considered one of the good polymers to stabilize PLGA nanoparticles (Vandervoort and Ludwig 2002).

Drug targeting can be primarily divided into two types namely active and passive targeting (Wheatley and Langer 1987). In passive targeting, the inherent dispositions of the drug delivery system are taken advantage to reach the desired site of action. In active targeting, the natural characteristics of the particles are modified to achieve the desired targeted delivery. For active targeting, either surface modification of the particles or adding biomolecules that guide or bind to the targeted site is required (Rolland and Sullivan 2003). For a particular drug delivery application, required properties of the nanoparticles like hydrophilicity, and zeta potential can be attained by surface modification of nanoparticles. One of the most commonly used polymers for surface modification is PEG (Clancy 1998; Hans and Lowman 2002; Solaro 2002; Rolland and

Sullivan 2003). PEG is a biocompatible, non-ionic, and hydrophilic polymer. Chitosan is a cationic and hydrophilic polymer that is often used for surface modification (Lee 2001; Kumar, Bakowsky et al. 2004; Duan, Wu et al. 2007). Apart from being mucoadhesive and biodegradable, chitosan confers positive zeta potential to PLGA nanoparticles (Hans and Lowman 2002; Kumar, Bakowsky et al. 2004; Tahara, Sakai et al. 2008). This results in an increased DNA binding capacity of PLGA nanoparticles. Chitosan enhances the penetration of the nanoparticles across the mucosal surface. Mucoadhesive polymers like chitosan have prolonged residence time increasing the bioavailability (Dhawan, Singla Anil et al. 2004; Kumar, Bakowsky et al. 2004).

Static Mixers

Static mixer consists of a series of identical mixing elements placed in a pipe, column or reactor (Maa and Hsu 1996; Thakur, Vial et al. 2003; Ouzineb, Lord et al. 2006; Kumar, Shirke et al. 2008). Static mixers are being extensively used in chemicals, petrochemicals, pharmaceuticals, food engineering, paper, and pulp industries. Depending on the requirement we can choose from more than 30 different types of commercial static mixers available. These models offer different variety of basic geometries and variable parameters. Number of mixing elements can be varied to achieve the desired mixing. Aspect ratio, ratio of length to diameter of each mixing element, is another important parameter considered for static mixers. Generally commercial models are designed using standard values of parameters that enable good mixing over wide range of applications.

Static mixers are used for continuous mixing operations in process industries. Based upon the design and geometry of the mixing elements, static mixers can be divided into five categories viz., open designs with helices, open designs with blades, corrugated plates, multi-layers designs, and closed designs with channels and holes (Thakur, Vial et al. 2003). The principle involved in mixing of flowing streams in a static mixer is the redistribution of fluid in the radial and tangential direction to the flow (Thakur, Vial et al. 2003). Three main mechanisms that occur in a static mixer that result in production of uniform product are - division of the flowing stream leading to twice the number of previous ones, cross current mixing by recombining the divided streams, and back mixing (Maa and Hsu 1996). The predominant of the three steps depends upon the design of the mixing element. Pressure difference is the driving force for the fluid to flow through the static mixer and is often provided by a pump (Kumar, Shirke et al. 2008). As the fluids flow through the mixer, pressure drop across the mixer is observed (Ouzineb, Lord et al. 2006).

Static mixers are used for four different types of applications namely mixing of miscible fluids, interface generation of immiscible phases, heat transfer, and axial mixing. Emulsifying an immiscible phase in a continuous phase to enhance the mass transfer between immiscible phases is one of the common processes observed in a process industry. Static mixers are used to reduce the droplet size of the dispersed phase and thereby increase the surface area for mass transfer. Emulsion formation depends upon the generation of the droplets by a device that can rupture the oil phase. Static mixers can be considered for nanoparticle preparation because it can produce liquid-liquid emulsions (Maa and Hsu 1996; Lemenand, Della Valle et al. 2003). Static mixers can produce local

shear rates high enough for interfacial generation. Static mixers are generally used for generating emulsions of phases involving stabilizer that is used to overcome the surface tension. Colloidal forces also play an important role in systems involving droplets with nanometer size range. Processing multiple phases with stabilizer through static mixers results in drop break-up followed by stable emulsion formation because of electrostatic forces of stabilizers. Static mixers require very low energy to generate stable and polymerizable emulsions that result in particles in nanometer size range (Ouzineb, Lord et al. 2006). Static mixers can produce emulsions with smaller size droplets with uniform size distribution compared to that of agitated vessels (Thakur, Vial et al. 2003).

The main advantages of static mixers over other conventional mixers are their compact size, comparatively low cost, close approach to plug flow, continuous processing, short residence time, low shear rates, absence of moving parts, easy cleaning, and no power requirement except for the process pump (Maa and Hsu 1996; Thakur, Vial et al. 2003; Ouzineb, Lord et al. 2006). The degree of mixing in a static mixer depends upon physicochemical properties and flow rates of the streams and on the type of the static mixer selected: static mixer performance may vary for different systems (Maa and Hsu 1996; Thakur, Vial et al. 2003).

Scale-up methods. Scale-up correlations for static mixers vary depending on the transport or physical mechanisms being modeled. Two mechanisms are relevant for the production of nanoparticles for drug delivery: fluid mixing, in the case that two miscible streams with different components are being mixed, and droplet formation, in the case that two immiscible streams with components are being mixed. Sauter mean diameter d_{32} or mass transfer coefficient $K_L A$ are appropriate metrics for evaluating static mixer performance for these mechanisms. Sauter mean diameter is the diameter of a sphere that has the same volume to surface area ratio as that of the droplet being examined. Correlations predict either the droplet diameter or the mass transfer coefficient based upon dimensionless numbers like Weber number (We), and Reynolds number (Re).

Many correlations have been proposed for co-current liquid-liquid systems. The First correlation to estimate Sauter diameter was proposed by Middleman for Kenics static mixer and is $d_{32}/D = A * We^{a1} * Re^{a2}$, where D is the column diameter (Thakur, Vial et al. 2003). Many other correlations are published following the first one, one of them is $d_{32}/D = 1.12 * We^{-0.65} * Re^{0.2} * R_{\mu}^{0.5}$ by Haas, where R_{μ} represents the ratio of dispersed to continuous phase viscosity (Thakur, Vial et al. 2003). One more correlation for kenics static mixer is $d_{32}/D = 0.49 * We^{-0.6} * \{1 + 1.38 V_i (d_{32}/D)^{1/3}\}^{0.6}$ by Berkman and Calabrese, where V_i is viscosity group on capillary number $V_i = (\mu_d V / \sigma)(\rho_c / \rho_d)^{1/2}$ (Berkman and Calabrese 1988; Thakur, Vial et al. 2003). The negative exponent on weber number signifies that droplet size decreases on increasing flow rate or decreasing surface tension. The positive exponent on the reynolds number implies that increase in the viscosity of the continuous phase results in decreased droplet size.

3. Materials and methods

Materials

PLGA 65:35 (CAS Registry No. 25013 – 16 – 5, MW 40,000 – 75,000) and PVA (CAS Registry No. 9002 – 89 – 5, MW 13,000 – 23,000, 98% hydrolyzed) are purchased from Sigma Aldrich, USA. Chitosan (CAS Registry No. 9012 – 76 – 4, deacetylation 75 – 92%) is obtained from Spectrum Chemicals, USA. Ethyl acetate (EA) (CAS Registry No. 141 – 78 – 6, FW 88.11, 99.5+%) is purchased from Acros Organics, USA. Hydrochloric acid (HCl) (CAS Registry No. 7647 – 01 – 0, FW 36.46, 32 – 38%) and deionized ultra filtered water (DIUF H₂O) (CAS Registry No. 7732 – 18 – 5, FW 18.02) are purchased from Fisher Scientific, USA. All the chemicals are used as obtained without further purification.

Chitosan chloride was synthesized using chitosan, HCl, and DIUF H₂O. First 0.005 wt% of 38% HCl was added to DIUF H₂O in a beaker. To this solution 0.0015 wt% of chitosan was added under stirring. This beaker was placed in a water bath at 80⁰C and the contents of the beaker were stirred at 1000 rpm using a magnetic stirrer for 2 hr. After 2 hr, the solution was filtered using a 25 μm filter paper. This solution was dried overnight in an oven at 80⁰ C to remove water present in it resulting in the formation of chitosan chloride powder. This chitosan chloride powder was stored for future use in some batches during the synthesis of PLGA nanoparticles.

Organic phase is prepared by dissolving 1 wt% of PLGA in required amount of EA in a closed vial bottle at 900 rpm using a magnetic stirrer for 2 hr at room temperature. Aqueous phase consists of PVA, and chitosan chloride dissolved in DIUF H₂O. Initially 1 wt% of PVA is added to the amount of DIUF H₂O five times as that of EA. This was stirred at 900 rpm in a water bath at 80⁰C for 2 hr until all the PVA was dissolved. After this solution was cooled down to room temperature, (0.3 wt %) of chitosan chloride prepared previously was added to the solution. The stirring of the solution is continued until all the chitosan chloride is completely dissolved. Thus the ratio of the organic phase to the aqueous phase is maintained at 1:5. The amount of EA and DIUF H₂O is selected based upon the minimum requirement of the equipments used for each batch but the ratio of the materials is maintained constant.

Sonication

A Torbeo ultrasonic cell disruptor (36810 – series) is used to generate primary oil – in – water emulsion. The vial bottle containing 5 ml of aqueous phase and 1ml of organic phase is placed in a water bath at room temperature. The tip of the sonicator was positioned in the middle of the liquid contents of the vial bottle. The sonicator is operated at 30 Watts for 2 min resulting in the formation of primary oil – in – water emulsion.

Colloid Mixer

In some batches, a SILVERSON L4RT – A lab mixer is used. A beaker containing organic and aqueous phase is placed under the rotor such that the mixing rotor head is completely immersed in the liquid. The mixer is switched on and the rotor speed is gradually increased to 9600rpm. The stirring is continued for 10 min resulting in the formation of the emulsion.

Static mixer

A Chemineer Kenics KM Static mixer is used in this work to generate secondary oil – in – water emulsions. Static mixers are used for diffusion step of the synthesis of the PLGA nanoparticles. Static mixer with size 3/16, housing ID 0.13in, 27 elements, material 316s/s, plain ends, edge sealed, and overall length 7.50in was selected for this application.



Figure 3.1. Series of helical mixing elements in a KM static mixer.

© Chemineer products and services

Two pumps are connected to the inlet provision of the Static mixer so that DIUF H₂O and primary oil – in – water emulsion can be simultaneously fed through the static mixer. A Fisher scientific mini – pump is used to pump primary oil – in – water emulsion through one input and DIUF H₂O is pumped using a COLE – PARMER Master flex console drive through another input provision of the static mixer. The speeds of both the pumps are adjusted so that the volumetric ratio of the emulsion to the DIUF H₂O pumped through the static mixer is maintained at 1:10. To send the secondary emulsion multiple times through the static mixer only Cole – Parmer Master flex console drive pump is used and the Fisher scientific mini – pump is switched off. After the secondary emulsion is sent 2 more times through the static mixer a good PLGA nanoparticles suspension is observed. The equipment arrangement for generating secondary emulsion using static mixer is shown in Figure2.

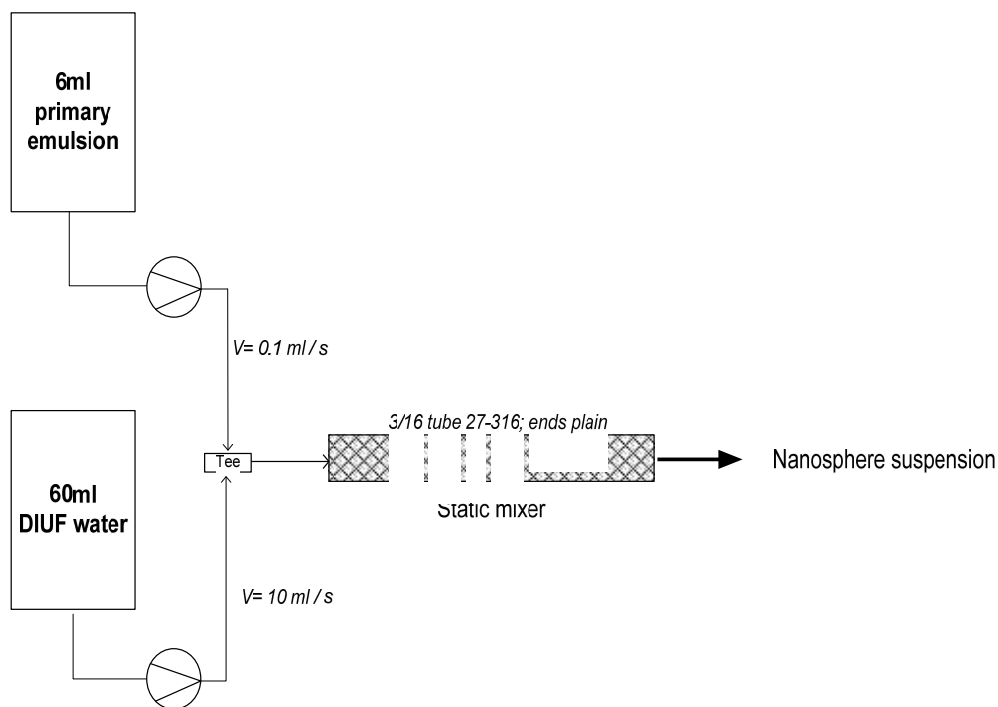


Figure 3.2. Process flow diagram of Static mixer.

Characterization of nanoparticles

Light scattering particle size analysis

The polymeric nanoparticles size measurement was made on a 90Plus/ BI-MAS particle size analyzer, Brookhaven Instruments Corporation. Each of the secondary oil – in – water samples were analyzed at a scattering angle of 90^0 at 23^0 C. The samples obtained to determine mechanism of formation of particles, and effect of static mixer on primary emulsion droplets have a run time of 15 min. The samples generated for TEM analysis have a run time of 30 min and all the remaining samples have a run time of 4 min. As average count rate is an indicator of signal quality, all the samples must have an average count rate of at least 100 Kcps. Care is also to be taken to verify that all the samples have a baseline index of at least 7.5 or above and a good correlation function graph before the data is collected. Baseline index is a measure of how good the scattering data are. If the data is corrupted by scattering from dust in the sample then turn the dust filter on. If the dust filter value is too low then we obtain low effective diameter. The mean particle size is obtained from multimodal size distribution (MSD) curves based on volume and number of the nanoparticles of each sample. The number based (NB) and volume based (VB) particle size for each sample is summarized in tables.

The mean diameter in MSD is calculated from diameter d and weighting factor $G(d)$ and the formula is

$$\text{Mean Diameter for MSD} = \frac{\sum (d \cdot G(d))}{\sum G(d)}$$

Zeta potential Measurements

The surface charge of the polymeric nanoparticles was measured by the Zetasizer2000, Malvern Instruments Limited. The zeta potential measurements of the secondary oil – in – water emulsion samples are carried out in an aqueous dip cell at 25⁰C. The solvent used is water for all the samples.

Transmission electron microscope (TEM) analysis

TEM measurement was carried out to get the information of the actual surface and morphology characteristics of PLGA nanoparticles. This can be used to verify and compare the particle size from MSD data of the sample. Transmission electron microscopy (TEM) analysis was performed on a JEOL 2010F instrument operated at 200 KeV. The TEM sample was prepared by dipping lacey carbon-coated copper grid into secondary emulsion of PLGA nanoparticles. After copper grid was taken out, it was dried at room temperature over night before measurement.

4. Results and discussion

All the results of the subsections are presented in the respective tables of the subsections and are followed by the volume based MSD figures. The corresponding number based MSD figures are included in the appendix.

Mechanisms for formation of nanoparticles

A key element of this study is to determine how nanoparticles form when solutions of PLGA and PVA are mixed.

Dissolution of polymers in their solvents

The individual polymers are tested for their solubility in respective solvents to make sure that the polymers are completely miscible in their solvents and the polymer solutions do not have any particles prior to the nanoparticle synthesis process. PLGA is dissolved in ethyl acetate, and PVA is dissolved in DIUF H₂O as a part of the encapsulation process. Both solutions were evaluated to determine whether the polymers were completely dissolved, or whether they were merely swollen by their solvents. A 2wt% solution of PLGA in ethyl acetate was prepared and the MSD of solution was analyzed by light scattering. The resulting solution was optically clear, and no particles were observed by light scattering. The lower limit of detection by Brookhaven instrument is 1nm. A 1wt% of PVA in DIUF H₂O was prepared as described in materials and methods. The solution is optically clear. After the solution is cooled down to room temperature, its particle size is measured. It was found that there were no particles in the solution, implying complete dissolution of PVA in DIUF H₂O at 80⁰ C. The results of the tests are summarized in rows 2 and 3 of Table 4.1 for PLGA in EA and PVA in DIUF H₂O respectively.

To confirm the solubility of Chitosan chloride, a solution of 0.3 wt% chitosan chloride in DIUF H₂O is prepared by dissolving chitosan chloride in DIUF H₂O for 15min until the solution was optically clear. This solution had 91% of the particles based on volume and 100% of particles based on number with size range 134 nm<D_{avg}<521 nm, as shown in Figure 4.1 and row 4 of Table 4.1. They had a polydispersity of 0.168. Based on volume, 9% of the particles with D_{avg}=1179 nm are found in the solution but they are very few in number as same range could not be found in number based MSD. This dispersion is stable as its zeta potential is 33.4±2.2 mV. It is possible that the chitosan suspension has agglomerates, which can be tested by diluting the sample and remeasuring the particle size distribution. When the solution was diluted by a factor of 10, its transparency improved, and 100% of the particles are found in the size range 132 nm<D_{avg}<295 nm based on number and volume as shown in Figure 4.2. It has a polydispersity of 0.072, as mentioned in row 5 of Table 4.1. It was observed that particles with smaller size and narrow size range are present in the 10 folds diluted chitosan chloride solution. The zeta potential of this solution was 57.4±1.3 mV, and it was deemed to be stable. These results demonstrate that PLGA and PVA are completely miscible in their respective solvents, while chitosan chloride is swollen, but forms a stable dispersion in its solvent.

The formation of nanoparticles if any by using only chitosan chloride for primary emulsion generation was checked in one batch. This batch was prepared by sonicating 1ml of EA with 5 ml of 0.3 wt% chitosan chloride in DIUF H₂O. The emulsion was diluted 100 folds and MSD of the emulsion was obtained by light scattering and results

are displayed in row 6 of Table 4.1 and Figure 4.3. There are no good signs of nanoparticle formation as the count rate is very low. All the results are summarized in Table 4.1 and the volume based MSD of the batches are presented following the Table 4.1.

Table 4.1. Summary of particles found in individual polymer solutions used.

System- Single component	Emulsion method and parameters	Appearance	D _v (nm) (% of particles in the range)	D _n (nm) (% of particles in the range)	Poly dispersity	Zeta Potential (mV)
2wt% PLGA in EA	N/A	transparent	Not detected	Not detected	N/A	N/A
1wt% PVA in DIUF H ₂ O	N/A	transparent	Not detected	Not detected	N/A	1.3 ±2.2
0.3wt% chitosan chloride in DIUF H ₂ O	N/A	Stone yellow clear	Peak 1 (91%) D _{min} =134, D _{avg} =390, D _{max} =521	Peak 1 (100%) D _{min} =134, D _{avg} =190, D _{max} =521	0.168	33.4±2.2
			Peak 2 (9%) D _{avg} =1179			
0.03wt% chitosan chloride in DIUF H ₂ O	N/A	transparent	Peak 1 (100%) D _{min} =132, D _{avg} =182, D _{max} =295	Peak 1 (100%) D _{min} =132, D _{avg} =162, D _{max} =295	0.072	57.4±1.3

Table 4.1(continued). Summary of particles found in individual polymer solutions used.

1ml EA and 5ml 0.3wt% chitosan chloride in DIUF H2O	Sonication 30watt, 2min, room temperature.	Turbid yellow	Peak 1 (40%) $D_{\min}=79, D_{\text{avg}}=119, D_{\max}=177$ abnormal low countrate	Peak 1 (100%) $D_{\min}=79, D_{\text{avg}}=104, D_{\max}=177$ abnormal low countrate	0.410	48.6±2.6
			Peak 2 (55%) $D_{\min}=644, D_{\text{avg}}=762, D_{\max}=889$			
			Peak 3 (5%) $D_{\min}=7242, D_{\text{avg}}=8460, D_{\max}=10^4$			

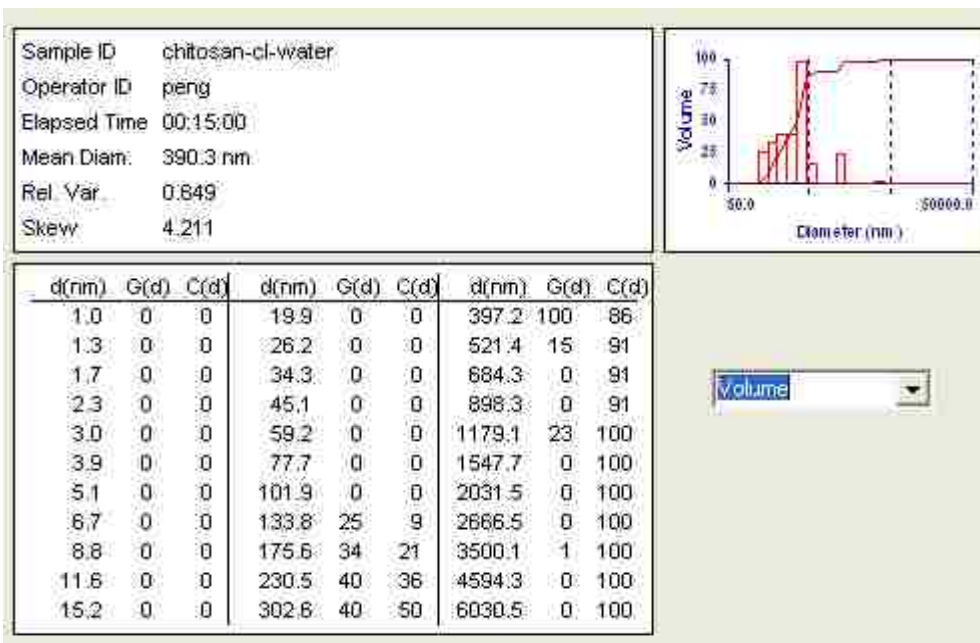


Figure 4.1. Volume based MSD of 0.3wt% chitosan chloride in DIUF H₂O [Table 4.1, row 3]

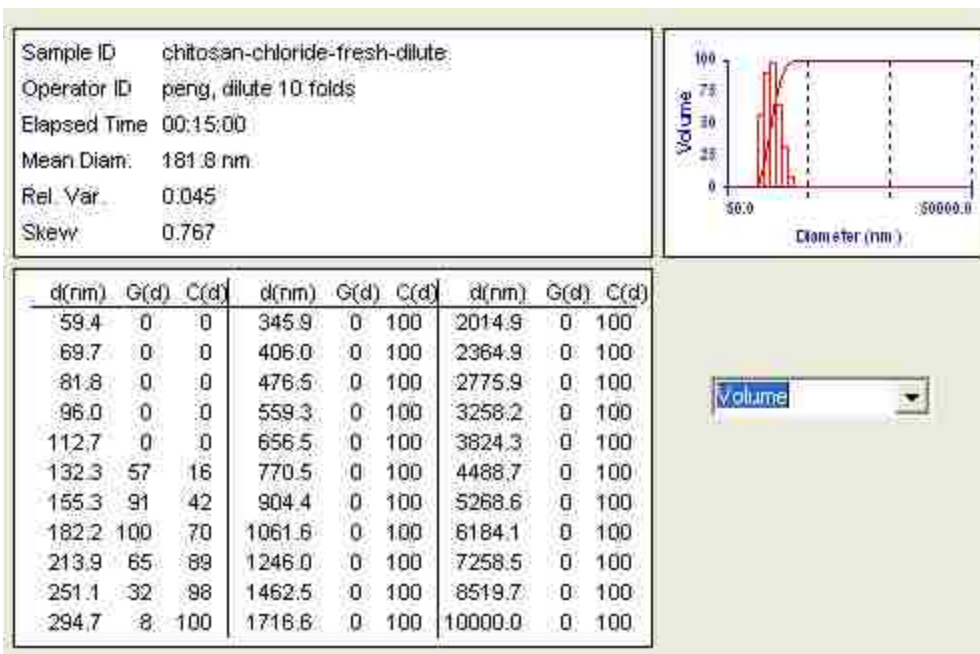


Figure 4.2. Volume based MSD of 0.03wt% chitosan chloride in DIUF H₂O. [Table 4.1, row 5]

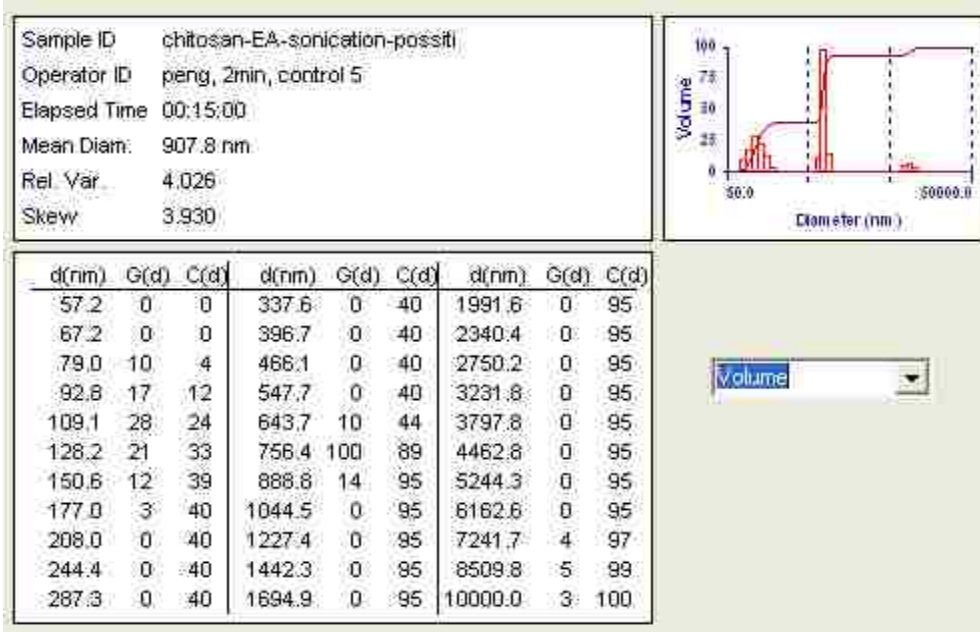


Figure 4.3. Volume based MSD of particles formed by emulsifying 1 ml EA in 5 ml solution of 0.3wt% chitosan chloride in DIUF H₂O. [Table 4.1, row 6]

Different possible binary polymer emulsions

Interaction between chitosan chloride and PVA in aqueous phase is tested in this batch. This is done to confirm the absence of nanoparticles in the aqueous phase before it is used for generating primary emulsion. A 5 ml aqueous solution of 1wt% PVA and 0.3wt% chitosan chloride in DIUF H₂O was prepared by following the procedure for aqueous phase as mentioned in materials and methods. The aqueous phase is analyzed for particle size and zeta potential. The particle size is found to be $D_{avg} = 15$ nm based on both volume and number. 62% of the nanoparticles based on volume and 100% of the particles based on number are found with $D_{avg} = 15$ nm. Based on volume, 38% of the particles with size in the range $192 \text{ nm} < D_{avg} < 614$ nm based on volume are observed but there are very few in number as no such range particles are observed in the number based multimodal size distribution. The comparison of the particle size distribution of this batch with that of the batch with no PVA in aqueous phase mentioned in previous section shows that smaller chitosan chloride particles are found in aqueous solution with PVA. The particle size distributions of aqueous solution of chitosan chloride without and with PVA are stated with S.No.1 and 2 respectively in Table 4.2 and are shown in Figure 4.4 and 4.5 respectively. The zeta potential of this batch is found to be 27.1 ± 1.9 mV. The decrease in the positive zeta potential compared to that of the batch with only chitosan chloride in DIUF H₂O can be explained by the presence of PVA in this batch. It is clear that broad ranged multimodal distribution of the particles is observed in the chitosan chloride solution where as much narrower distribution of particles is observed with the presence of the PVA in the solution. It can be concluded that the PVA acts as a compatibilizer of chitosan chloride.

This is confirmed by preparing 2 more batches. For this, two batches of 10ml 0.3wt% chitosan chloride in DIUF H₂O were prepared and particle size was analyzed. Two batches of 10ml 1wt% PVA in DIUF H₂O are prepared at 80⁰C and after cooled down to room temperature, each of them is added to the 10ml 0.3wt% chitosan chloride and stirred together with aid of magnetic stirrer for 15min at room temperature. The MSD of both the batches were analyzed to confirm the effect of PVA on chitosan chloride. In the absence of PVA, 0.3wt% of chitosan chloride in DIUF H₂O has with sizes in range 180 nm < D_{avg} < 222 nm and 417 nm < D_{avg} < 515 nm in first batch and 127 nm < D_{avg} < 639 nm in second batch. For both batches with PVA, much narrower distribution of particles with D_{avg}=24 nm and 89 nm < D_{avg} < 483 nm in the first and D_{avg}=11 nm in the second batch were observed. The effect of PVA on chitosan chloride in all the three batches is listed in Table 4.2.

The role of each component in generating the desired product, uniform sized cationic PLGA nanoparticles, is tested. For this, PLGA nanoparticles formation with different possible combinations of the polymers was tested. All resulting primary emulsions after sonication were diluted 100 times for testing their MSD by light scattering. This was done by diluting 0.1 ml of emulsion with 10ml of DIUF H₂O.

The importance of PVA in generation of PLGA nanoparticles was tested. First a batch of 1ml of 1wt% PLGA in EA and 5ml of 1wt% PVA in DIUF H₂O were prepared as described in materials and methods. Sonication of organic phase and aqueous phase at 30 Watt for 2 min resulted in a primary emulsion. The MSD of the diluted emulsion was analyzed. Based on volume 1%, and based on number 66% of the nanoparticles are of size D_{avg}=74 nm. In addition to that, based on volume 12% and based on number 33% of the particles in the range 134 nm < D_{avg} < 308 nm are also found in the diluted primary emulsion. This concludes that based on volume 13% and number 99% of the particles below 300 nm in size are generated using PVA as stabilizer. The size range of the particles is summarized in row 3, Table 4.3 and shown in Figure 4.11. This emulsion also has 87% of the particles in the range 894 nm < D_{avg} < 1615 nm based on volume. This indicates that the PVA generates PLGA nanoparticles with narrow size range and the performance of PVA as stabilizer for PLGA nanoparticles is proved in this batch. The zeta potential of the emulsion is obtained as -17.3±0.3 mV indicating formation of unstable anionic nanoparticles, which is not desired. The PLGA nanoparticles are required to possess a positive charge on its surface.

To test if chitosan chloride alone can produce the required stable cationic PLGA nanoparticles in the required size range, a batch of primary emulsion is prepared using only chitosan chloride in DIUF H₂O as the aqueous phase. A batch of primary emulsion is prepared same as mentioned above except for 5 ml of 0.3wt% chitosan chloride in DIUF H₂O is used instead of 5 ml of 1wt% PVA in DIUF H₂O. The aqueous phase for this batch is prepared by adding 15 mg of chitosan chloride to 5 ml of DIUF H₂O and dissolving at room temperature using a magnetic stirrer for 15 min till the chitosan chloride solution is optically clear. The MSD of 100 folds diluted primary emulsion and zeta potential of the sample are analyzed. The range of nanoparticle sizes present in the emulsion is summarized in row 4, Table 4.3 and Figure 4.12. Based on volume 9% and based on number 70% of the nanoparticles with size range 134 nm < D_{avg} < 237 nm are

observed in emulsion. Presence of 67% of the particles based on volume and 30% of the particles based on number with large size in the range of $364 \text{ nm} < D_{\text{avg}} < 645 \text{ nm}$ is observed in this batch. There are also 24% of the particles in size range $2335 \text{ nm} < D_{\text{avg}} < 3586 \text{ nm}$ based on volume in this batch. It can be observed that fewer particles with size below 300 nm are present in this batch compared to that of the previous batch, confirming the necessity of stabilizer PVA in obtaining PLGA nanoparticles of required size range. Zeta potential of $56.9 \pm 3.0 \text{ mV}$ represents formation of a highly stable emulsion and cationic particles due to presence of chitosan chloride. Summary of MSD of nanoparticles in all emulsions formed by different possible binary polymer pairs in system is presented in Table 4.3.

Table 4.2. Effect of PVA on MSD of chitosan chloride particles in DIUF H₂O.

S. No.	System	Appearance	D _v (nm) (% of particles in the range)	D _n (nm) (% of particles in the range)	Poly dispersity
1	0.3wt%chitosan chloride in DIUF H ₂ O-batch-1	Stone yellow clear	Peak 1 (91%) D _{min} =134, D _{avg} =390, D _{max} =521	Peak 1 (100%) D _{min} =134, D _{avg} =190, D _{max} =521	0.168
			Peak 2 (9%) D _{avg} =1179		
2	1wt% PVA and 0.3wt% chitosan chloride in DIUF H ₂ O-batch-1	Stone yellow clear	Peak 1 (62%) D _{min} =15, D _{avg} =15, D _{max} =15	Peak 1 (100%) D _{min} =15, D _{avg} =15, D _{max} =15	0.200
			Peak 2 (38%) D _{min} =192, D _{avg} =448, D _{max} =614		
3	0.3wt%chitosan chloride in DIUF H ₂ O-batch-2	Stone yellow clear	Peak 1 (4%) D _{min} =180, D _{avg} =196, D _{max} =213	Peak 1 (33%) D _{min} =180, D _{avg} =198, D _{max} =222	0.147
			Peak 2 (96%) D _{min} =417, D _{avg} =462, D _{max} =515		

Table 4.2(continued). Effect of PVA on MSD of chitosan chloride particles in DIUF H2O.

4	1wt% PVA in DIUF H ₂ O and 0.3wt% chitosan chloride in DIUF H ₂ O-batch-2	Light stone yellow clear	Peak 1 (39%) $D_{\min}=24, D_{\text{avg}}=24, D_{\max}=24$	Peak 1 (100%) $D_{\min}=24, D_{\text{avg}}=24, D_{\max}=24$	0.206
			Peak 2 (59%) $D_{\min}=89, D_{\text{avg}}=395, D_{\max}=483$		
			Peak 3 (2%) $D_{\min}=1672, D_{\text{avg}}=2255, D_{\max}=2678$		
5	0.3wt%chitosan chloride in DIUF H ₂ O-batch-3	Stone yellow clear	Peak 1 (97%) $D_{\min}=127, D_{\text{avg}}=458, D_{\max}=639$	Peak 1 (100%) $D_{\min}=127, D_{\text{avg}}=247, D_{\max}=639$	0.142
			Peak 2 (3%) $D_{\min}=1433, D_{\text{avg}}=1433, D_{\max}=1433$		
6	1wt% PVA in DIUF H ₂ O and 0.3wt% chitosan chloride in DIUF H ₂ O-batch-3	Light stone yellow clear	Peak 1 (72%) $D_{\min}=11, D_{\text{avg}}=11, D_{\max}=11$	Peak 1 (100%) $D_{\min}=11, D_{\text{avg}}=11, D_{\max}=11$	0.208
			Peak 2 (28%) $D_{\min}=328, D_{\text{avg}}=446, D_{\max}=593$		

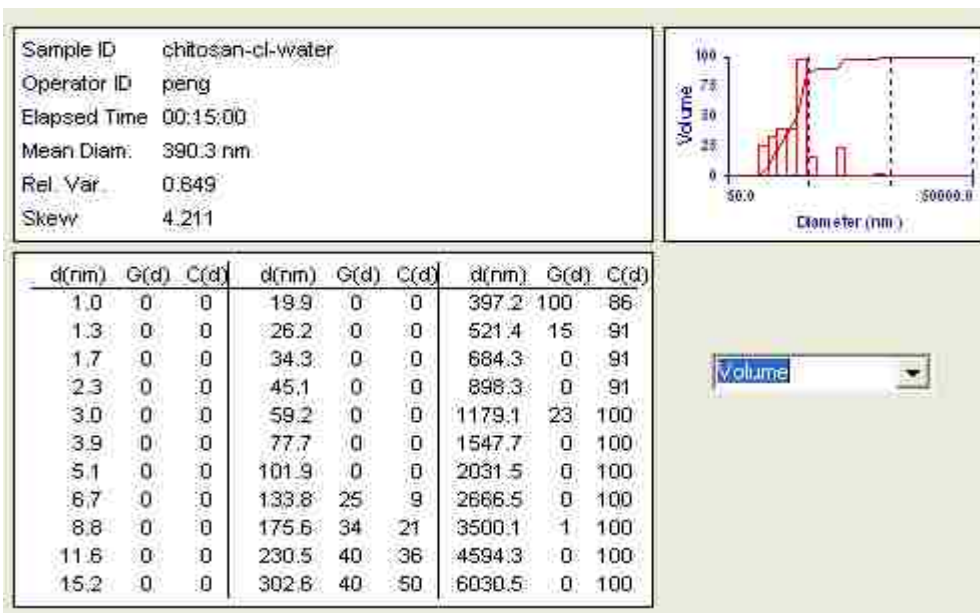


Figure 4.4. Volume based MSD of 0.3wt% chitosan chloride in DIUF H₂O – batch-1. [Table 4.2, S.No.1]

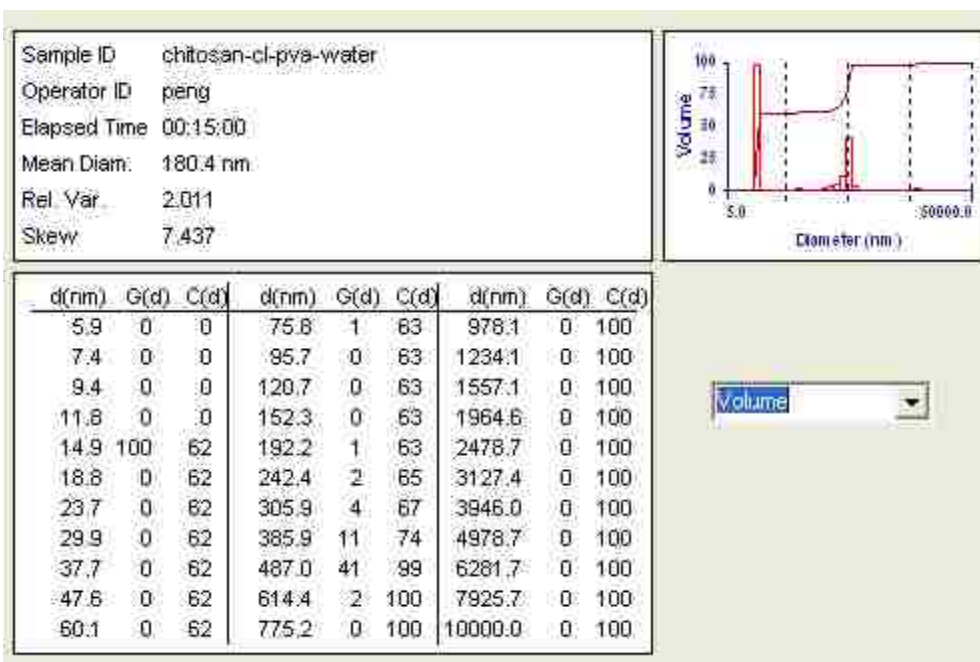


Figure 4.5. Volume based MSD of 1wt% PVA and 0.3wt% chitosan chloride in DIUF H₂O – batch-1. [Table 4.2, S.No.2]

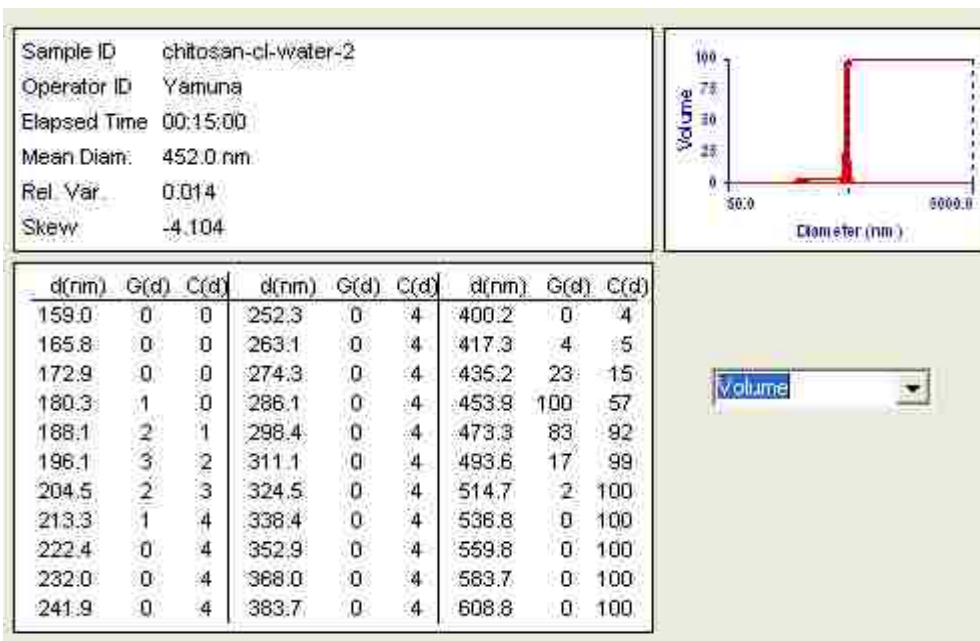


Figure 4.6. Volume based MSD of 0.3wt% chitosan chloride in DIUF H₂O – batch-2. [Table 4.2, S.No.3]

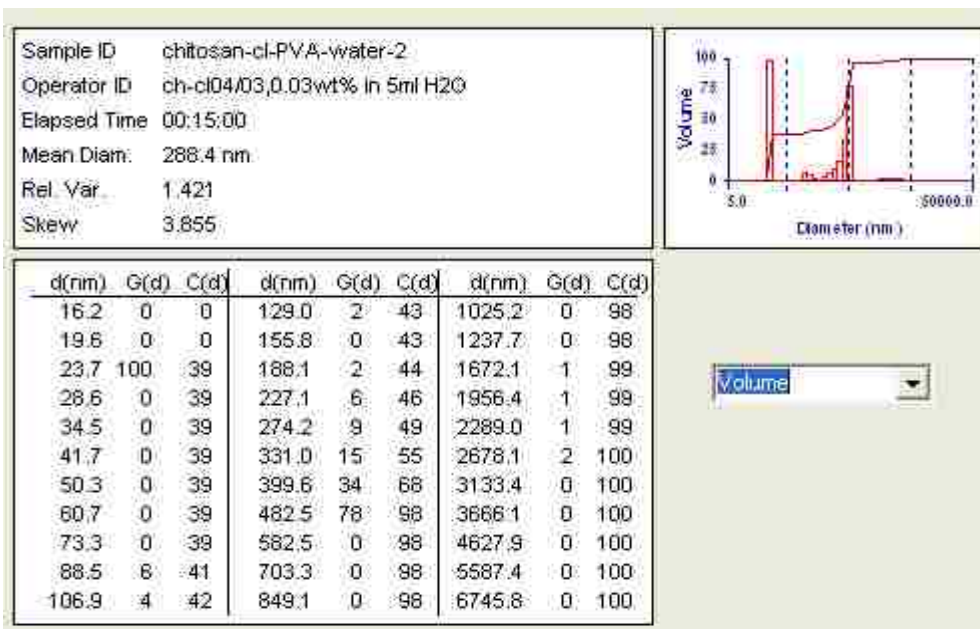


Figure 4.7. Volume based MSD of 1wt% PVA and 0.3wt% chitosan chloride in DIUF H₂O – batch -2. [Table 4.2, S.No.4]

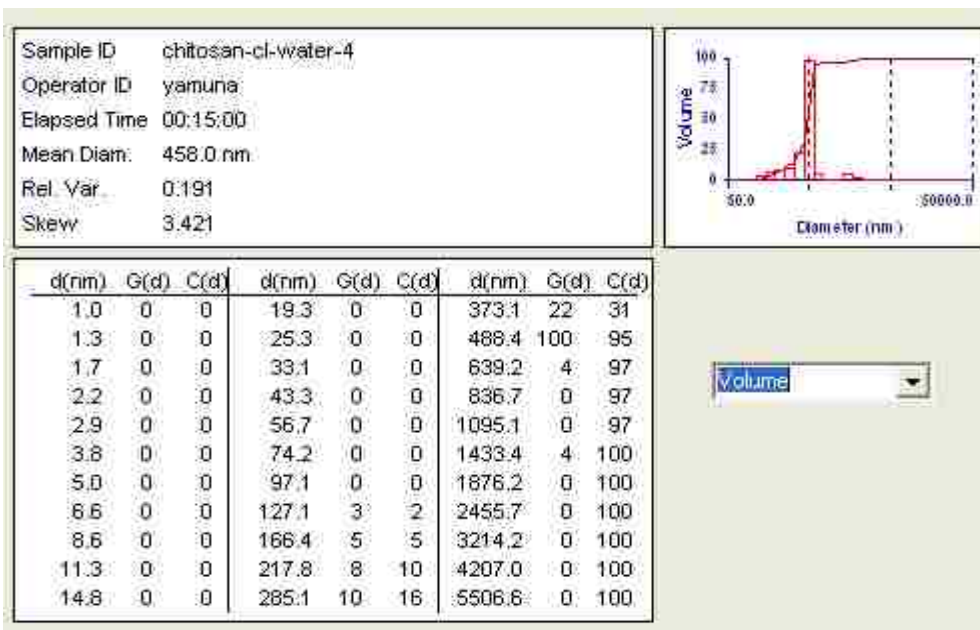


Figure 4.8. Volume based MSD of 0.3wt% chitosan chloride in DIUF H₂O – batch-3. [Table 4.2, S.No.5]

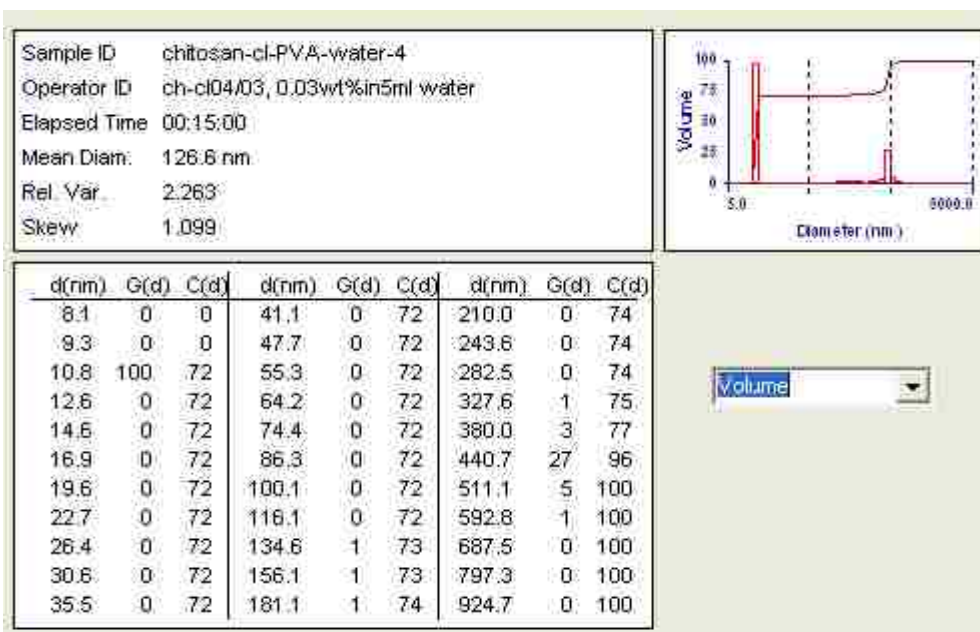


Figure 4.9. Volume based MSD of 1wt% PVA and 0.3wt% chitosan chloride in DIUF H₂O – batch -3. [Table 4.2, S.No.6]

Table 4.3. Summary of particle formation with different possible binary combinations of polymers used.

Binary polymer pairs	Emulsion method and parameters	Appearance	D _v (nm) (% of particles in the range)	D _n (nm) (% of particles in the range)	Poly dispersity	Zeta Potential (mV)
1wt% PVA and 0.3wt% chitosan chloride in DIUF H ₂ O	N/A	Clear yellow stone	Peak 1 (62%) D _{min} =15, D _{avg} =15, D _{max} =15	Peak 1 (100%) D _{min} =15, D _{avg} =15, D _{max} =15	0.200	27.1±1.9
			Peak 2 (38%) D _{min} =192, D _{avg} =448, D _{max} =614			
1ml 1wt% PLGA in EA and 5ml 1wt% PVA in DIUF H ₂ O	Sonication 30watt, 2min, room temperature.	Turbid white	Peak 1 (1%) D _{min} =74, D _{avg} =74, D _{max} =74	Peak 1 (66%) D _{min} =74, D _{avg} =74, D _{max} =74	0.313	-17±0.3
			Peak 2 (12%) D _{min} =134, D _{avg} =210, D _{max} =308	Peak 2 (33%) D _{min} =134, D _{avg} =189, D _{max} =308		
			Peak 3 (87%) D _{min} =894, D _{avg} =1199, D _{max} =1615	Peak 3 (1%) D _{avg} =1133		

Table 4.3 (continued). Summary of particle formation with different possible binary combinations of polymers used.

1ml 1wt% PLGA in EA and 5ml 0.3wt % chitosan chloride in DIUF H2O	Sonication 30watt, 2min, room temperature.	Turbid light yellow	Peak 1 (9%) $D_{\min}=134, D_{\text{avg}}=184, D_{\max}=237$	Peak 1 (70%) $D_{\min}=134, D_{\text{avg}}=171, D_{\max}=237$	0.306	56.9±3.0
			Peak 2 (67%) $D_{\min}=364, D_{\text{avg}}=474, D_{\max}=645$			
			Peak 3 (24%) $D_{\min}=2335, D_{\text{avg}}=2696, D_{\max}=3586$	Peak 2 (30%) $D_{\min}=364, D_{\text{avg}}=461, D_{\max}=559$		

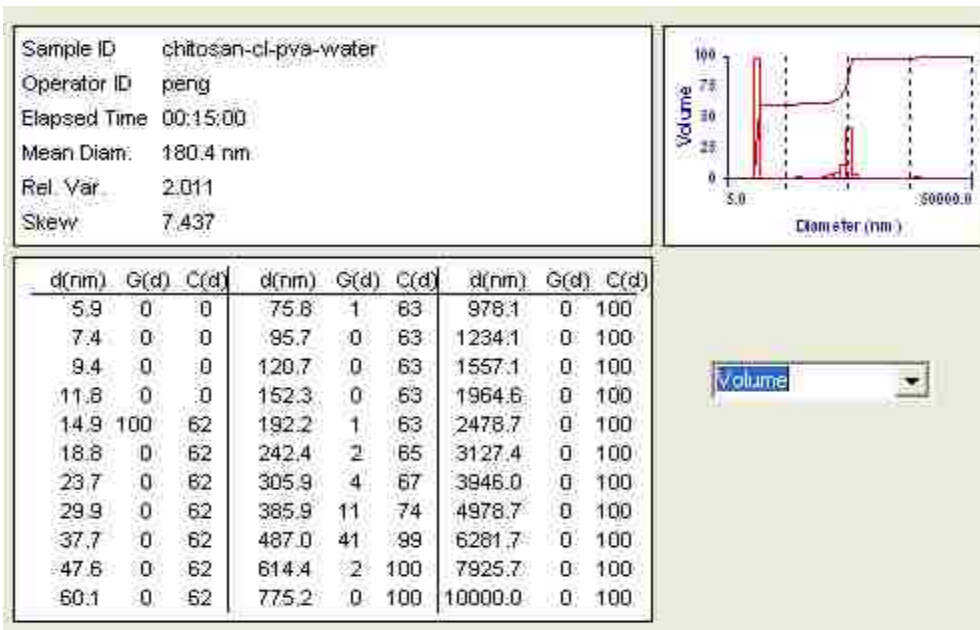


Figure 4.10. Volume based MSD of 1wt% PVA and 0.3wt% chitosan chloride in DIUF H2O. [Table 4.3, row 2]

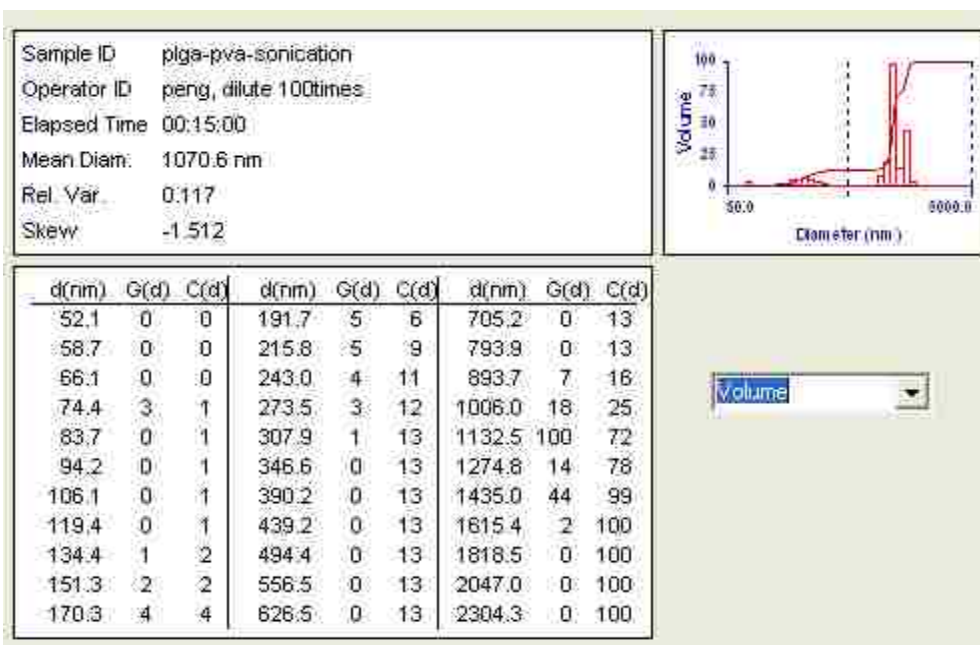


Figure 4.11. Volume based MSD of nanoparticles formed by 1 ml 1wt% PLGA in EA emulsified in 5 ml aqueous solution of 1wt% PVA. [Table 4.3, row 3]

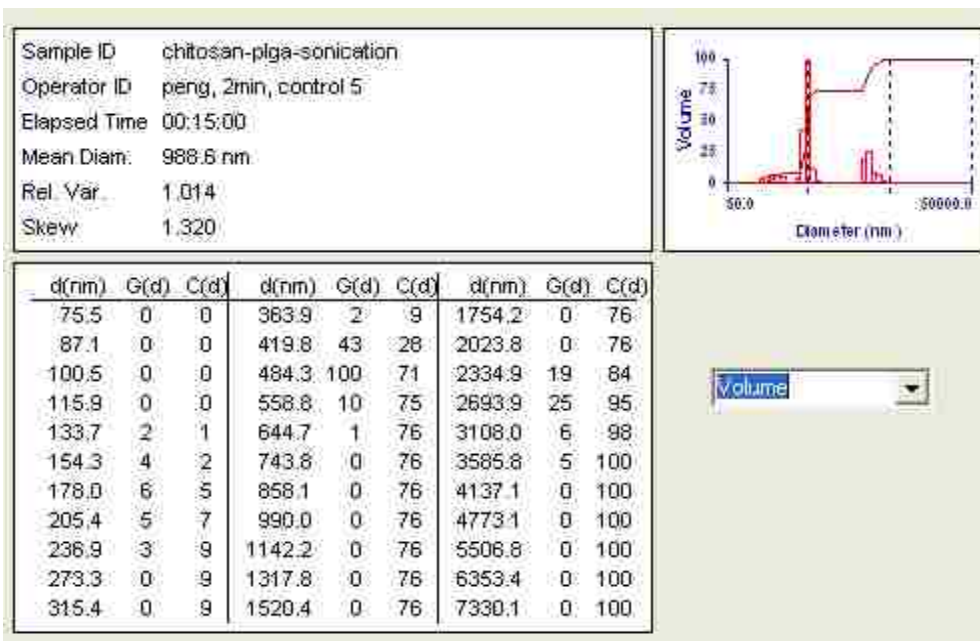


Figure 4.12. Volume based MSD of nanoparticles formed by 1 ml solution of 1wt% PLGA in EA emulsified in 5 ml aqueous solution of 0.3wt% chitosan chloride. [Table 4.3, row 4]

Emulsion formed by the ternary polymer system

From the above two batches it is observed that the combined effect of both PVA and chitosan chloride is required for generating the desired product. A batch of materials was prepared by using all the three polymers to test the combined effect of PVA and chitosan on PLGA nanoparticle formation. First 1 ml of organic phase and 5 ml of aqueous phase were prepared as mentioned in materials and methods section. Organic phase was added to aqueous phase and sonicated for 2 min at 30watt. The diluted emulsion was analyzed for MSD and it was found that 6% of the particles based on volume and 92% of the particles based on number are with size range $74 \text{ nm} < D_{\text{avg}} < 108 \text{ nm}$. Based on volume 8% of the particles and based on number 6% of the particles in size range $177 \text{ nm} < D_{\text{avg}} < 291 \text{ nm}$ are present in the emulsion indicating that majority of them are less than 300 nm based on number and the results are shown in row 2, Table 4.4. Based on volume, 58% of the particles and 28% of the particles are found with larger size in the range of $477 \text{ nm} < D_{\text{avg}} < 784 \text{ nm}$ and $1137 \text{ nm} < D_{\text{avg}} < 1867 \text{ nm}$ as shown in Figure 4.13. The zeta potential of the resulting primary emulsion was found to be $30.1 \pm 2.2 \text{ mV}$ representing cationic particles with good stability in emulsion. One more batch with all the three polymers is prepared to check the reproducibility of the results obtained. Based on volume 10%, and based on number 90% of the nanoparticles in this batch are of size in the range of $154 \text{ nm} < D_{\text{avg}} < 223 \text{ nm}$ with a zeta potential of $42.1 \pm 1.0 \text{ mV}$ and are presented in row 3, Table 4.4. 90% of the particles based on volume and 10% of the particles in this batch based on number are in the size range nearly 700 nm – 1000 nm. The two batches confirm the generation of the cationic PLGA nanoparticles in the required range starting from the individual polymeric solutions.

Table 4.4. Summary of particle formation in the ternary polymer system used.

Ternary polymer system	Emulsion method and parameters	Appearance	D _v (nm) (% of particles in the range)	D _n (nm) (% of particles in the range)	Poly dispersity	Zeta Potential (mV)
1ml 1wt% PLGA in EA and 5ml 1wt% PVA , 0.3wt% chitosan chloride in DIUF H2O- batch-1	Sonication 30watt, 2min, room temperature.	Turbid yellow	Peak 1 (6%) D _{min} =74, D _{avg} =87, D _{max} =108	Peak 1 (92%) D _{min} =74, D _{avg} =83, D _{max} =108	0.275	30.1±2.2
			Peak 2 (8%) D _{min} =177, D _{avg} =236, D _{max} =291	Peak 2 (6%) D _{min} =177, D _{avg} =220, D _{max} =291		
			Peak 3 (58%) D _{min} =477, D _{avg} =705, D _{max} =784	Peak 3 (1%) D _{avg} =477		
			Peak 4 (28%) D _{min} =1137, D _{avg} =1450, D _{max} =1867	Peak 3 (1%) D _{avg} =784		

Table 4.4(continued). Summary of particle formation in the ternary polymer system used.

1ml 1wt% PLGA in EA and 5ml 1wt% PVA , 0.3wt% chitosan chloride in DIUF H2O- batch-2	Sonication 30watt, 2min, room tempera- ture.	Turbid yellow	Peak 1 (10%) $D_{min}=154, D_{avg}=185, D_{max}=223$	Peak 1 (90%) $D_{min}=154, D_{avg}=181, D_{max}=223$	0.272	42.1±1.0
			Peak 2 (90%) $D_{min}=717, D_{avg}=805, D_{max}=1033$	Peak 2 (10%) $D_{min}=717, D_{avg}=796, D_{max}=960$		

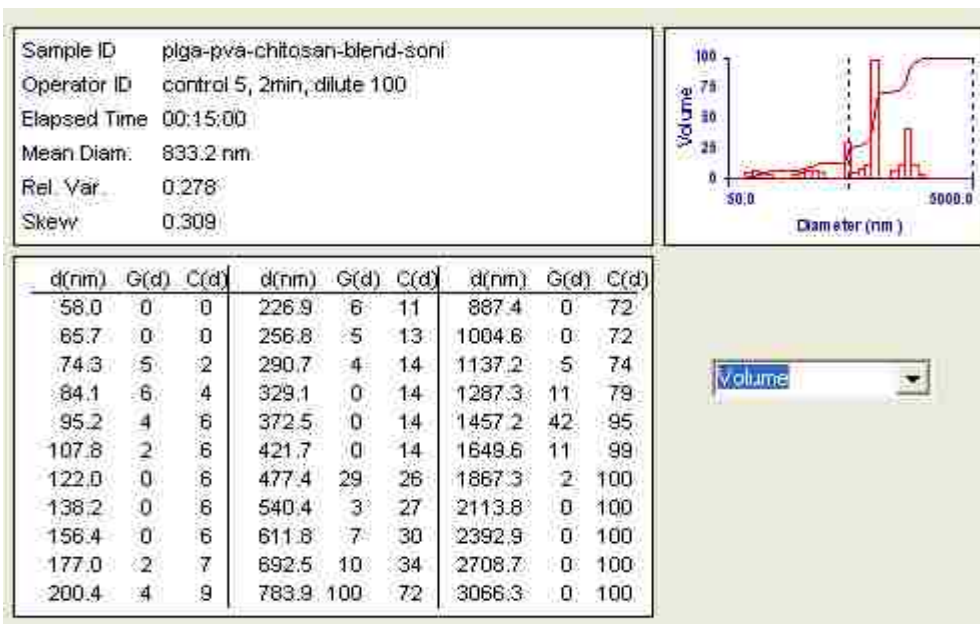


Figure 4.13. Volume based MSD of nanoparticles formed by 1 ml 1wt% PLGA in EA emulsified in 5 ml of 1wt% PVA and 0.3wt% chitosan chloride in DIUF H₂O. [Table 4.4, row 2]

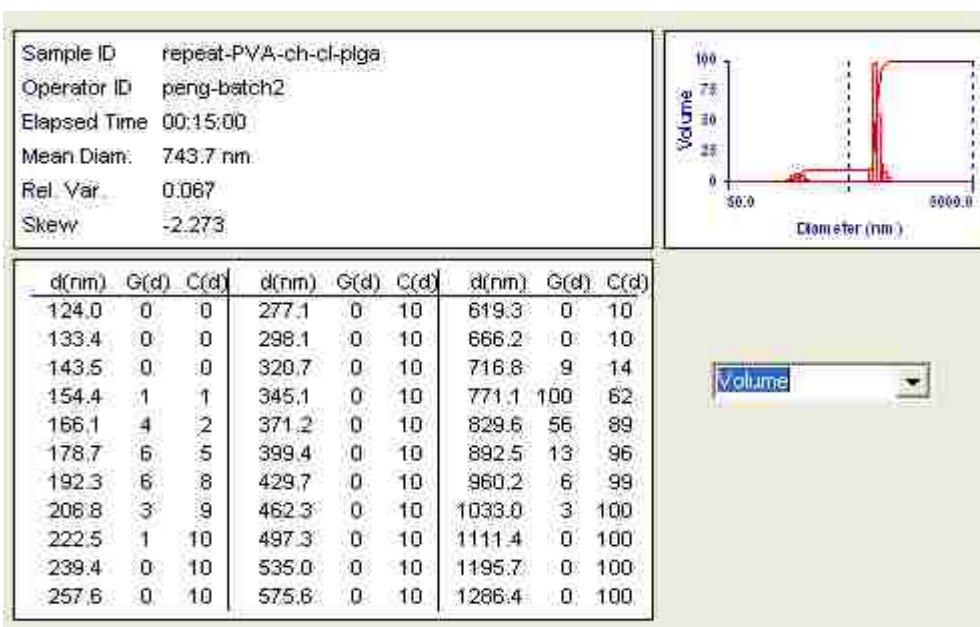


Figure 4.14. Volume based MSD of 2nd batch of nanoparticles formed by 1 ml 1wt% PLGA in EA emulsified in 5 ml aqueous solution of 1wt% PVA and 0.3wt% chitosan chloride. [Table 4.4, row 3]

Synthesis of cationic PLGA nanoparticles

Preliminary work

One batch of PLGA nanoparticles is prepared following a similar procedure as that described by Kumar et al (19). Organic phase is prepared by adding 400 mg of PLGA (2 wt %) to 20 ml EA under stirring at 1000rpm for 2 hr at room temperature. Aqueous phase is prepared by adding 200 mg of PVA (1 wt %), in 20 ml DIUF H₂O and stirring at 1000rpm for 2 hrs at 80⁰C. After it is cooled down to room temperature, 60mg of chitosan chloride (0.3 wt %) is added to the aqueous phase and stirred till all the chitosan chloride is completely dissolved. Both the organic and aqueous phases are filtered using a 4 – 8 µm filter paper to remove any dust if present in both solutions. Only in this batch, ratio of organic phase to aqueous phase is 1:1. Organic phase is slowly added drop wise using a glass pipette into aqueous phase under stirring at 1000 rpm. After the completion of adding of one phase into another, stirring of this primary oil – in – water emulsion at 1000rpm is continued for 3 hrs. This emulsion is homogenized at 9600rpm for 10min using SILVERSON L4RT. The homogenized primary emulsion is added drop by drop using a pipette into 40ml DIUF H₂O under stirring at 1000 rpm resulting in the formation of a secondary emulsion. Secondary emulsion is stirred over night to evaporate the organic solvent leading to the nanoparticles formation.

Nanoparticles with particle size 2271 nm based on volume and 1436 nm based in number are obtained and are much higher than expected. These particles have a polydispersity of 0.185. A polymer film at the top of the liquid and precipitation at the bottom of the beaker is observed indicating lot of wastage of materials. So the concentrations of chemicals are lowered in the following synthesis processes. To decrease the PLGA nanoparticle size the concentration of the stabilizer PVA is increased by changing ratio of organic to aqueous phase to 1:5.

Effect of static mixer on size of nanoparticles

Static mixer could be used for different mixing problems associated with the nanoparticle formation, such as in further size reduction of the polymer droplets of primary emulsion or in diffusion step for generating secondary oil-in-water emulsion. In this section, the nanoparticles synthesis process is focused on using static mixer for the reduction of droplet size of primary emulsion. One batch of PLGA nanoparticles synthesis is carried out with initial homogenization to generate a primary emulsion similar to that stated in the literature. Then subsequent use of static mixer multiple times is done to test the role of static mixer in decreasing polymer droplet size.

First 1wt% PLGA in 10ml ethyl acetate and 1 wt% PVA, 0.3 wt% chitosan chloride in 50 ml of DIUF H₂O is prepared as described in materials and methods. Organic phase is added to aqueous phase in a beaker and homogenized at 9600 rpm for 10 min resulting in the formation of emulsion. The size of the nanoparticles is measured by taking a small sample of the emulsion out and diluting 100 times. In this case 0.1 ml of the emulsion is diluted with 10 ml water for particle size measurement and the corresponding results are assigned S.No.1 in Table 4.5. The correlation function of the sample is not good and is as shown in the Figure 4.15. An example of good correlation function, baseline index and average count rate are shown for 0.3 wt% chitosan chloride in DIUF H₂O in Figure 4.16.

The baseline index is obtained as zero for this sample. So, the MSD with dust filter on is considered for this set of results. The percentage of data retained after switching on the dust filter is mentioned for each sample in the brackets in Table 4.5.

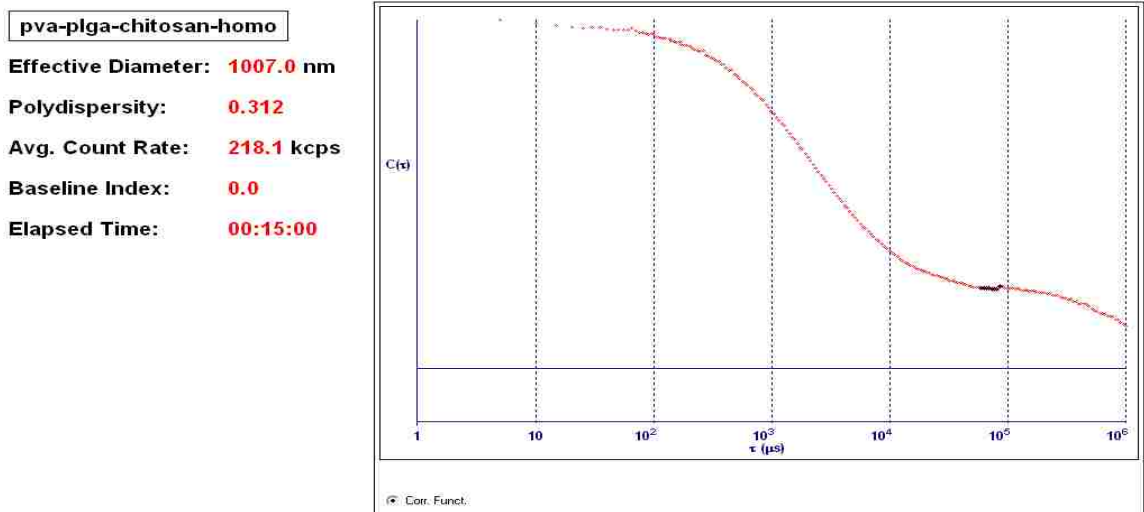


Figure 4.15. Correlation function of nanoparticles in 100 times dilute primary emulsion from homogenization of 10ml organic phase and 50ml of aqueous phase. [Table 4.5, S.No.1]

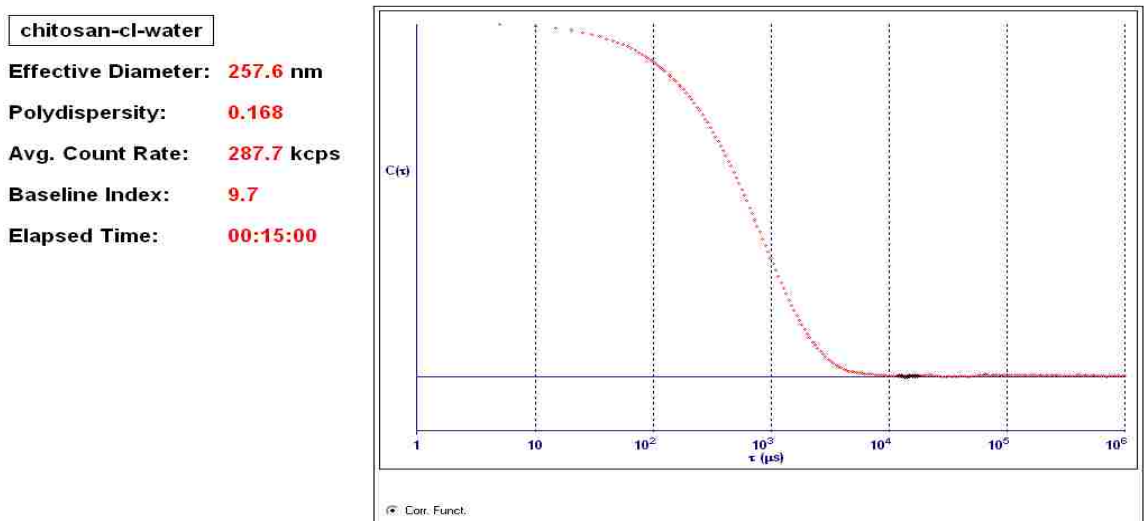


Figure 4.16. Correlation function of 0.3wt% chitosan chloride in DIUF H2O [Table 4.1, row 3]

Based on volume 4% and based on number 76% of the particles in this batch are of size in the range $91 \text{ nm} < D_{\text{avg}} < 204 \text{ nm}$. The size range of $332 \text{ nm} < D_{\text{avg}} < 747 \text{ nm}$ is found among 91% of nanoparticles based on volume and 24% of the nanoparticles based on number. The original emulsion is fed thrice through the static mixer at 135 ml/min speed. The size of the nanoparticles is tested again as mentioned earlier by taking a small sample out and the results are presented with S.No.2 in Table 4.5. Based on volume 11% and based on number 97% of the nanoparticles are in size range of $191 \text{ nm} < D_{\text{avg}} < 305 \text{ nm}$. The size range of 1200nm – 2000nm is found among nearly 89% of the nanoparticles based on volume and 3% of the nanoparticles based on number in this batch. The emulsion is again pumped through the static mixer at the same speed three more times and the size of the nanoparticles is measured one more time. The results obtained are summarized with S.No.3 in Table 4.5. Based on volume 1% and based on number 75% of the nanoparticles are with size $D_{\text{avg}}=83 \text{ nm}$ in this batch. The size range of $168 \text{ nm} < D_{\text{avg}} < 268 \text{ nm}$ is found among nearly 6% of the nanoparticles based on volume and 23% of the nanoparticles based on number in this batch. Based on volume 93% of the nanoparticles are in the size range of 1000nm – 2000nm. There is no decrease in the average particle size and no fixed pattern of size reduction of secondary emulsion is observed with increase in the number of primary emulsion passes through the static mixer. The nanoparticle size is not in the expected range so an alternate method to generate a primary emulsion is employed in next batch. In addition, large quantity of chemicals involved in primary emulsion generation using homogenization, forced to search for an effective alternate method to generate primary emulsion that needs only small quantity of chemicals.

Table 4.5. Nanoparticle size obtained by using homogenizer for primary emulsion and subsequent use of static mixer for particle size reduction.

S. No	Emulsion method	Parameters	Appearance	D_v (nm) (% of particles in the range)	D_n (nm) (% of particles in the range)	Poly dispersity
1.	Homogenization	9600rpm, 10min homogenizer.	Turbid yellow	Peak 1 (4%) $D_{min}=91, D_{avg}=128, D_{max}= 174$ (dust filter 43.9%)	Peak 1 (76%) $D_{min}=91, D_{avg}=111, D_{max}= 204$ (dust filter 43.9%)	0.289
				Peak 2 (91%) $D_{min}=332, D_{avg}=484, D_{max}=747$	Peak 2 (24%) $D_{min}=332, D_{avg}=465, D_{max}=747$	
				Peak 3 (5%) $D_{min}=2324, D_{avg}=2626, D_{max}=3214$		
2.	Homogenization followed by static mixer	9600rpm, 10min homogenizer. 3 times through static mixer at135ml/min.	Turbid yellow	Peak 1 (11%) $D_{min}=191, D_{avg}=246, D_{max}=305$ (52%)	Peak 1 (97%) $D_{min}=191, D_{avg}=237, D_{max}= 305$ (52%)	0.346
				Peak 2 (89%) $D_{min}=1238, D_{avg}=1493, D_{max}=1975$	Peak 2 (3%) $D_{min}=1238, D_{avg}=1453, D_{max}=1799$	

Table 4.5 (continued). Nanoparticle size obtained by using homogenizer for primary emulsion and subsequent use of static mixer for particle size reduction.

3.	Homogenization followed by static mixer	9600rpm, 10min homogenizer. 6 times through static mixer at 135ml/min.	Turbid yellow	Peak 1 (1%) D _{avg} =83 (49.4%)	Peak 1 (75%) D _{avg} =83 (49.4%)	0.361
				Peak 2 (6%) D _{min} =168, D _{avg} =216, D _{max} =268	Peak 2 (23%) D _{min} =168, D _{avg} =207, D _{max} =268	
				Peak 3 (93%) D _{min} =1086, D _{avg} =1362, D _{max} =1945	Peak 3 (1%) D _{avg} =1086	

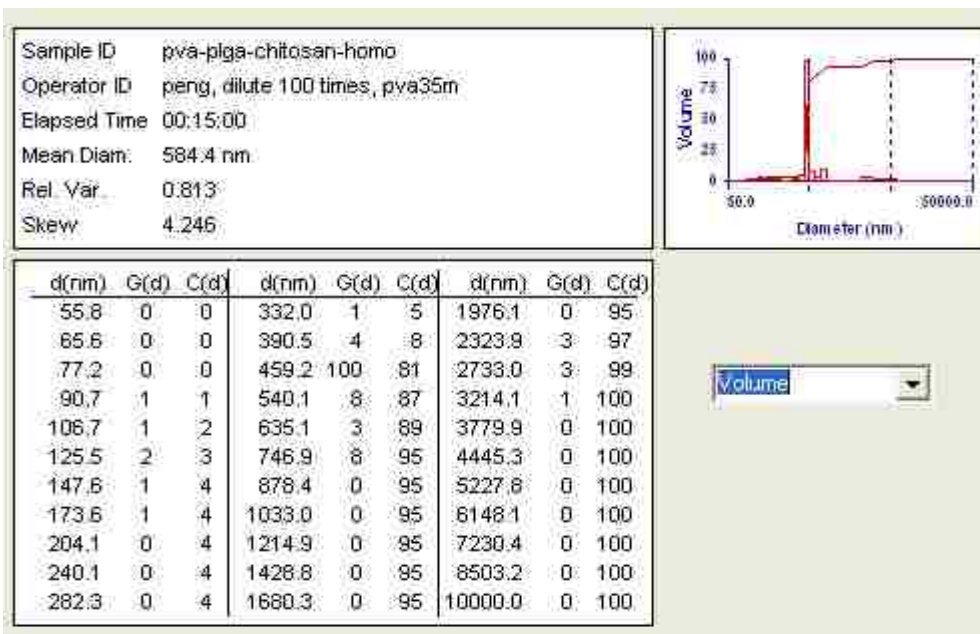


Figure 4.17. Volume based MSD of nanoparticles in 100 times dilute primary emulsion from homogenization of 10ml organic phase and 50ml of aqueous phase. [Table 4.5, S.No.1]

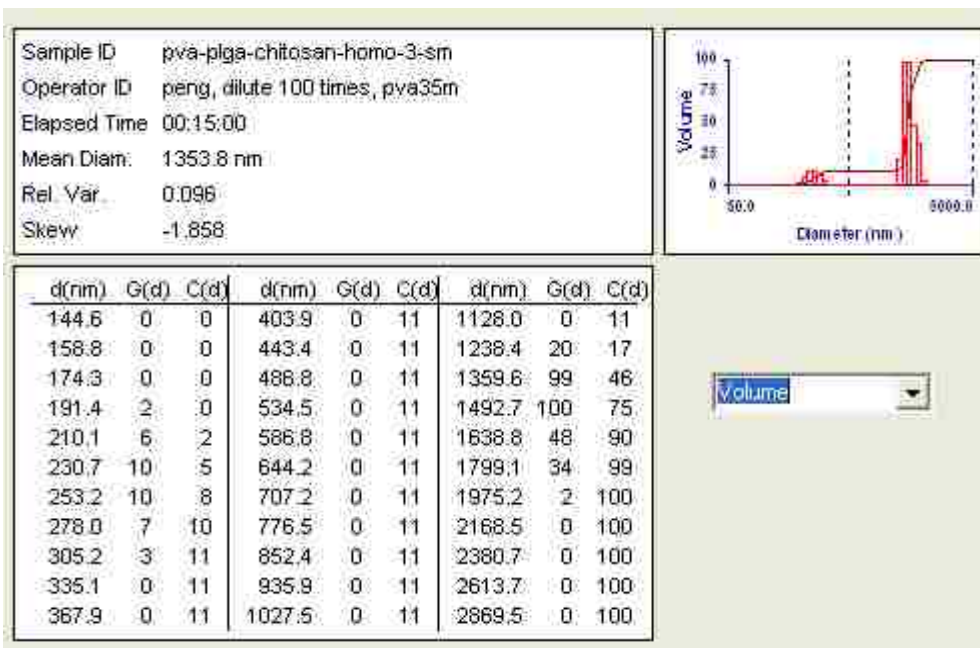


Figure 4.18. Volume based MSD in 100 times diluted emulsion from homogenization of 10ml of organic and 50ml of aqueous phase and subsequently processing 3 times through static mixer at 135ml/min. [Table 4.5, S.No.2]

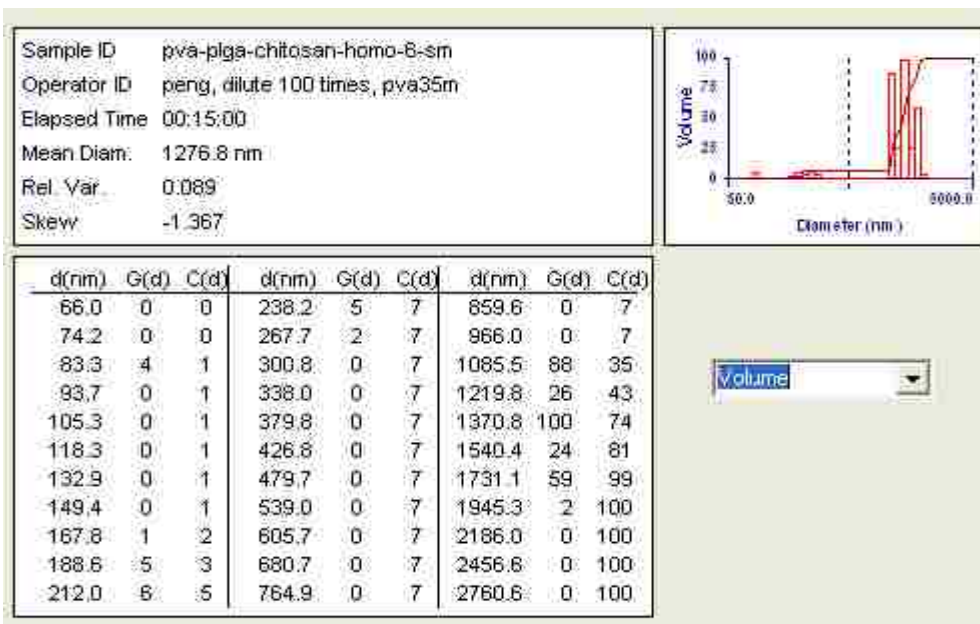


Figure 4.19. Volume based MSD in 100 times diluted emulsion from homogenization of 10ml of organic and 50ml of aqueous phase and subsequently processing 6 times through static mixer at 135ml/min. [Table 4.5, S.No.3]

Sonication and Homogenization

As the homogenization requires minimum 60ml of raw material for each batch as rotor head is to be completely immersed, in order to save the chemicals an equally efficient technique for emulsion generation, sonication which needs only 6ml raw material for each batch is considered for generating primary emulsion. Homogenization is used for diffusion step as enough quantity is present for 1:10 or 1:100 dilution ratio. Primary emulsion is generated by sonicating 1ml of an organic phase and 5 ml of aqueous phase in a vial bottle. For secondary emulsion, a beaker containing 100 ml of DIUF H₂O is placed at centre under rotor of SILVERSON L4RT and switched on. The speed of the rotor is gradually increased to 9600 rpm and 1 ml of the primary emulsion is added drop by drop by a glass pipette into the beaker containing 100ml DIUF H₂O so that the dilution ratio is 1:100. The stirring is continued for 10min after the completion of adding primary emulsion. The size distribution of the generated PLGA nanoparticles in the resulting secondary emulsion is measured and is shown in S.No.1 of Table 4.6. Based on volume 6% of the nanoparticles and based on number 93% of the nanoparticles of this batch are in the size range of 69 nm<D_{avg}<114 nm. Based on volume 12% of the nanoparticles and based on number 7% of the nanoparticles are in the size range of 189 nm<D_{avg}<355 nm. Also in this batch, based on volume, 82% of nanoparticles are of size range 1100 – 2100nm. Second batch is repeated with the same procedure but the primary emulsion is added very slowly to the beaker containing DIUF H₂O with the pipette tip placed inside nearly at the bottom of the liquid. The particle size obtained by employing this procedure is summarized with S.No.2 in Table 4.6. Based on volume 10% of the nanoparticles and based on number 95% of the nanoparticles of this batch are in the size range of 163 nm<D_{avg}<246 nm. Based on volume 90% of the nanoparticles and based on number 5% of the nanoparticles nearly with a size range of 850 nm<D_{avg}<1300 nm are

also found in this batch. One more batch is repeated same as the second batch mentioned above, but with a dilution ratio of 1:10. The particle size distribution of nanoparticles of this batch is summarized in row with S.No.3 of Table 4.6. Based on volume 4% of the nanoparticles and based on number 90% of the nanoparticles of this batch are with size $D_{avg}=65$ nm. Based on volume 77% and 19% of the nanoparticles with a broad size range of $172 \text{ nm} < D_{avg} < 865 \text{ nm}$ and $1940 \text{ nm} < D_{avg} < 3703 \text{ nm}$ respectively are also found in this batch. But based on number nearly all the remaining 9% of the nanoparticles are in the size range $202 \text{ nm} < D_{avg} < 385 \text{ nm}$.

Presence of good number of nanoparticles with size below and around 300nm based on volume and number in first two batches prepared by this process was observed. These results show that a combination of sonication and homogenization result in PLGA nanoparticles with preferred particle size range. The batch with dilution rate 1:10 does not contain good number of nanoparticles in desired range as compared to that of the first two batches with 1:100 dilution ratio. This is because of chances of comparatively more agglomeration with dilution rate 1:10 than with that of 1:100.

Table 4.6. Particle sizes obtained by using sonication for primary emulsion and homogenization for secondary emulsion generation.

S.No.	Secondary emulsion method	Dilution times	D _v (nm) (% of particles in the range)	D _n (nm) (% of particles in the range)	Poly dispersity
1	Homogenization (9600rpm,10min)	100	Peak 1 (6%) D _{min} =69, D _{avg} =84, D _{max} =114	Peak 1 (93%) D _{min} =69, D _{avg} =79, D _{max} =114	0.288
			Peak 2 (12%) D _{min} =189, D _{avg} =258, D _{max} =355	Peak 2 (7%) D _{min} =189, D _{avg} =232, D _{max} =313	
			Peak 3 (82%) D _{min} =1106, D _{avg} =1370, D _{max} =2079		
2	Homogenization (9600rpm,10min)	100	Peak 1 (10%) D _{min} =163, D _{avg} =201, D _{max} =246	Peak 1 (95%) D _{min} =163, D _{avg} =188, D _{max} =246	0.315
			Peak 2 (90%) D _{min} =853, D _{avg} =1060, D _{max} =1291	Peak 2 (5%) D _{min} =853, D _{avg} =1042, D _{max} =1188	

Table 4.6 (continued). Particle sizes obtained by using sonication for primary emulsion and homogenization for secondary emulsion generation.

3	Homogenization (9600rpm,10min)	10	Peak 1 (4%) $D_{avg}=65$	Peak 1 (90%) $D_{avg}=65$	0.250
			Peak 2 (77%) $D_{min}=172, D_{avg}=554, D_{max}=865$	Peak 2 (9%) $D_{min}=202, D_{avg}=261, D_{max}=385$	
			Peak 3 (19%) $D_{min}=1940, D_{avg}=2576, D_{max}=3703$		

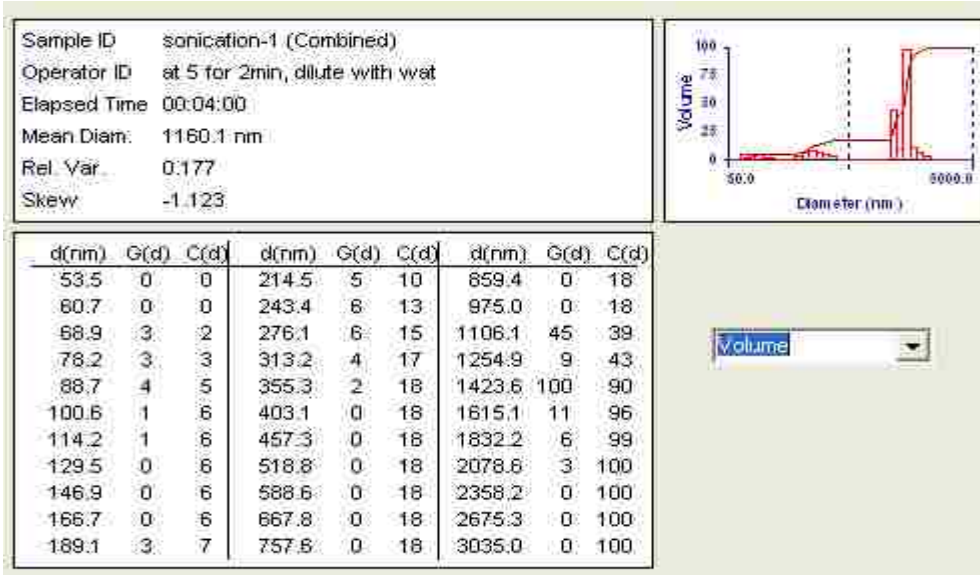


Figure 4.20. Volume based MSD in secondary emulsion generated by homogenization at dilution rate 1:100 of primary emulsion formed by sonication of 1ml 1wt% PLGA in EA and 5ml of 1wt% PVA and 0.3wt% chitosan chloride aqueous solution. [Table 4.6, S.No.1]

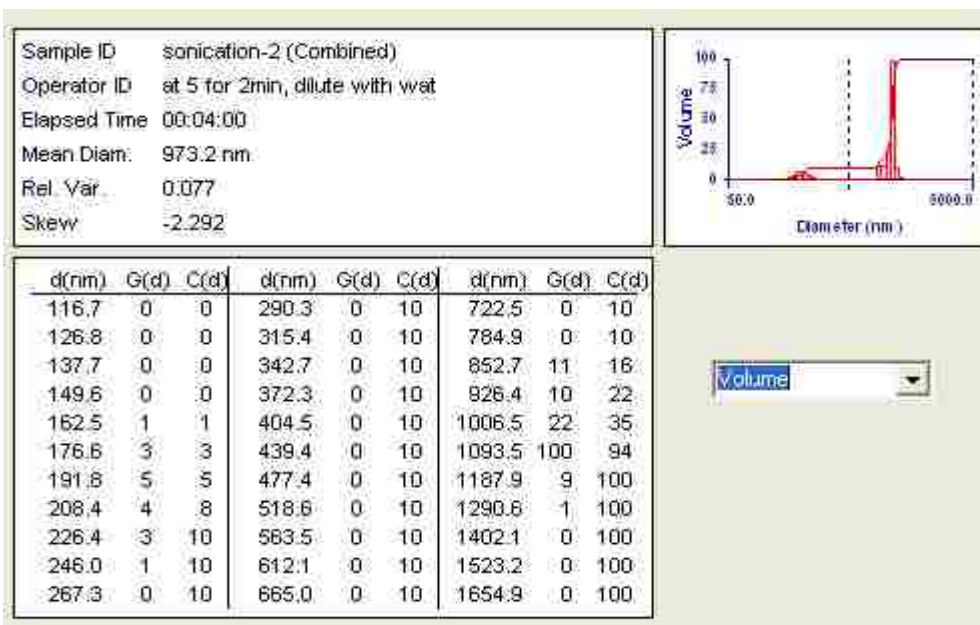


Figure 4.21. Volume based MSD in secondary emulsion generated by homogenization at dilution rate 1:100 of primary emulsion formed by sonication of 1ml 1wt% PLGA in EA and 5ml of 1wt% PVA and 0.3wt% chitosan chloride aqueous solution. [Table 4.6, S.No.2]

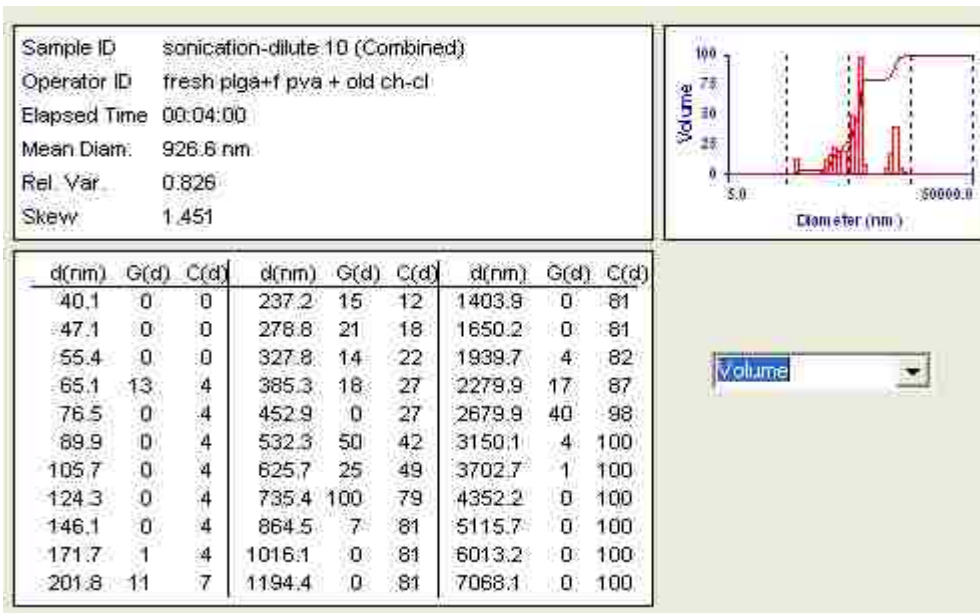


Figure 4.22. Volume based MSD in secondary emulsion generated by homogenization at dilution rate 1:10 of primary emulsion formed by sonication of 1ml 1wt% PLGA in EA and 5ml of 1wt% PVA and 0.3wt% chitosan chloride aqueous solution. [Table 4.6, S.No.3]

Dilution effect on the size of the particles

The effect of dilution ratio on the size of PLGA nanoparticles is examined. As the sonication followed by homogenization resulted in good PLGA nanoparticles, the effect of dilution on the nanoparticle size is tested using this technique. Batches with different dilution ratios of primary emulsion are made to test the effect of dilution ratio on the particle size of PLGA nanoparticles. First 1ml of organic phase and 5 ml of aqueous phase is sonicated for 2 min resulting in formation of primary emulsion. This emulsion is diluted at different ratios under stirring at 9600 rpm using SILVERSON L4RT as described in the previous two batches. Initially, 0.5 ml of primary emulsion is diluted 100 times with 50 ml of DIUF H₂O as described previously resulting in the formation of secondary emulsion. Then 5 ml of the primary emulsion is diluted 10 times with 50 ml of DIUF H₂O following the same procedure as described previously resulting in the formation of secondary emulsion. This secondary emulsion is further used to generate emulsions with different dilutions. An emulsion with total dilution ratio of 30 times is prepared by adding 30 ml of the secondary emulsion to 52 ml of DIUF H₂O as described previously. Similarly emulsions with total dilution ratios of 66, 88, and 100 are prepared by adding 10 ml, 8.6 ml, and 6 ml of secondary emulsion to 50ml, 54ml, and 48.5ml of DIUF H₂O respectively. The above procedure is repeated multiple times to get at least 3 values for average size of PLGA nanoparticles for each dilution rate. The particle size of the PLGA nanoparticles in the resulting emulsions is measured. The results are summarized in Table 4.7, Figure 4.1 (a) and (b).

All the volume and number based MSDs of this subsection are included in the appendix of the report. It can be concluded from Figures 4.1 (a) and (b) that there is no much

difference in the particle size because of dilution. However, the particle size of the 65 times dilution studies have very small particle size distributions, suggesting that this dilution rate provides a stable production on nanoparticles.

Table 4.7. Summary of dilution ratio effect on the PLGA nanoparticle particle size.

S. No.	Dilution times	Repetition times	Particle size (mean, nm)		Poly dispersity	Average particle size		Standard deviation of diameters	
			D _v (nm)	D _n (nm)		D _v (nm)	D _n (nm)	D _v (nm)	D _n (nm)
1.	11	4	296.0	159.3	0.250	274.4	132.8	18.4	17.9
			279.9	121.7	0.340				
			269.6	122.3	0.322				
			252.1	127.8	0.274				
2.	30	3	277.5	126.8	0.318	265.4	126.6	29.5	16.3
			287.0	142.8	0.282				
			231.8	110.3	0.301				
3.	66	3	247.9	121.4	0.289	245.0	111.3	2.6	8.8
			244.5	105.6	0.343				
			242.7	106.9	0.334				

Table 4.7 (continued). Summary of dilution ratio effect on the PLGA nanoparticle particle size.

4.	88	4	232.2	107.6	0.312	279.9	140.5	43.9	38.8
			277.0	127.4	0.315				
			272.0	130.2	0.298				
			338.5	196.6	0.218				
5.	100	3	284.7	136.7	0.297	307.3	166.4	46.7	52.4
			276.2	135.5	0.288				
			361.0	226.9	0.187				

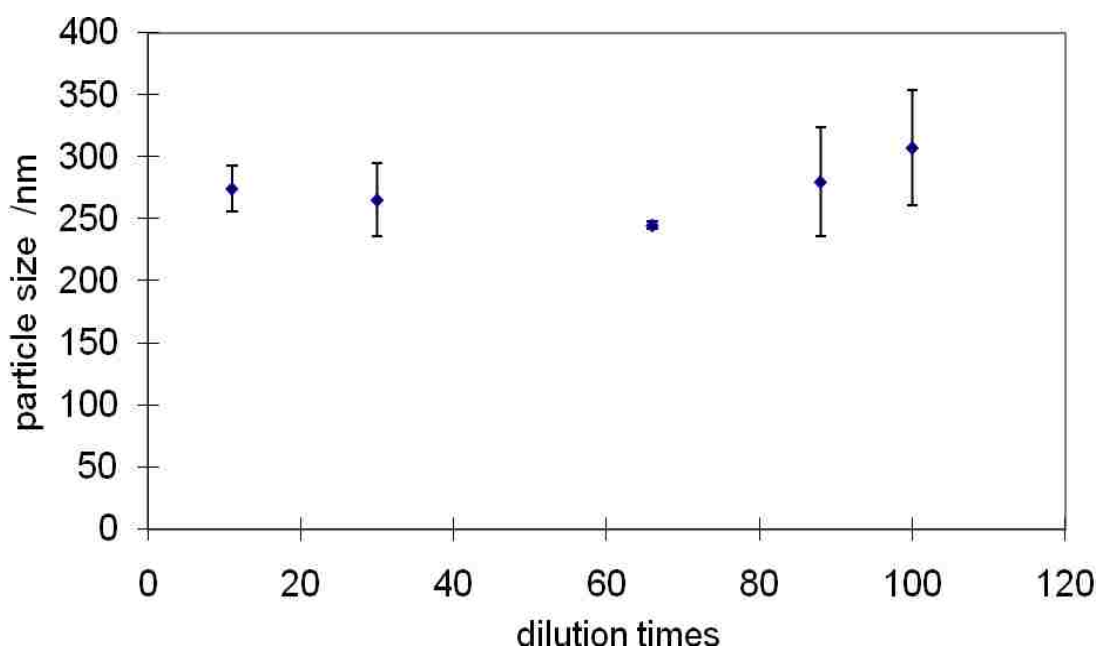


Figure 4.23. Effect of dilution ratio on volume based particle size distribution of PLGA nanoparticles.

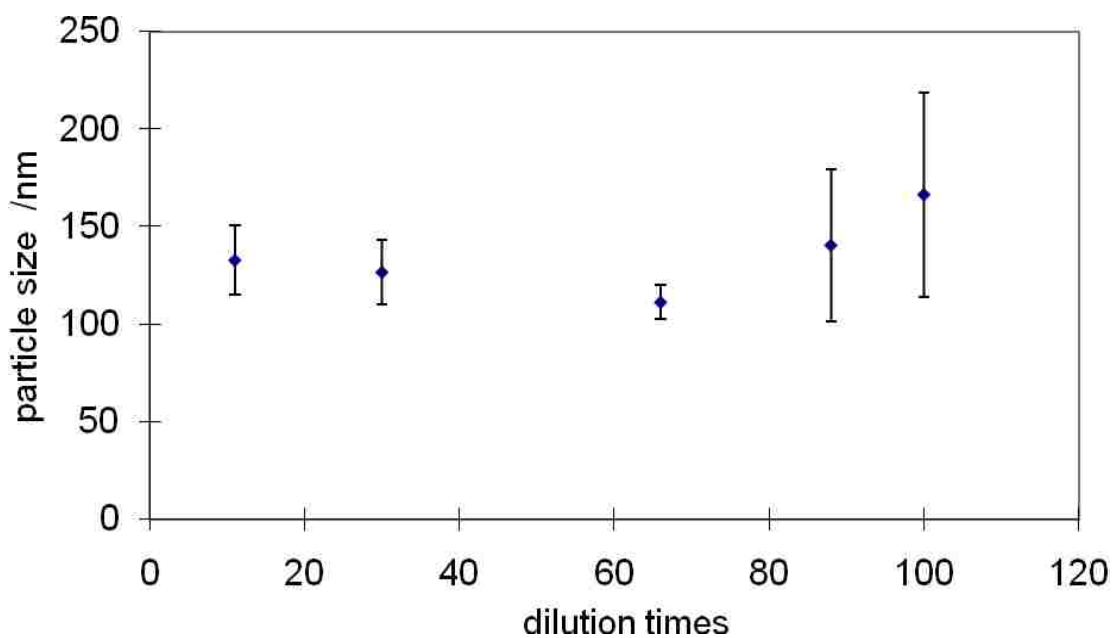


Figure 4.24. Effect of dilution ratio on number based particle size distribution of PLGA nanoparticles.

Sonication and Static mixer

The previous particle size distributions obtained by using sonication and homogenization are almost in the required range. Thus a batch of PLGA nanoparticles using static mixer as an alternative to homogenization is tried. If the static mixer can do the complete job of producing the desired MSD, then scale – up should be easier. First 18 ml of primary emulsion is prepared by sonication as described in materials and methods section. 18 ml of primary emulsion is used so that good enough emulsion to pump through the static mixer is present. One more beaker is filled with 180 ml of DIUF H₂O. The two beakers, one with primary emulsion and other with DIUF H₂O, are attached to the two input provisions of the static mixer and are fed simultaneously through the static mixer using the two pumps. The speeds of both the pumps are maintained at 1:10. Taking the speed limits of both the pumps into consideration the 1:10 ratio of pump speed is selected for the synthesis. The effect of speed through the static mixer on the size of the nanoparticles is tested by generating nanoparticles at three different speeds through the static mixer, while maintaining the same speed ratio of both the pumps in all the three batches. For the first batch, the speeds of pumps are 18 ml/min and 180 ml/min for emulsion and DIUF H₂O respectively. The output from the static mixer is pumped through the static mixer four more times using a single pump for all the three batches to further decrease the size of the nanoparticles. The resulting emulsion is checked for particle size distribution. Two more batches are prepared same as described above except that the speed through the static mixer is 20 ml/min and 26 ml/min for the primary emulsion and 200 ml/min and 260 ml/min for DIUF H₂O respectively. To test the effect of solvent removal on the nanoparticle size distribution, one of the batches is evaporated over night at 30⁰C temperature to remove EA and MSD of the particles is tested. The comparison between particle size distributions of nanoparticles obtained by employing different speeds through the static mixer to generate a secondary emulsion is summarized in Table 4.8.

In the batch that was processed at 180ml/min through the static mixer, 14 % of the partilces based on volume and 96% of the partilces based on number with desired range 154 nm < D_{avg} < 223 nm were observed along with 86% of particles based on volume and 4% of the partilces based on size having size around 850 nm < D_{avg} < 1350 nm. Based on volume 4% and based on number 61% of particles with desired size range 122 nm < D_{avg} < 157 nm were observed in the batch that was generated at 200 ml/min through static mixer. Based on volume 96% and based on number 39% of particles in the size range 405 nm < D_{avg} < 560 nm were also observed in this batch. Based on volume 23% and based on number 97% of particles with desired size range 152 nm < D_{avg} < 230 nm were observed in the batch that was generated at 260 ml/min through static mixer. Based on volume 77% and based on number 3% of particles in the size range 795 nm < D_{avg} < 1205 nm were also observed in this batch. In conclusion, there are good number of nanoparticles in required size range of 100-250 nm based on number in all the samples generated by using static mixer. In the ethyl acetate evaporated sample, 100% of the particles with size in the range of 97 nm < D_{avg} < 1886 nm based on volume are observed. In this batch, based on number 99% of the nanoparticles are in the size range of 97 nm < D_{avg} < 491 nm. The increase in the range of particle sizes present in the emulsion is because of agglomeration of the nanoparticles over the evaporation process. It can be concluded that the static mixer is a good substitute for homogenizer in generating

secondary emulsion with particles in the size range of 100-250 nm. The use of static mixer instead of homogenizer aids the scale up of the technique for industrial application.

Table 4.8. Particle sizes obtained by using sonication for primary emulsion and static mixer for secondary emulsion generation.

S. No.	Secondary emulsion method	Dilution times	D _v (nm) (% of particles in the range)	D _n (nm) (% of particles in the range)	Poly dispersity
1	Static mixer (180ml/min, 5times)	10	Peak 1 (14%) D _{min} =165, D _{avg} =206, D _{max} =255	Peak 1 (96%) D _{min} =165, D _{avg} =199, D _{max} =255	0.307
			Peak 2 (86%) D _{min} =872, D _{avg} =1085, D _{max} =1351	Peak 2 (4%) D _{min} =872, D _{avg} =1056, D _{max} =1134	
2	Static mixer (200ml/min, 5times)	10	Peak 1 (4%) D _{min} =122, D _{avg} =138, D _{max} =157	Peak 1 (61%) D _{min} =122, D _{avg} =135, D _{max} =157	0.234
			Peak 2 (96%) D _{min} =405, D _{avg} =463, D _{max} =557	Peak 2 (39%) D _{min} =405, D _{avg} =460, D _{max} =522	
3	Static mixer (260ml/min, 5times)	10	Peak 1 (23%) D _{min} =152, D _{avg} =192, D _{max} =230	Peak 1 (97%) D _{min} =152, D _{avg} =186, D _{max} =230	0.256
			Peak 2 (77%) D _{min} =796, D _{avg} =759, D _{max} =1205	Peak 2 (3%) D _{min} =796, D _{avg} =902, D _{max} =1109	

Table 4.8(continued). Particle sizes obtained by using sonication for primary emulsion and static mixer for secondary emulsion generation.

4	Static mixer (260ml/min, 5 times) evaporated over night	10	Peak 1 (100%) $D_{\min}=97, D_{\text{avg}}=693, D_{\max}=1886$	Peak 1 (99%) $D_{\min}=97, D_{\text{avg}}=161, D_{\max}=491$	0.222
---	--	----	---	---	-------

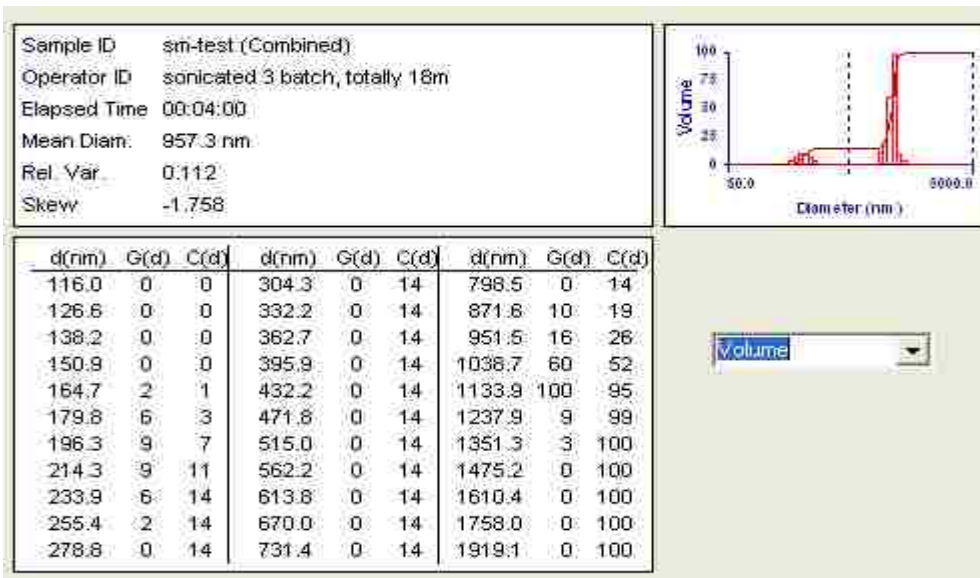


Figure 4.25. Volume based MSD of nanoparticles generated by sonication of 1ml organic solution and 5ml aqueous solution resulting in primary emulsion followed by using static mixer at 180ml/min and dilution ratio 1:10 to generate secondary emulsion. [Table 4.8, S.No.1]

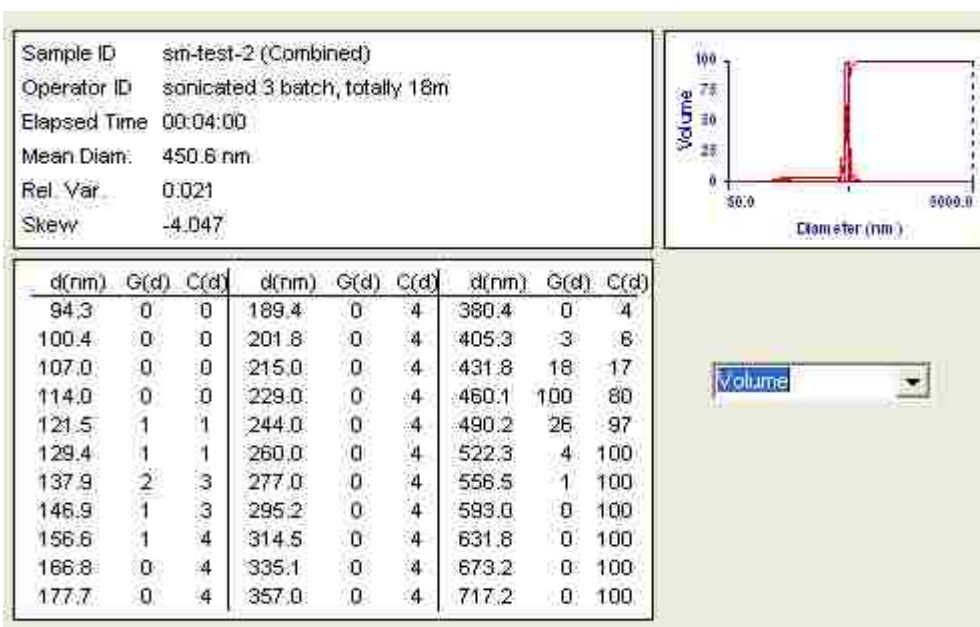


Figure 4.26. Volume based MSD of nanoparticles generated by sonication of 1ml organic solution and 5ml aqueous solution resulting in primary emulsion followed by using static mixer at 200ml/min and dilution ratio 1:10 to generate secondary emulsion. [Table 4.8, S.No.2]

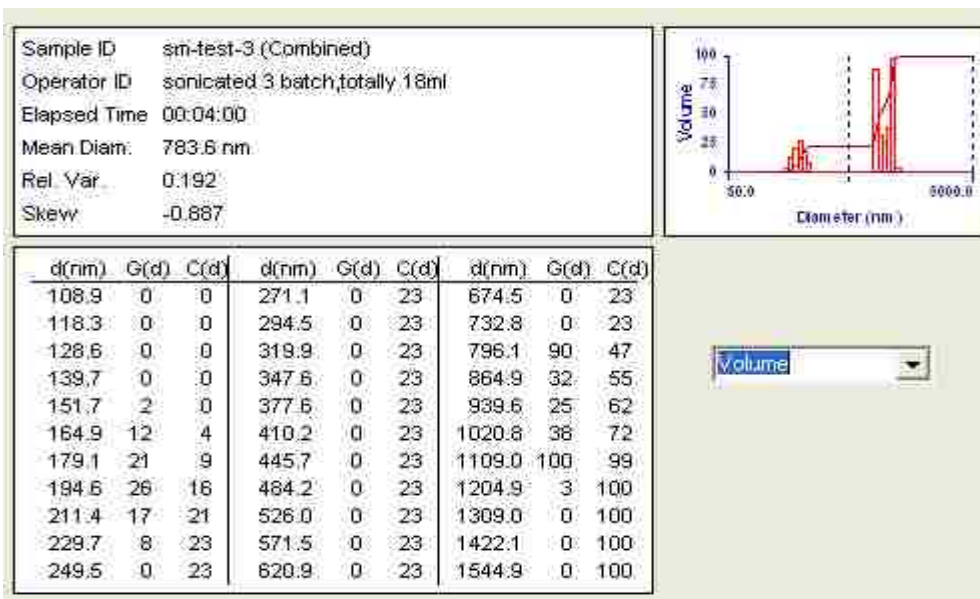


Figure 4.27. Volume based MSD of nanoparticles generated by sonication of 1ml organic solution and 5ml aqueous solution resulting in primary emulsion followed by using static mixer at 260ml/min and dilution ratio 1:10 to generate secondary emulsion. [Table 4.8, S.No.3]

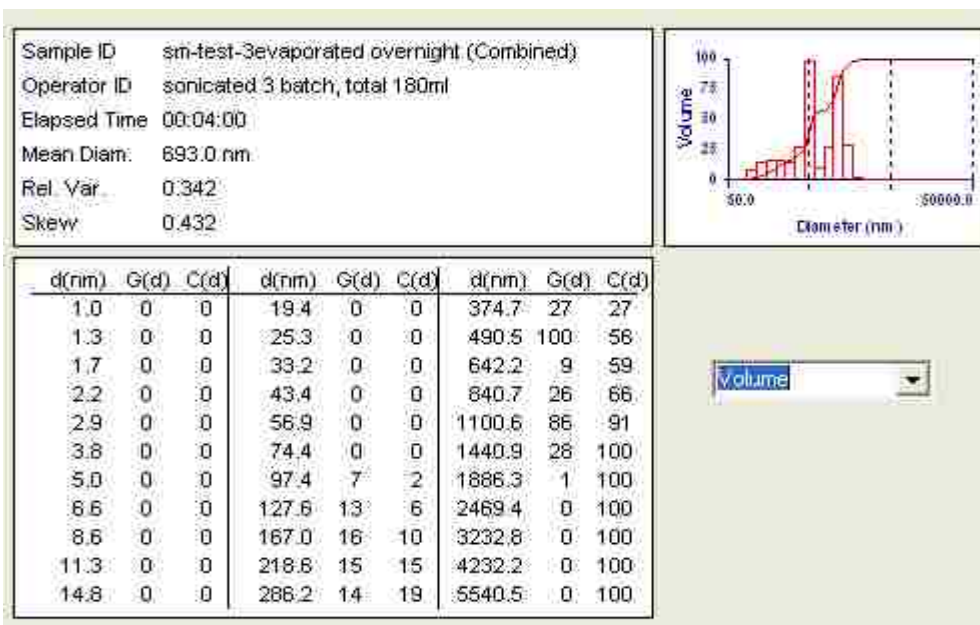


Figure 4.28. Volume based MSD of secondary emulsion, after removing EA, generated by sonication of 1ml organic and 5ml aqueous phase resulting in primary emulsion followed by use of static mixer at 260ml/min and dilution ratio 1:10. [Table 4.8, S.No.4]

Transmission electron microscopy measurement

To confirm the presence of the nanoparticles in the secondary emulsion synthesized by a static mixer, TEM and MSD images of the secondary emulsion are compared for this batch. One batch of PLGA nanoparticles is produced as mentioned in previous section with speed through the static mixer being 39 ml/min and 390 ml/min of primary emulsion and DIUF H₂O respectively. The MSD of the secondary emulsion was obtained. The TEM sample was prepared as mentioned in materials and methods section.

The volume and number based MSD of the nanoparticles sample were determined and are shown in Figure 4.27 and Figure 4.28 respectively. The summary of the range of size of the nanoparticles sample based on MSD is presented in Table 4.9. It can be observed that majority of the particles with size range $75 \text{ nm} < D_{\text{avg}} < 95 \text{ nm}$ and $197 \text{ nm} < D_{\text{avg}} < 360 \text{ nm}$ are present in the emulsion. There are few particles in the range of $1 \mu\text{m} - 2 \mu\text{m}$. TEM images of the sample are presented in Figure 4.29 through Figure 4.33. No clear images and boundaries of the PLGA nanoparticles are observed as distinguishing the carbon based PLGA nanoparticles coated over lacey carbon-coated copper grid is difficult. TEM images are analyzed and compared to the MSD of the samples to verify the results obtained. In Figure 4.29, clusters of spherical nanoparticles can be observed in the top left hand corner and bottom right hand corner of the picture. It is evident from the TEM image Figure 4.29 of the secondary emulsion that there are nanoparticles in size range $50 \text{ nm} < D_{\text{avg}} < 100 \text{ nm}$. A close up image of a PLGA nanoparticle with size around 100 nm is shown in Figure 4.30. Figures 4.31 and 4.32 represent TEM images of a PLGA nanoparticle with diameter around 300 nm. In Figure 4.33, nanoparticles with a wide range of particle size are found. Nanoparticles with size around 1000 nm in size can be clearly seen all over the image in Figure 4.33. The volume based MSD of the sample also indicate the presence of the PLGA nanoparticles with diameter around 1000 nm, but they are very small in number as no particles in such range are observed in the number based MSD. Small clusters of PLGA nanoparticles in size range around 100nm-500nm are also found in the TEM image of Figure 4.33. The range of particles found in all the TEM images is also found in MSD data of the sample. It is concluded that MSD data of the sample and the TEM images are in well agreement with each other.

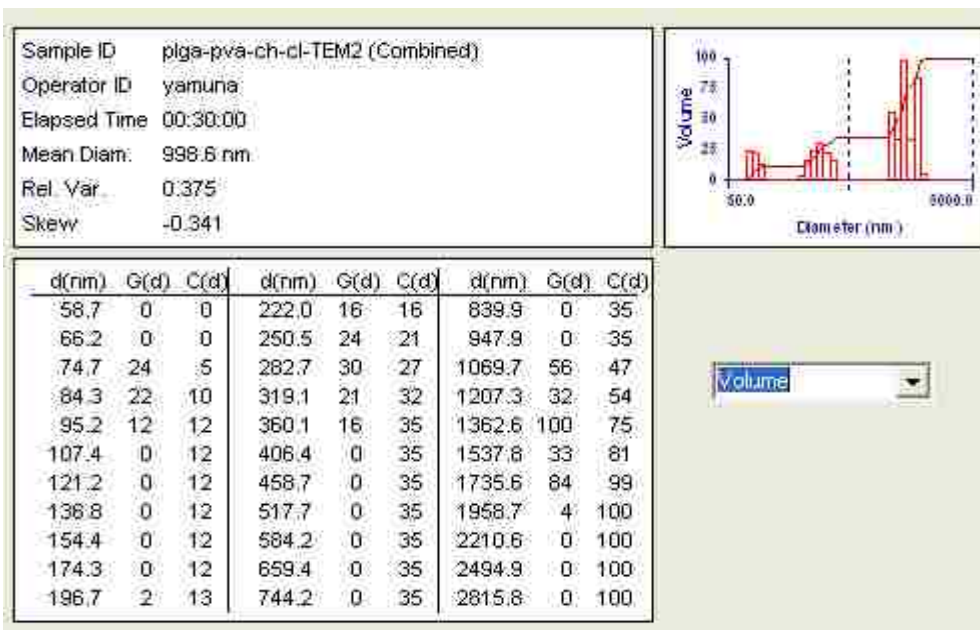


Figure 4.29. Volume based MSD of PLGA nanoparticles in TEM sample.

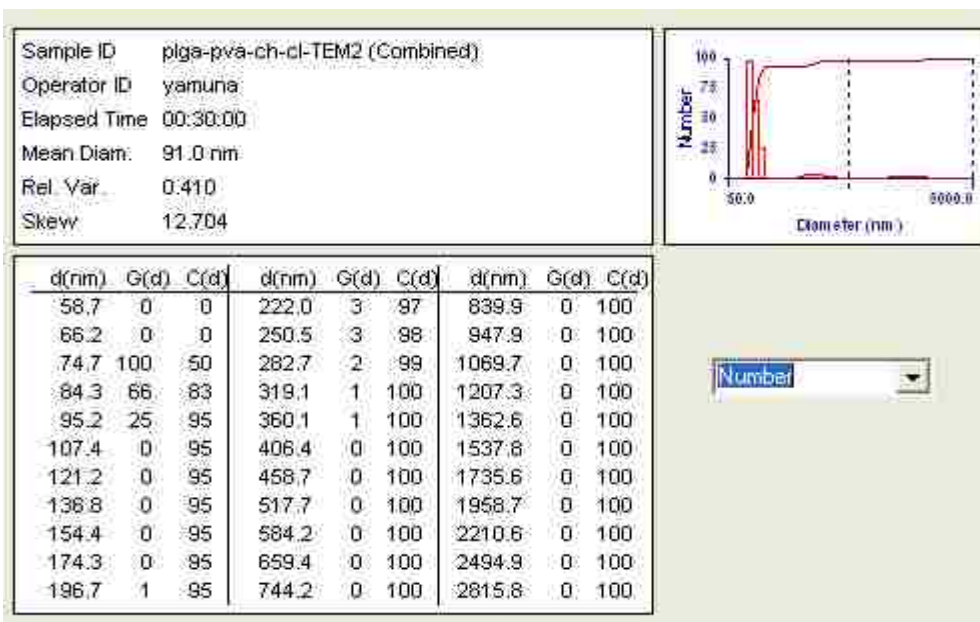


Figure 4.30. Number based MSD of PLGA nanoparticles in TEM sample.

Table 4.9. MSD summary of secondary emulsion from the static mixer for TEM measurement.

Batch. No.	System	Secondary emulsion method	Dilution times	D _v (nm)	D _n (nm)	Poly dispersity
1.	1ml 1wt% PLGA in EA and 5ml 1wt% PVA, 0.3wt% Chitosan chloride in DIUF H2O	Static mixer (390ml/min, 5 times)	10	Peak 1 D _{min} =75,D _{avg} =83, D _{max} =95	Peak 1 D _{min} =75,D _{avg} =81,D _{max} =95	0.265
				Peak 2 D _{min} =197,D _{avg} =283,D _{max} =360	Peak 2 D _{min} =197,D _{avg} =260,D _{max} =360	
				Peak 3 D _{min} =1070,D _{avg} =1421,D _{max} =1959		

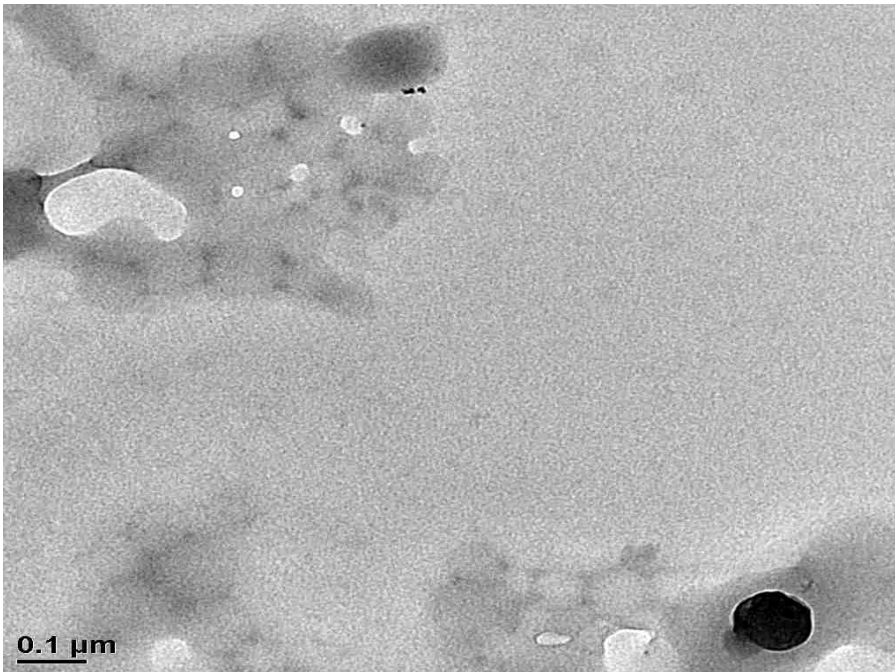


Figure 4.31. TEM images of the PLGA nanoparticles with size around 100nm in the secondary emulsion processed through the static mixer at 390ml/min.

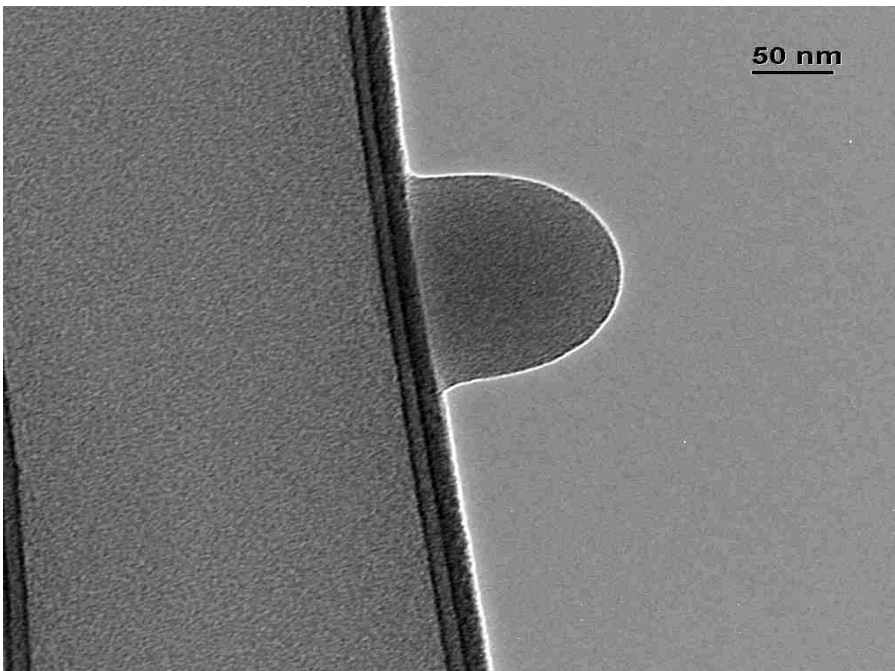


Figure 4.32. TEM images of the PLGA nanoparticles with size around 100nm in the secondary emulsion processed through the static mixer at 390ml/min.

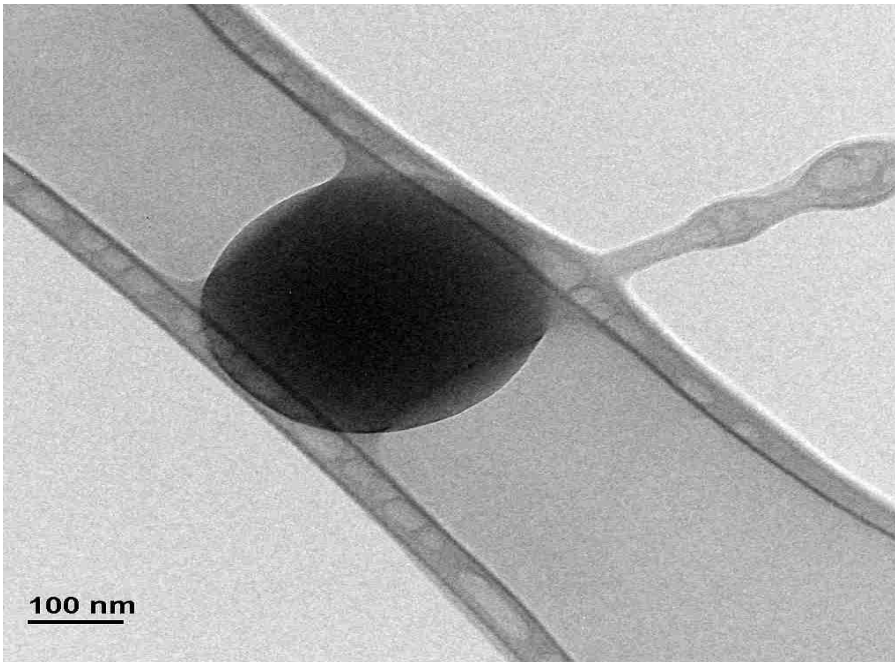


Figure 4.33. TEM images of the nanoparticles with diameter around 300nm in the secondary emulsion processed through the static mixer at 390ml/min.

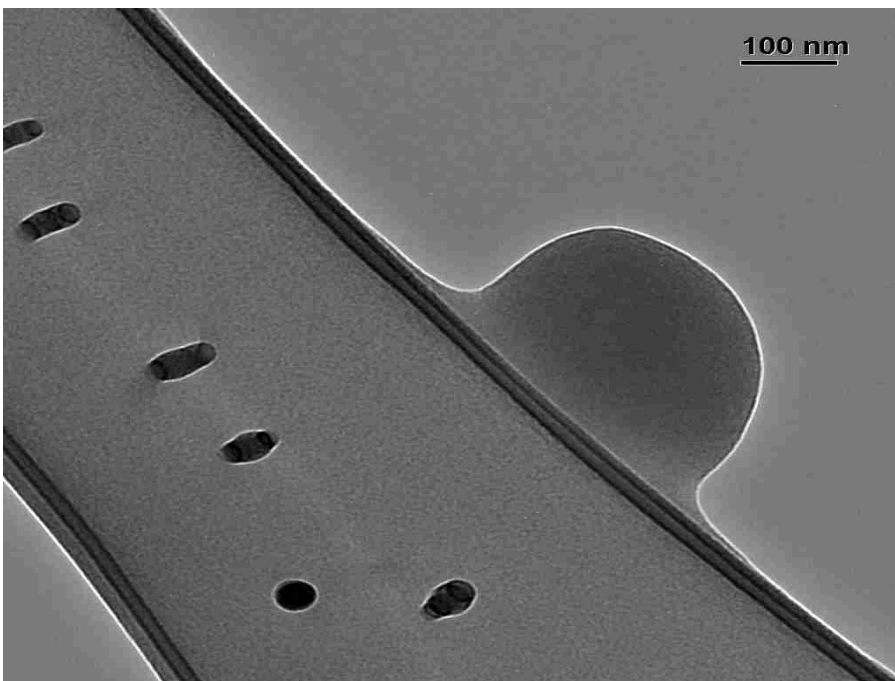


Figure 4.34. TEM images of the nanoparticles with diameter around 300nm in the secondary emulsion processed through the static mixer at 390ml/min.

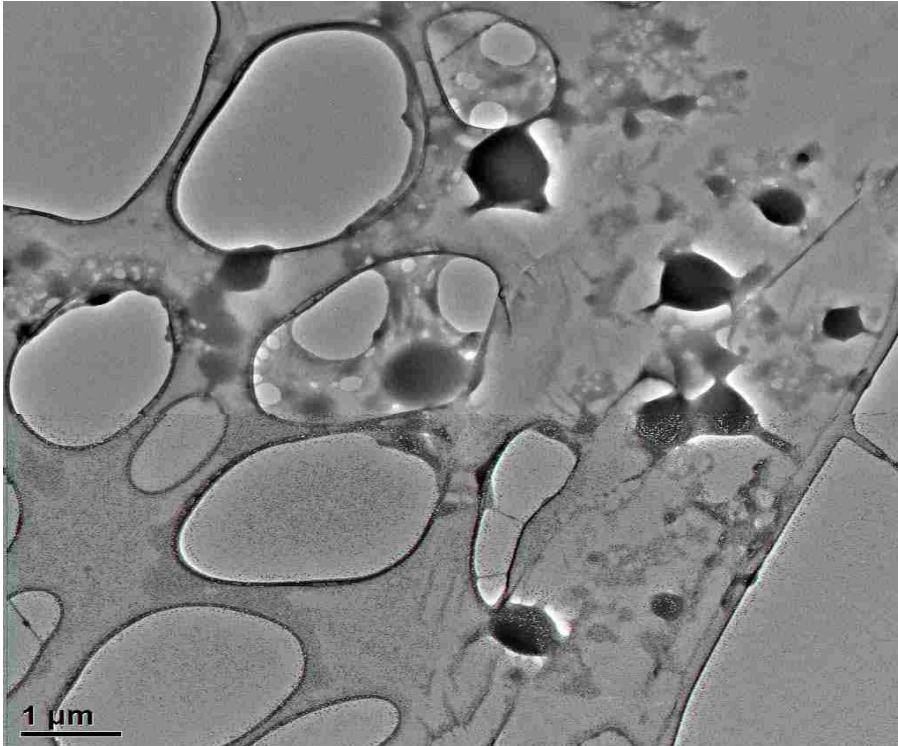


Figure 4.35. TEM images of spherical nanoparticles with sizes in the range of 100-1000nm in the secondary emulsion processed through the static mixer at 390ml/min.

5. Conclusions

The present study reports the formation of cationic PLGA nanoparticles with a portion of their distribution below 250nm using PVA as stabilizer and chitosan chloride for surface modification. The nanoparticles are generated by emulsion – diffusion – evaporation method and sonication is used for generating primary emulsion followed by static mixer for diffusion step. In the process of analyzing nanoparticle formation it is observed that the PVA acts as a compatibilizer for chitosan chloride in DIUF H₂O. It is also confirmed in this report that chitosan chloride alone cannot generate nanoparticles in required size range and PVA alone cannot confer positive charge to the nanoparticles and generate a good stable emulsion.

The static mixer was used to modify the formed colloidal droplet size after homogenizer. Data in Table 4.5 demonstrate that the particle size of primary emulsion were not further reduced, rather they seem to have agglomerated. The dilution ratio of secondary emulsion in diffusion step has little effect on the final PLGA nanoparticles size. However a dilution ratio of 65 times generated stable nanoparticles size. The use of sonication for emulsion generation followed by static mixer for diffusion step successfully generated a fraction of PLGA nanoparticles below 250nm. The use of static mixer enables easy scale – up for industrial use of this method. TEM images of the nanoparticles and the multi – modal distribution of particle sizes of nanoparticles are in correspondence with one another.

6. Appendices

Abbreviations

Polymers

Chlorin-cored PCL -b- mPEG – chlorin-core poly (ϵ -caprolactone)–poly (ethylene glycol) diblock copolymer

PDMAPAAm-PNIPAM – poly (*N,N*-dimethylaminopropyl acrylamide)- poly (*N*-isopropylacrylamide)

PEG – poly (ethylene glycol)

PEGDMA/PLA semi-IPN – poly (ethylene glycol) dimethacrylate/ poly (lactic acid) semi-interpenetrating network

PEI-graft-PCL (PEC) – polyethylenimine-graft-poly(ϵ -caprolactone)

PEG-PLLA-PEG - polyethylene glycol and poly (L-lactide) diblock copolymers

PHPMA – poly [*N*-(2-hydroxypropyl)methacrylamide]

PLGA – poly (lactic-co-glycolic acid)

PSMA – poly (styrene-co-maleic anhydride)

PVA – polyvinyl alcohol

PVP – polyvinylpyrrolidone

Nomenclature

G (d): relative percentage contribution of the size range.

C (d): cumulated percentage contribution.

d: diameter of dispersed phase

D_v : volume-based size.

D_n : number-based size.

μ_d : viscosity of dispersed phase

σ : surface tension

ρ_c : density of continuous phase

ρ_d : density of dispersed phase

Number based multimodal size distributions of all secondary emulsions in this work

Dissolution of polymers in their solvents (Table 4.1)

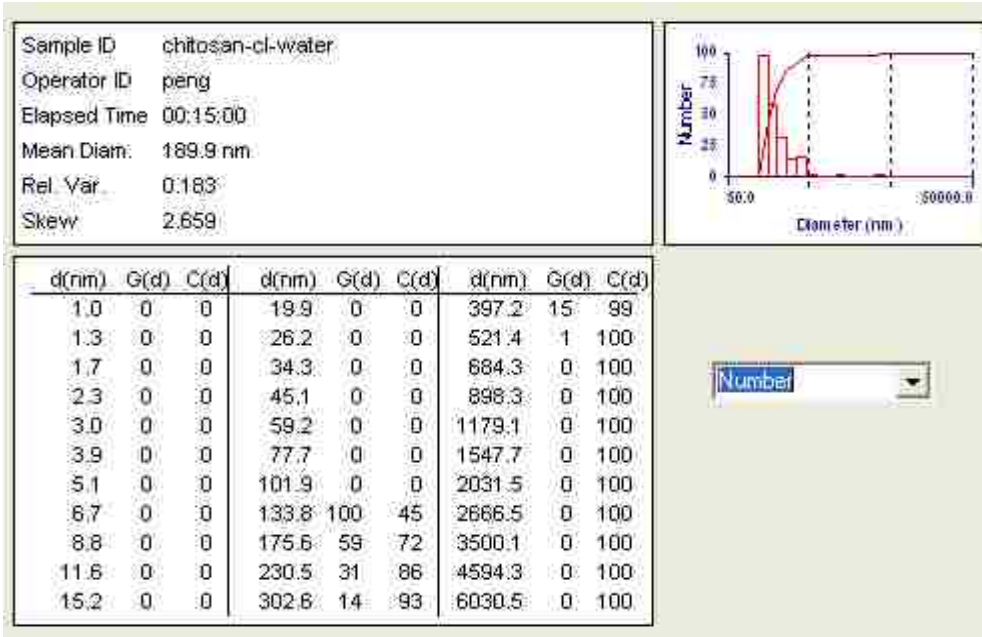


Figure 6.1. Number based MSD of 0.3wt% chitosan chloride in DIUF H2O [Table 4.1, row 3]

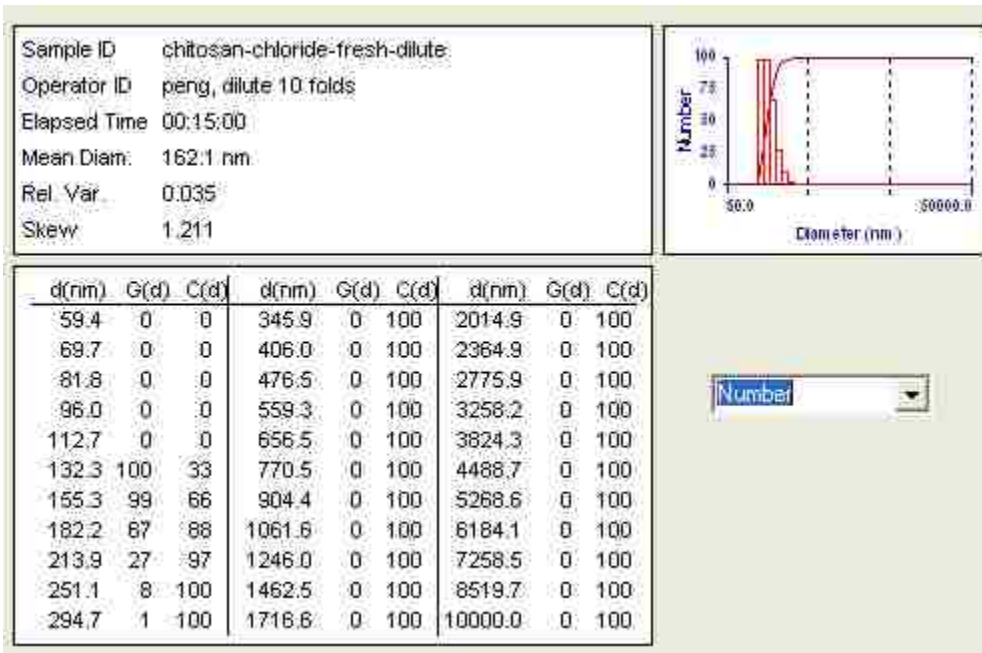


Figure 6.2. Number based MSD of 0.03wt% chitosan chloride in DIUF H2O. [Table 4.1, row 5]

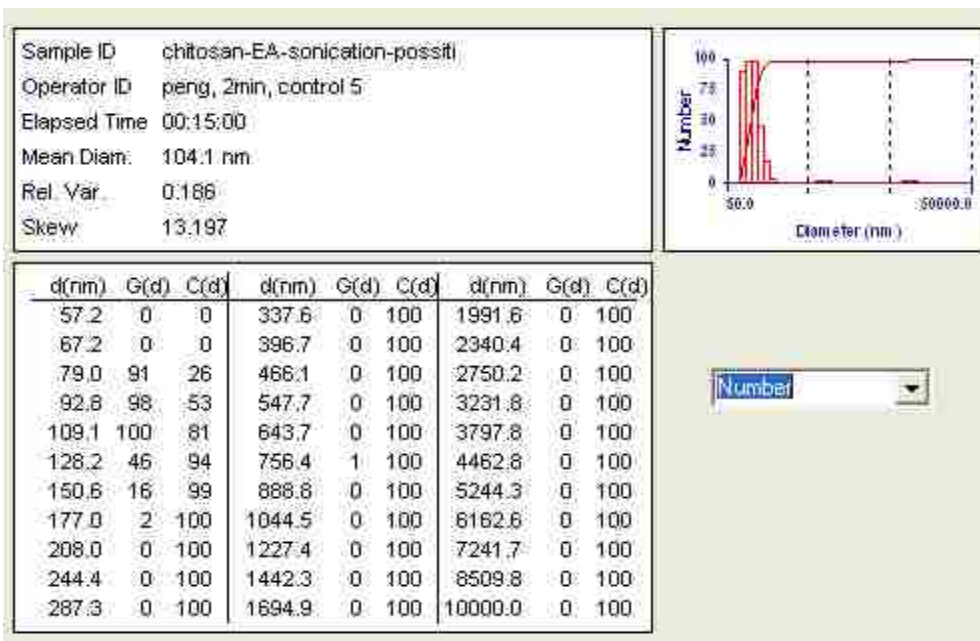


Figure 6.3. Number based MSD of particles formed by emulsifying 1 ml EA in 5 ml solution of 0.3wt% chitosan chloride in DIUF H₂O. [Table 4.1, row 6]

Effect of PVA on Chitosan chloride aqueous solution (Table 4.2)

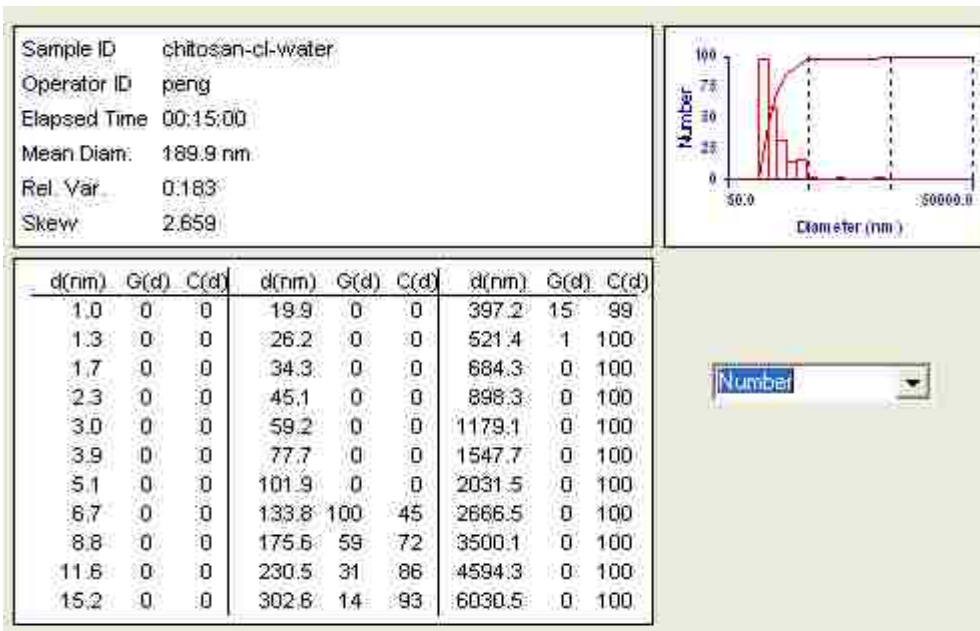


Figure 6.4. Number based MSD of 0.3wt% chitosan chloride in DIUF H₂O – batch-1. [Table 4.2, S.No.1]

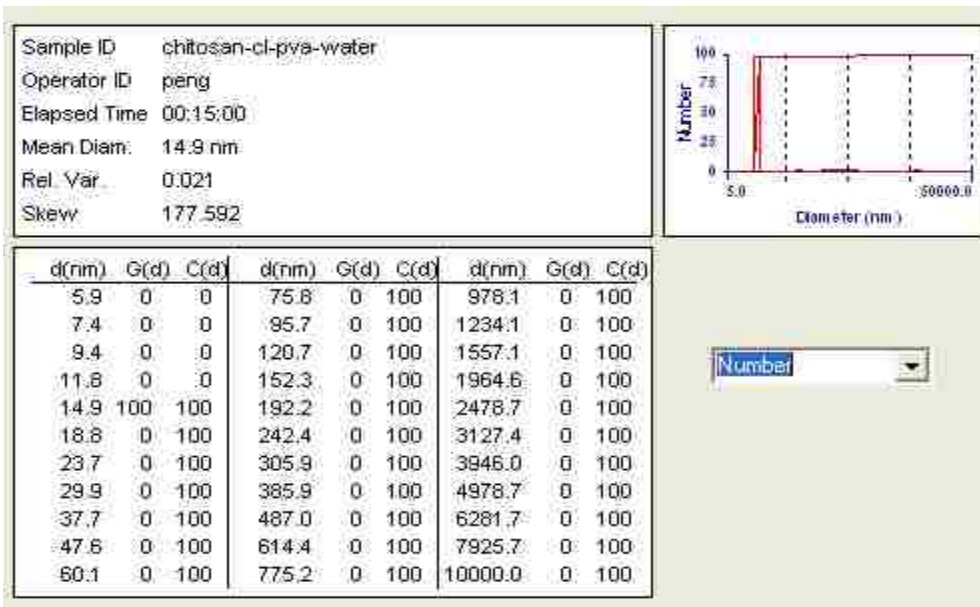


Figure 6.5. Number based MSD of 1wt% PVA and 0.3wt% chitosan chloride in DIUF H2O – batch -1. [Table 4.2, S.No.2]

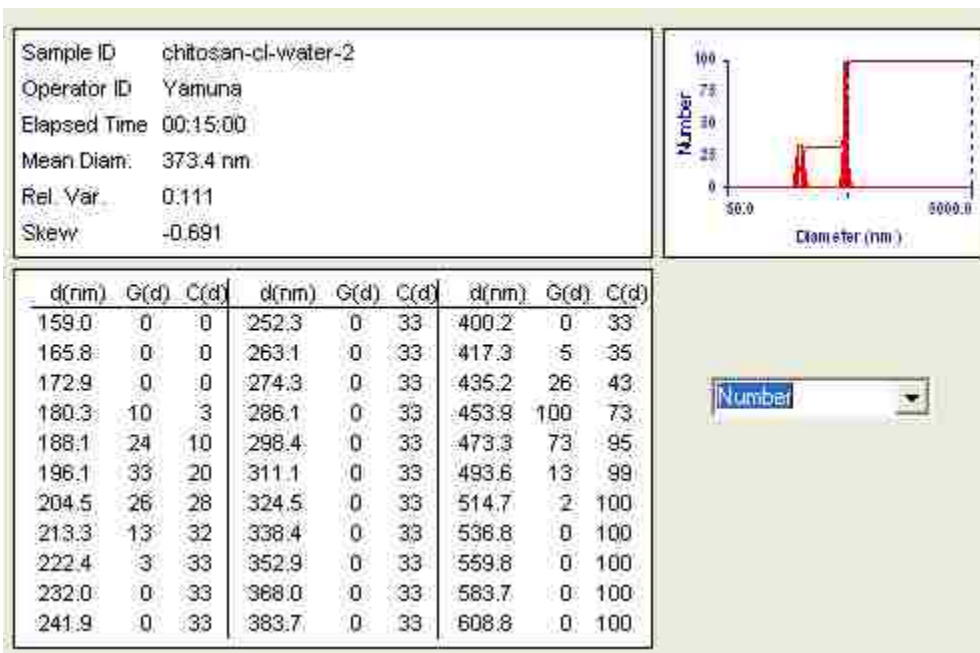


Figure 6.6. Number based MSD of 0.3wt% chitosan chloride in DIUF H2O – batch-2. [Table 4.2, S.No.3]

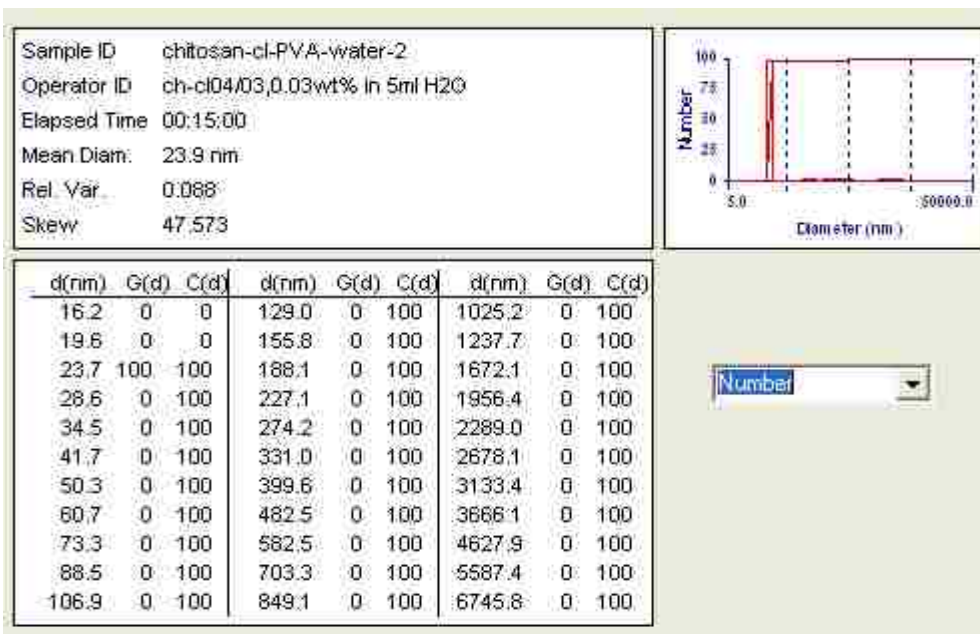


Figure 6.7. Number based MSD of 1wt% PVA and 0.3wt% chitosan chloride in DIUF H2O – batch -2. [Table 4.2, S.No.4]

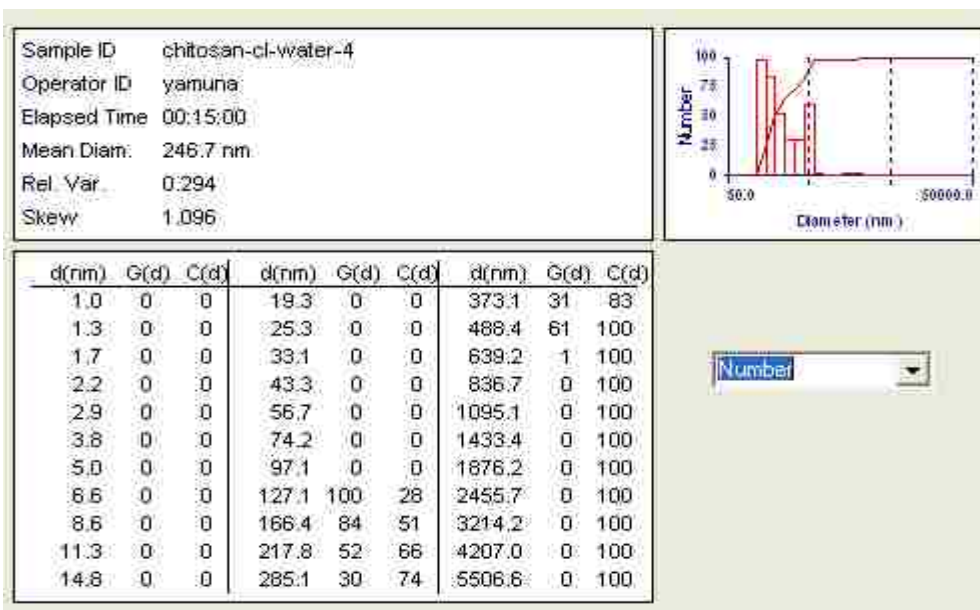


Figure 6.8. Number based MSD of 0.3wt% chitosan chloride in DIUF H2O – batch-3. [Table 4.2, S.No.5]

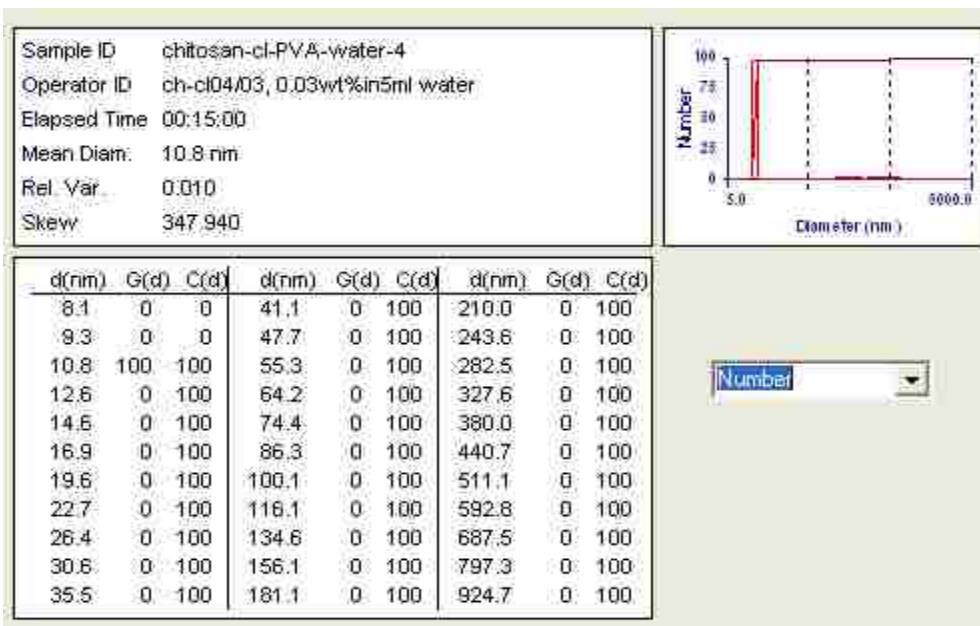


Figure 6.9. Number based MSD of 1wt% PVA and 0.3wt% chitosan chloride in DIUF H2O – batch -3. [Table 4.2, S.No.6]

Different possible binary polymer emulsions (Table 4.3)

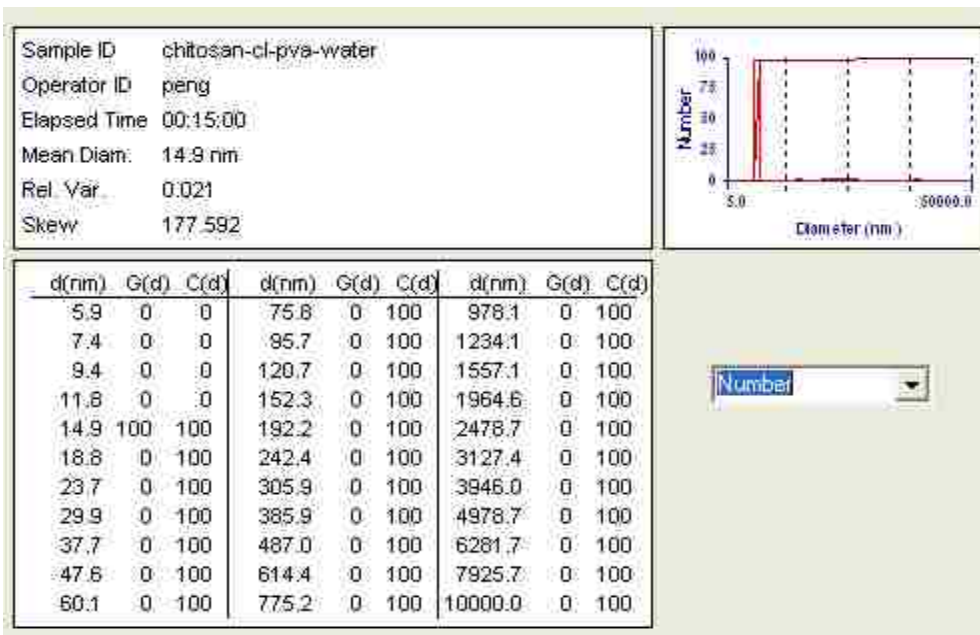


Figure 6.10. Number based MSD of 1wt% PVA and 0.3wt% chitosan chloride in DIUF H2O. [Table 4.3, row 2]

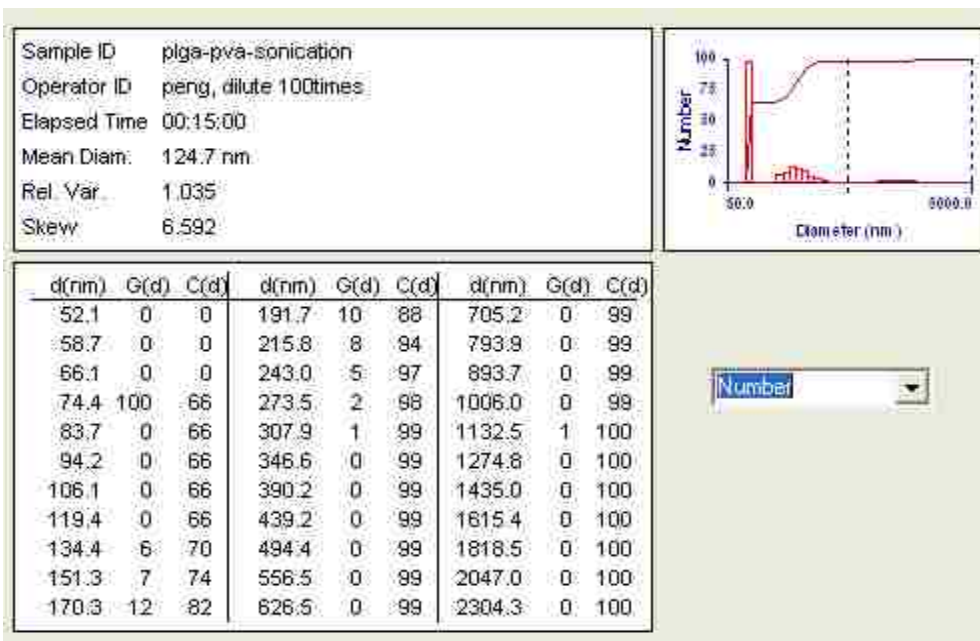


Figure 6.11. Number based MSD of nanoparticles formed by 1 ml 1wt% PLGA in EA emulsified in 5 ml aqueous solution of 1wt% PVA. [Table 4.3, row 3]

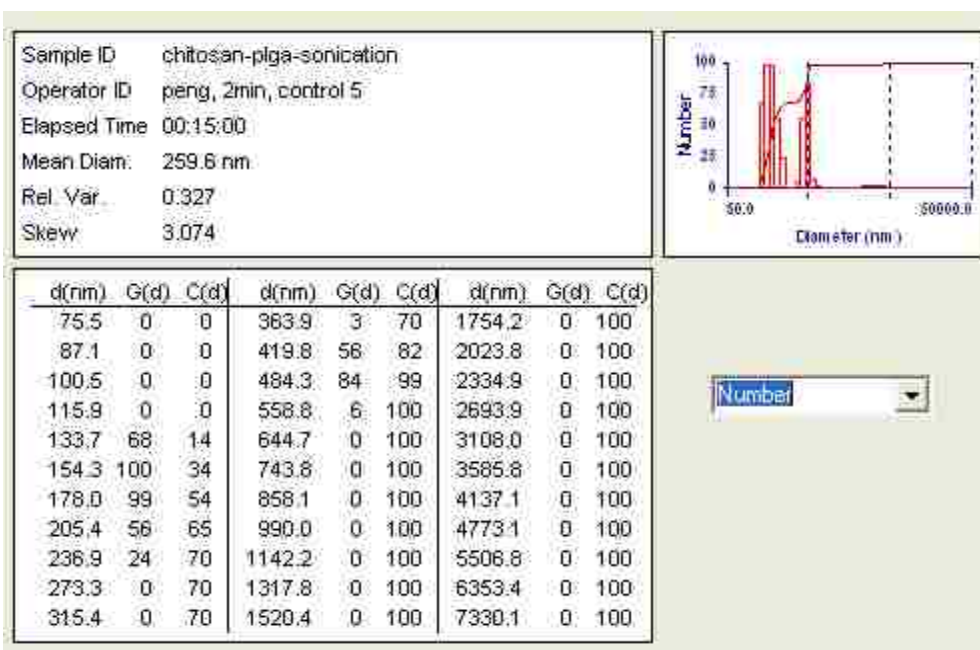


Figure 6.12. Number based MSD of nanoparticles formed by 1 ml solution of 1wt% PLGA in EA emulsified in 5 ml aqueous solution of 0.3wt% chitosan chloride. [Table 4.3, row 4]

Emulsion formed by the ternary polymer system (Table 4.4)

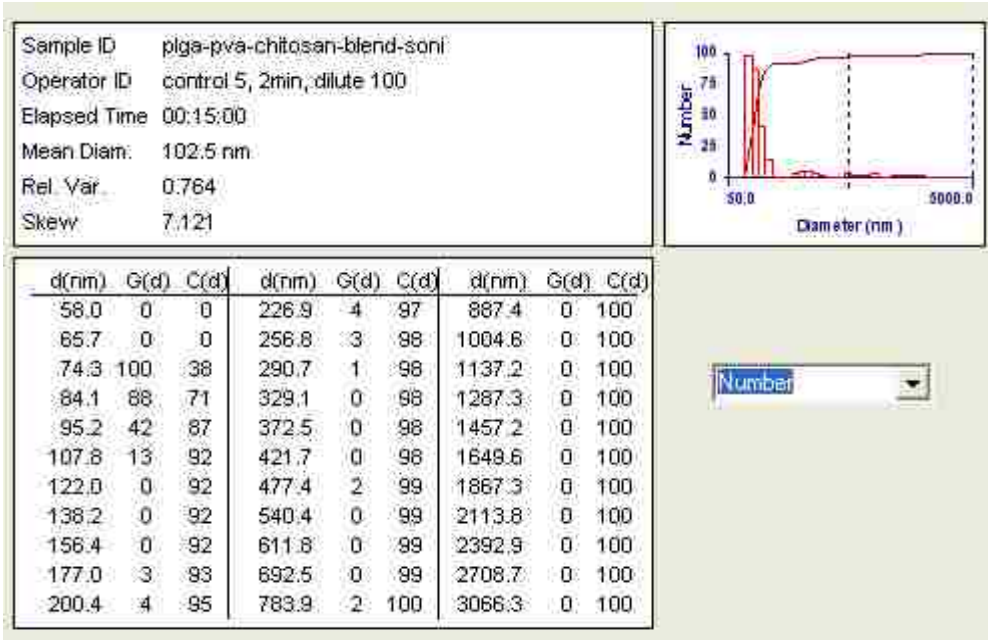


Figure 6.13. Number based MSD of nanoparticles formed by 1 ml 1wt% PLGA in EA emulsified in 5 ml of 1wt% PVA and 0.3wt% chitosan chloride in DIUF H₂O. [Table 4.4, row 2]

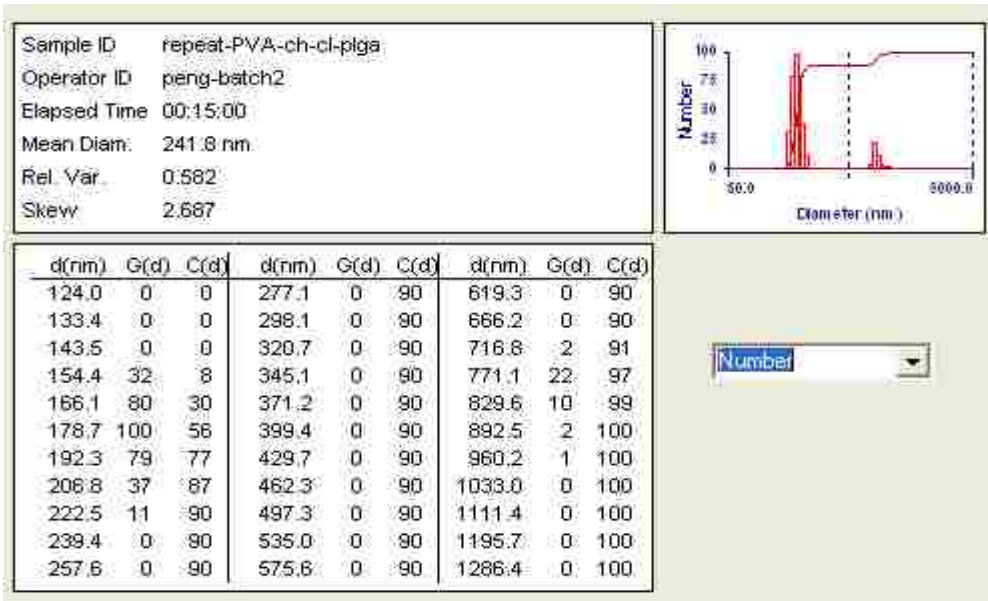


Figure 6.14. Number based MSD of 2nd batch of nanoparticles formed by 1 ml 1wt% PLGA in EA emulsified in 5 ml aqueous solution of 1wt% PVA and 0.3wt% chitosan chloride. [Table 4.4, row 3]

Effect of Static mixer (Table 4.5)

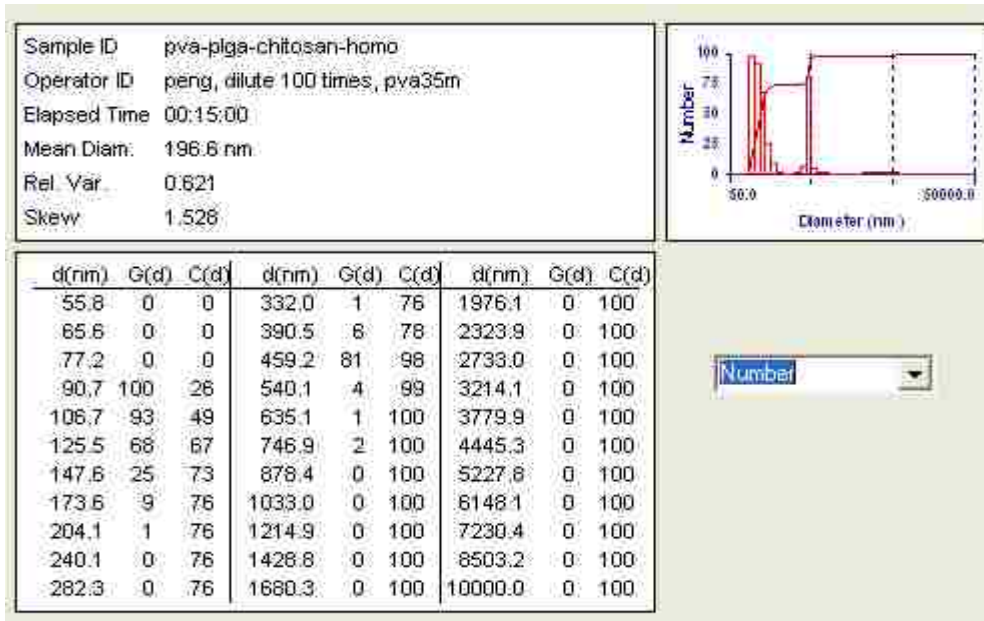


Figure 6.15. Number based MSD of nanoparticles in 100 times dilute primary emulsion from homogenization of 10ml organic phase and 50ml of aqueous phase. [Table 4.5, S.No.1]

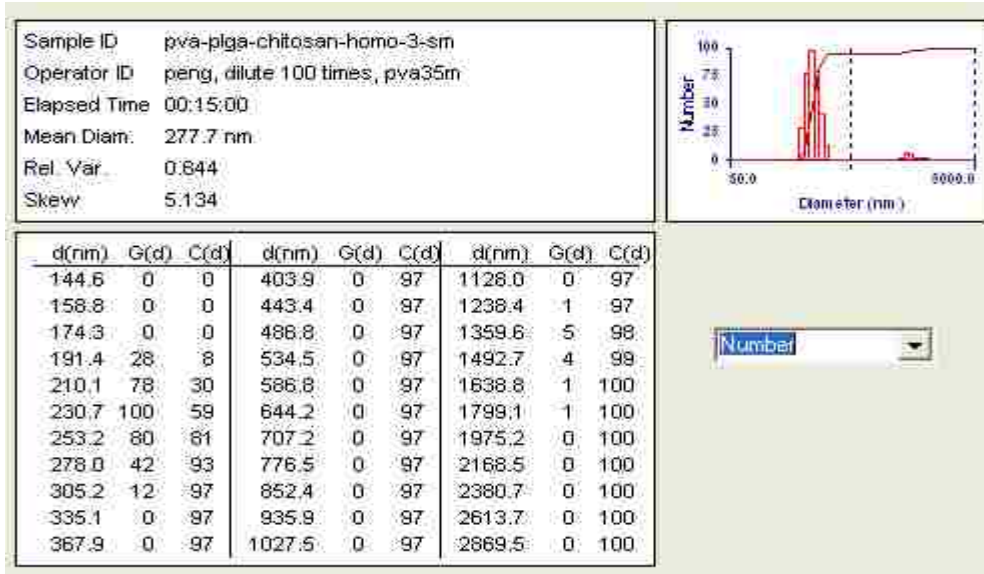


Figure 6.16. Number based MSD in 100 times diluted emulsion from homogenization of 10ml of organic and 50ml of aqueous phase and subsequently processing 3 times through static mixer at 135ml/min. [Table 4.5, S.No.2]

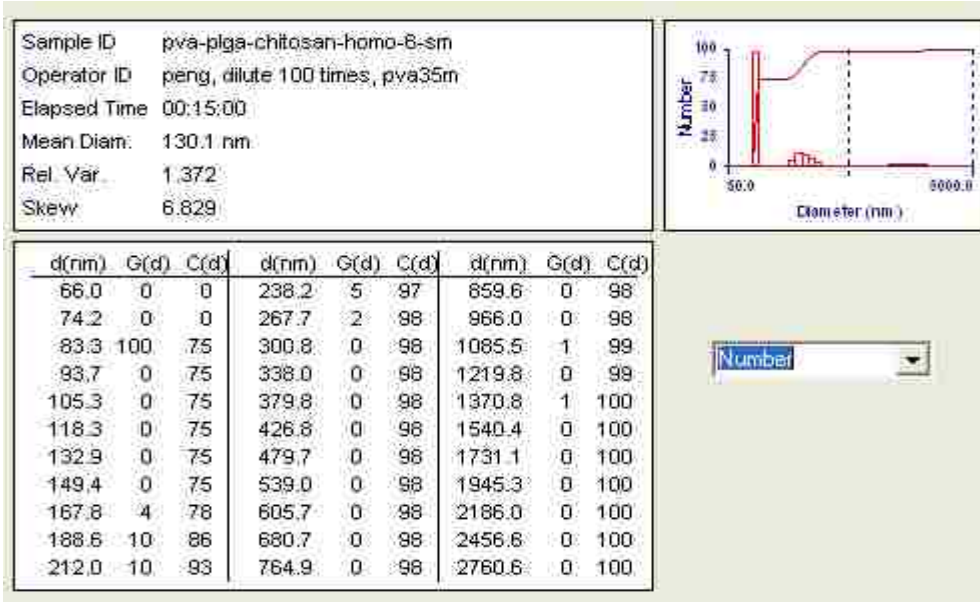


Figure 6.17. Number based MSD in 100 times diluted emulsion from homogenization of 10ml of organic and 50ml of aqueous phase and subsequently processing 6 times through static mixer at 135ml/min. [Table 4.5, S.No.3]

Sonication - homogenization (Table 4.6)

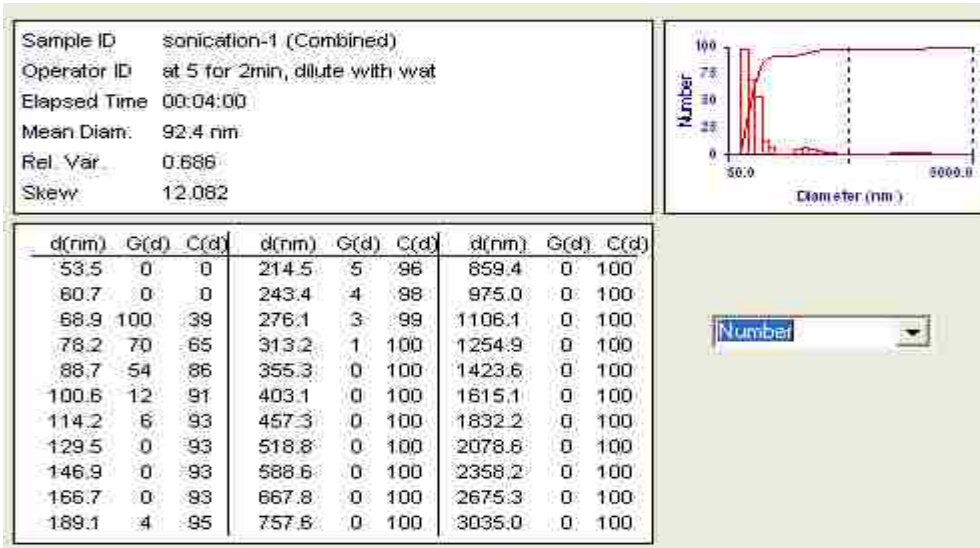


Figure 6.18. Number based MSD in secondary emulsion generated by homogenization at dilution rate 1:100 of primary emulsion formed by sonication of 1ml 1wt% PLGA in EA and 5ml of 1wt% PVA and 0.3wt% chitosan chloride aqueous solution. [Table 4.6, S.No.1]

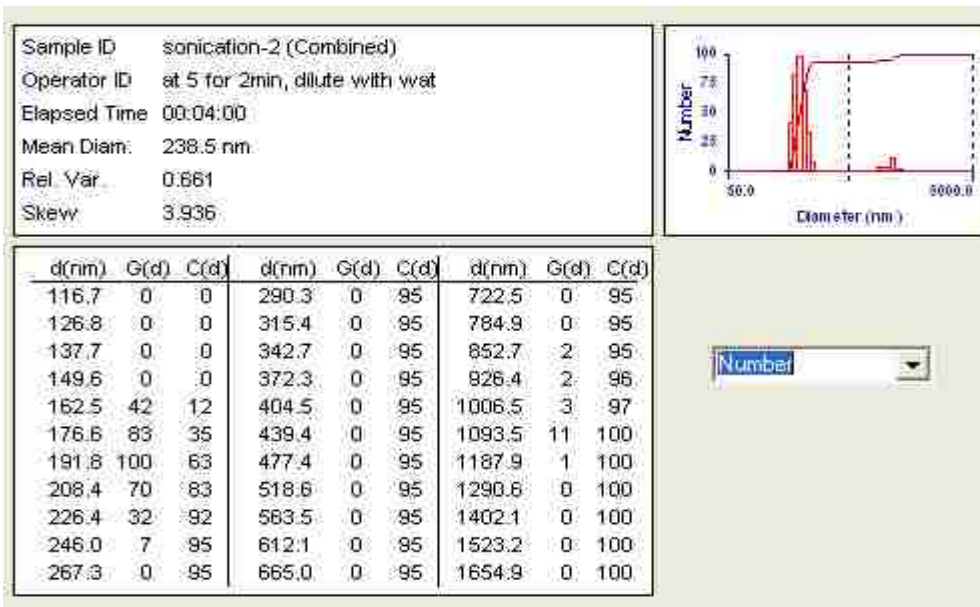


Figure 6.19. Number based MSD in secondary emulsion generated by homogenization at dilution rate 1:100 of primary emulsion formed by sonication of 1ml 1wt% PLGA in EA and 5ml of 1wt% PVA and 0.3wt% chitosan chloride aqueous solution. [Table 4.6, S.No.2]

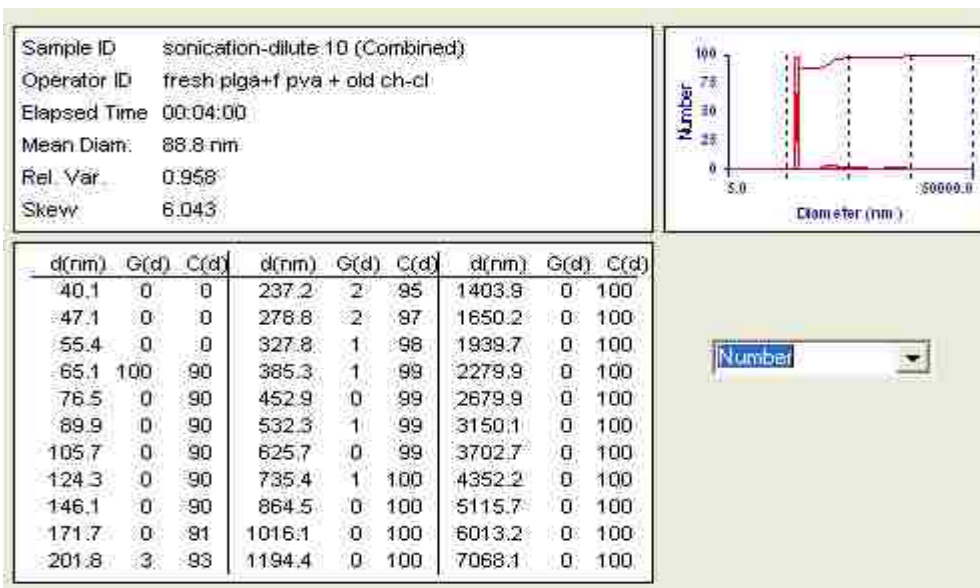


Figure 6.20. Number based MSD in secondary emulsion generated by homogenization at dilution rate 1:10 of primary emulsion formed by sonication of 1ml 1wt% PLGA in EA and 5ml of 1wt% PVA and 0.3wt% chitosan chloride aqueous solution. [Table 4.6, S.No.3]

Effect of dilution ratio on the PLGA nanoparticle size (Table 4.7)

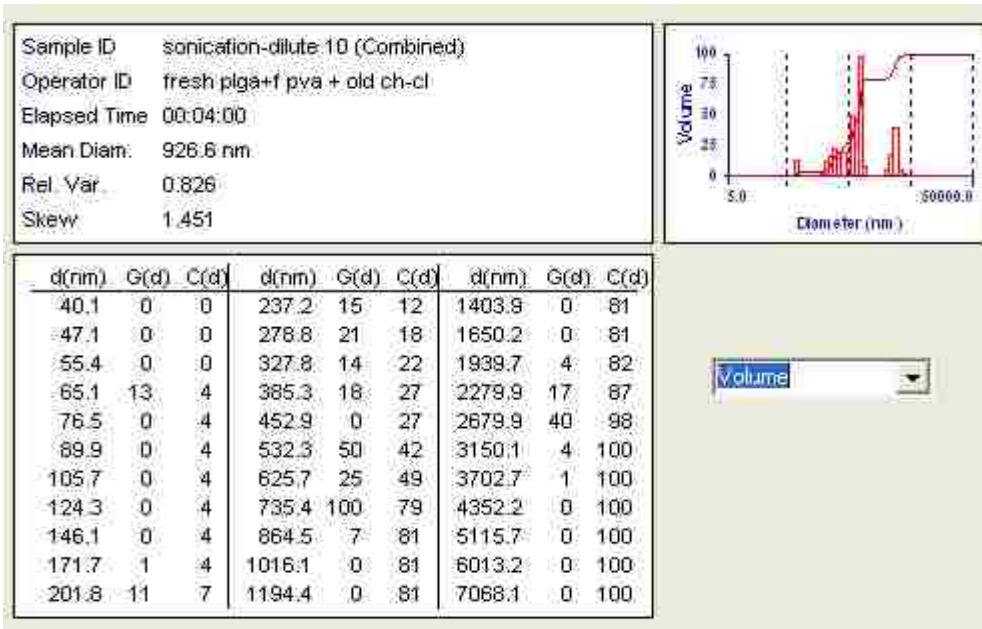


Figure 6.21. Volume based MSD of first batch of secondary emulsion with dilution ratio 1:10. [Table 4.7, row 2]

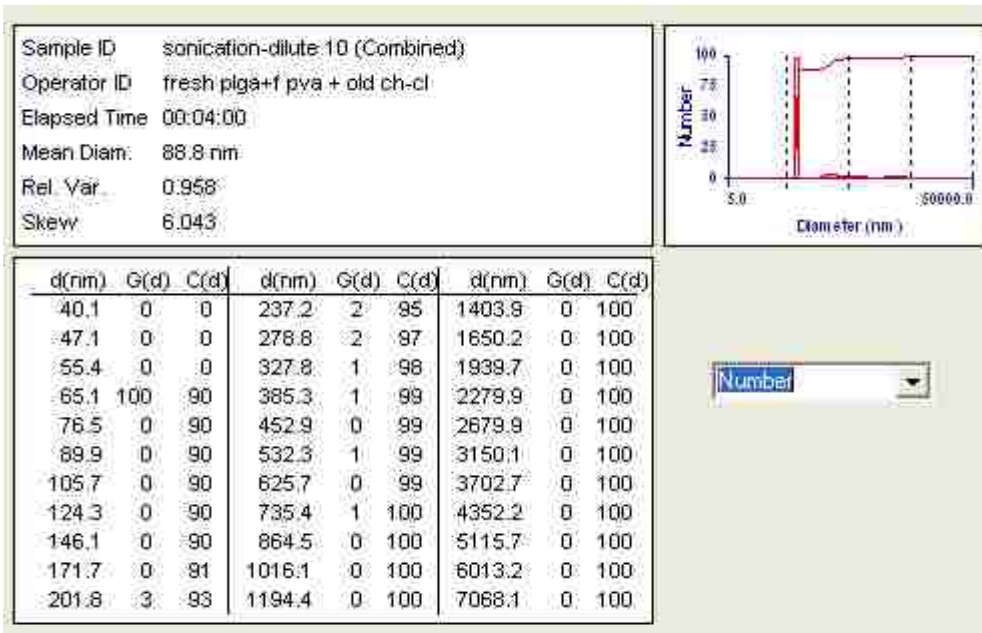


Figure 6.22. Number based MSD of first batch of secondary emulsion with dilution ratio 1:10. [Table 4.7, row 2]

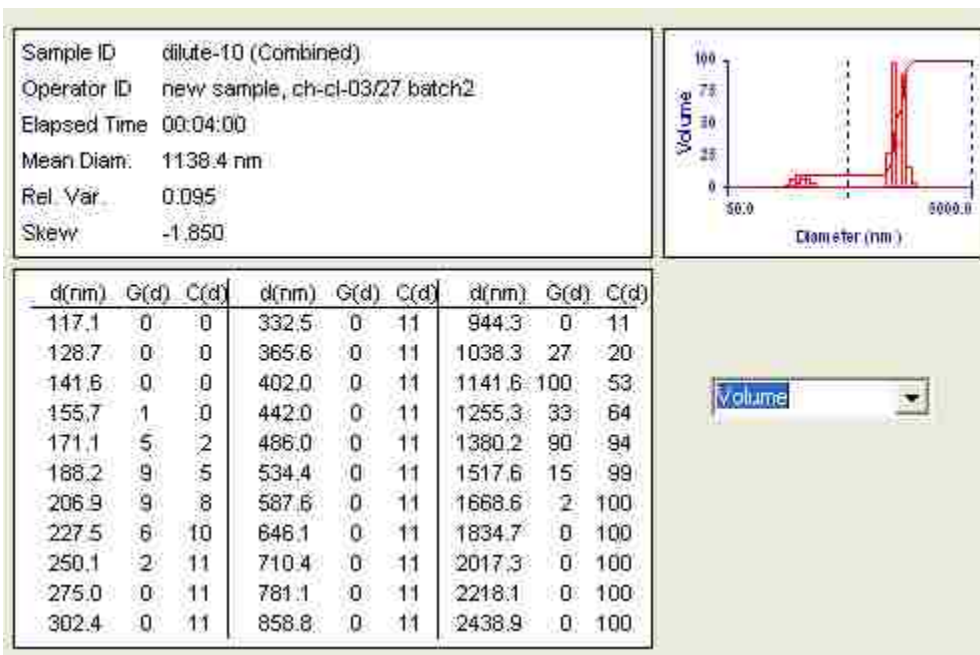


Figure 6.23. Volume based MSD of second batch of secondary emulsion with dilution ratio 1:10. [Table 4.7, row 3]

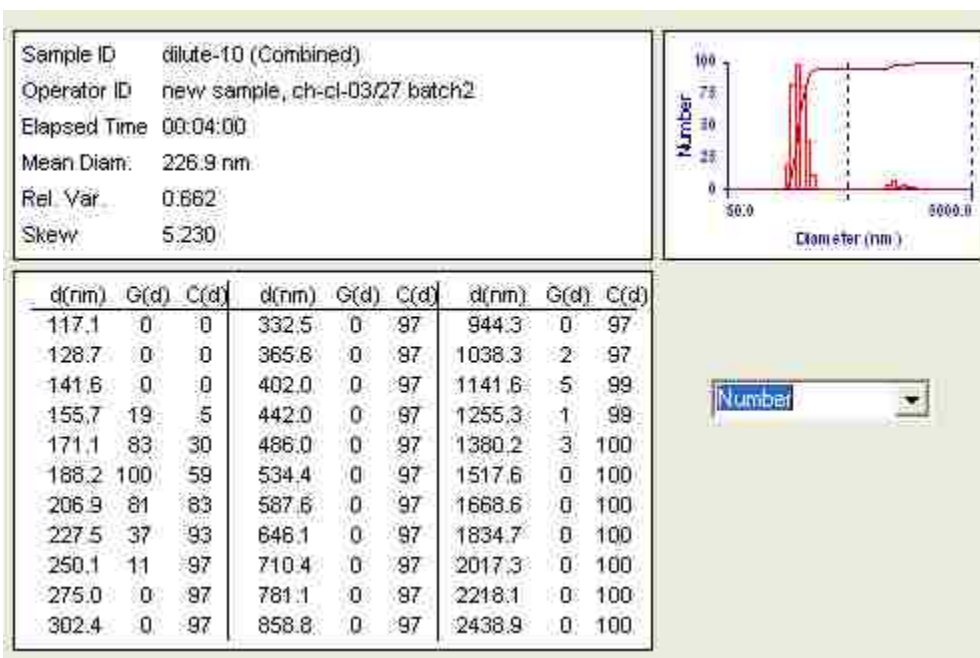


Figure 6.24. Number based MSD of second batch of secondary emulsion with dilution ratio 1:10. [Table 4.7, row 3]

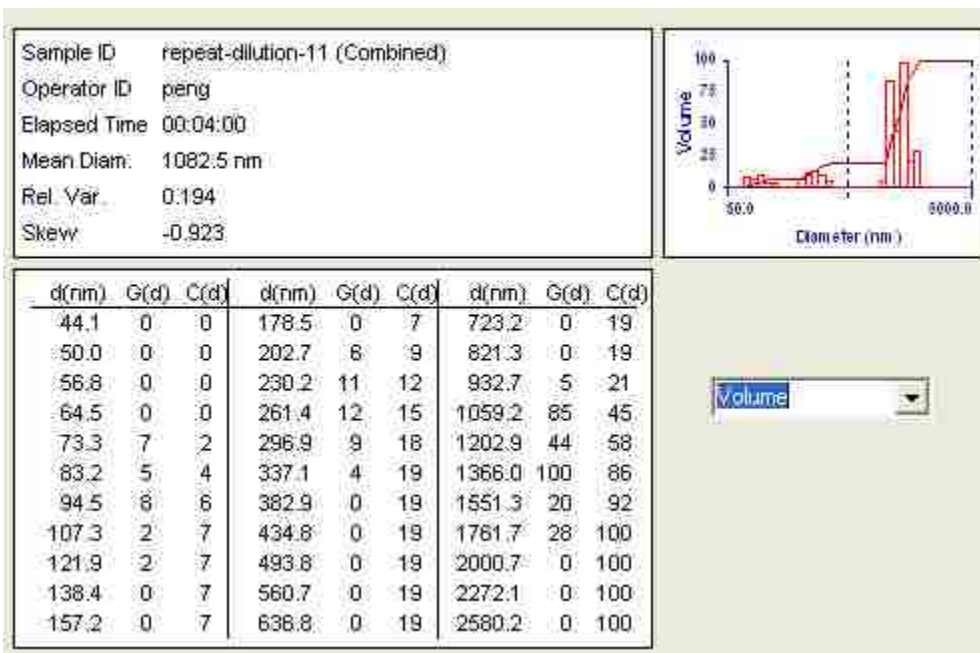


Figure 6.25. Volume based MSD of third batch of secondary emulsion with dilution ratio 1:10. [Table 4.7, row 4]

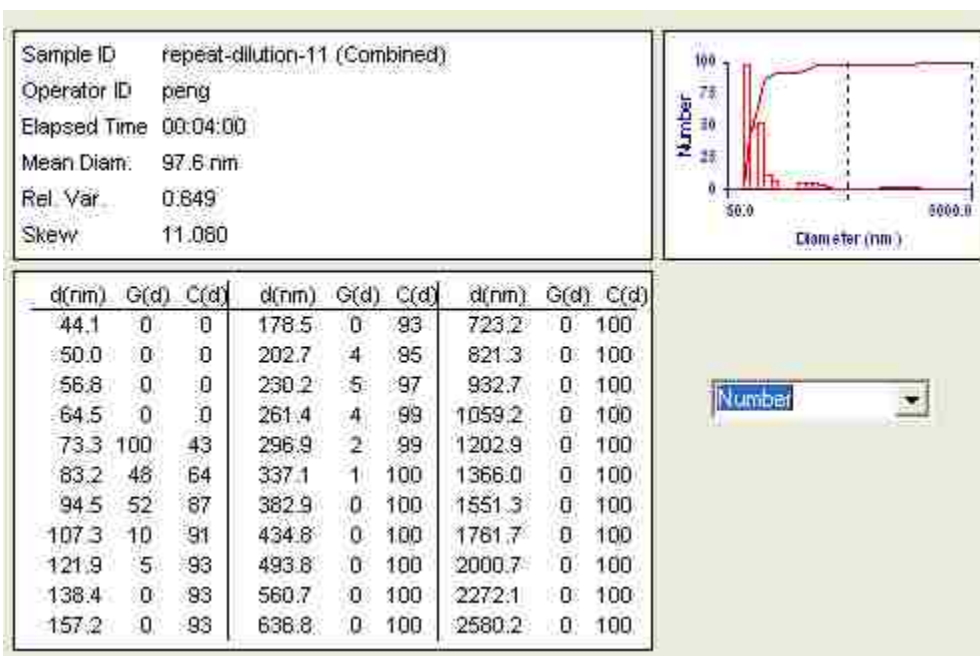


Figure 6.26. Number based MSD of third batch of secondary emulsion with dilution ratio 1:10. [Table 4.7, row 4]

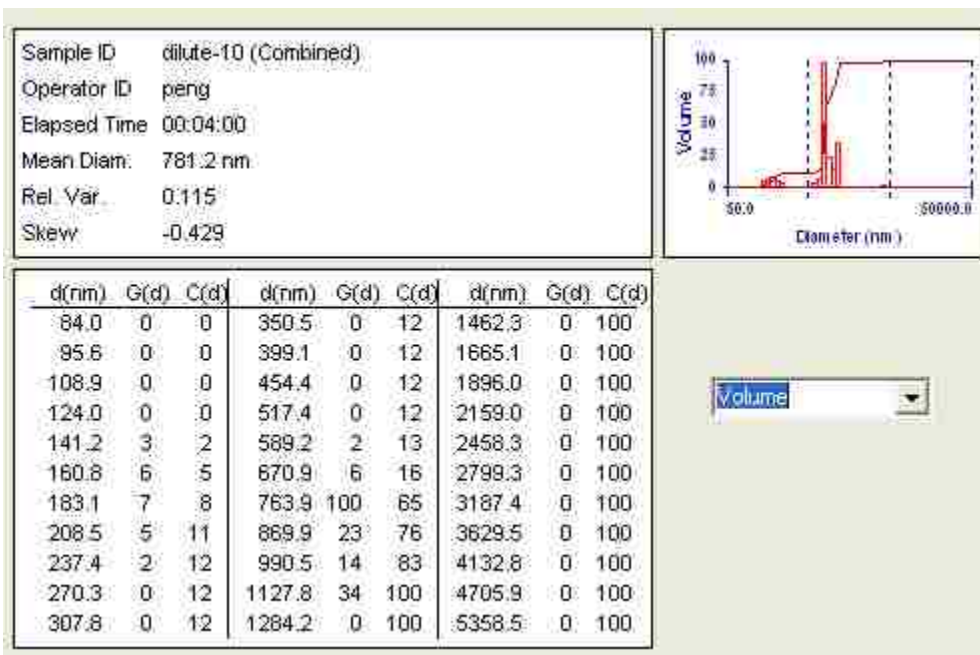


Figure 6.27. Volume based MSD of fourth batch of secondary emulsion with dilution ratio 1:10. [Table 4.7, row 5]

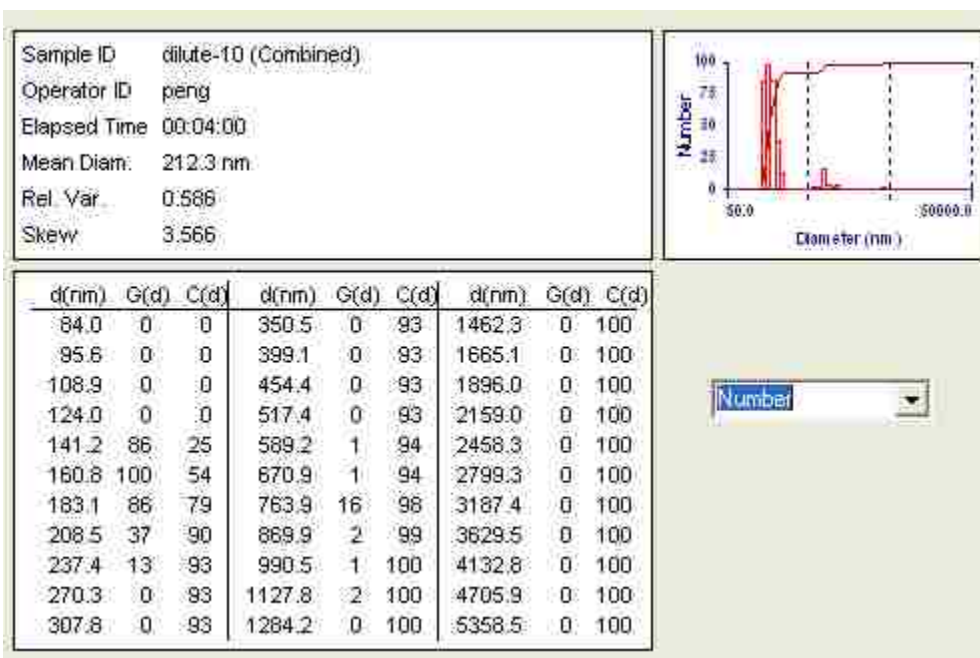


Figure 6.28. Number based MSD of fourth batch of secondary emulsion with dilution ratio 1:10. [Table 4.7, row 5]

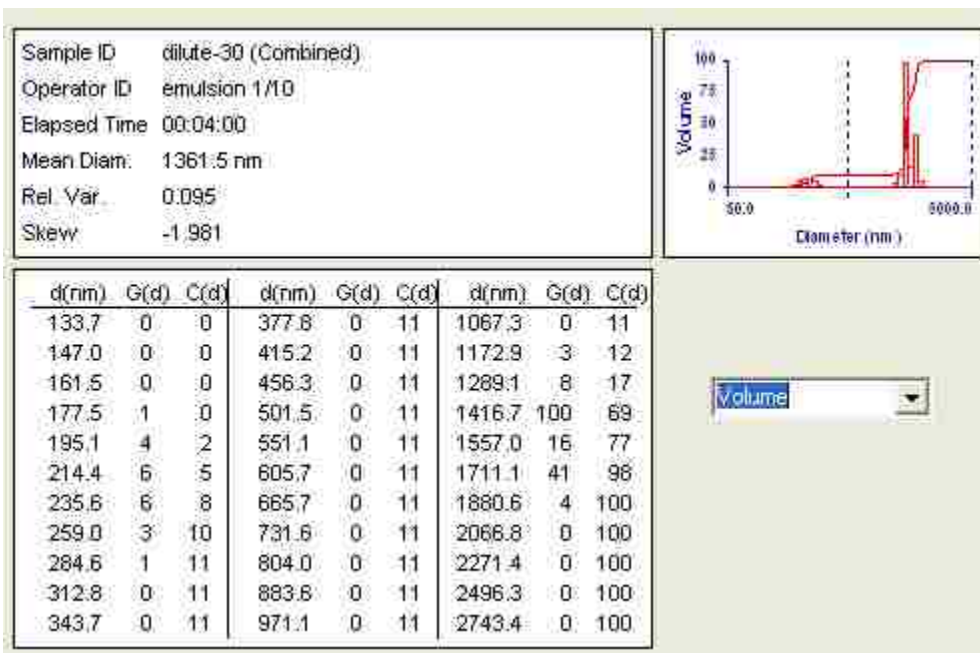


Figure 6.29. Volume based MSD of first batch of secondary emulsion with dilution ratio 1:30. [Table 4.7, row 6]

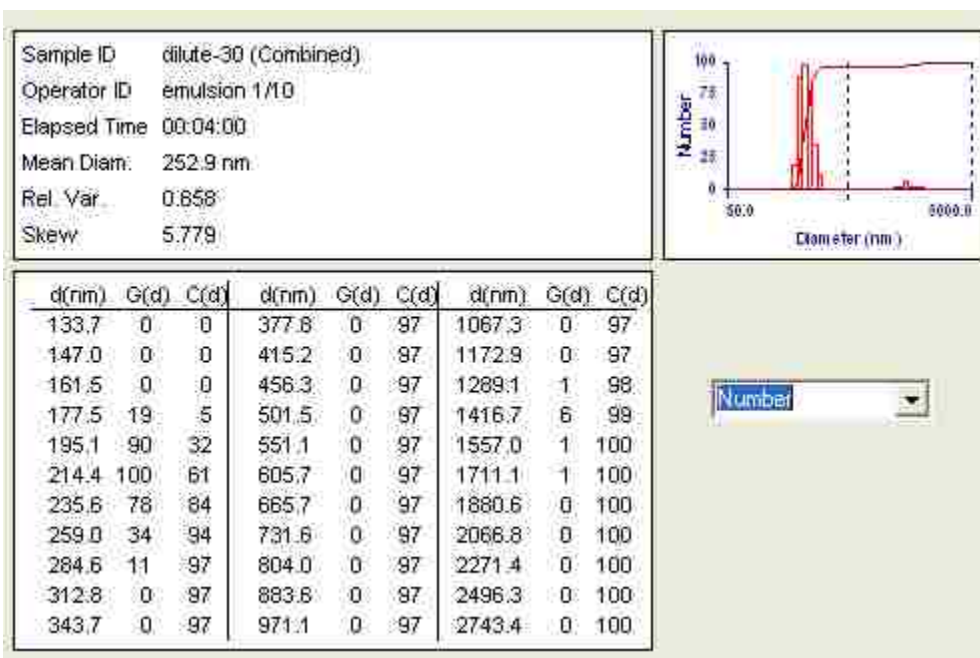


Figure 6.30. Number based MSD of first batch of secondary emulsion with dilution ratio 1:30. [Table 4.7, row 6]

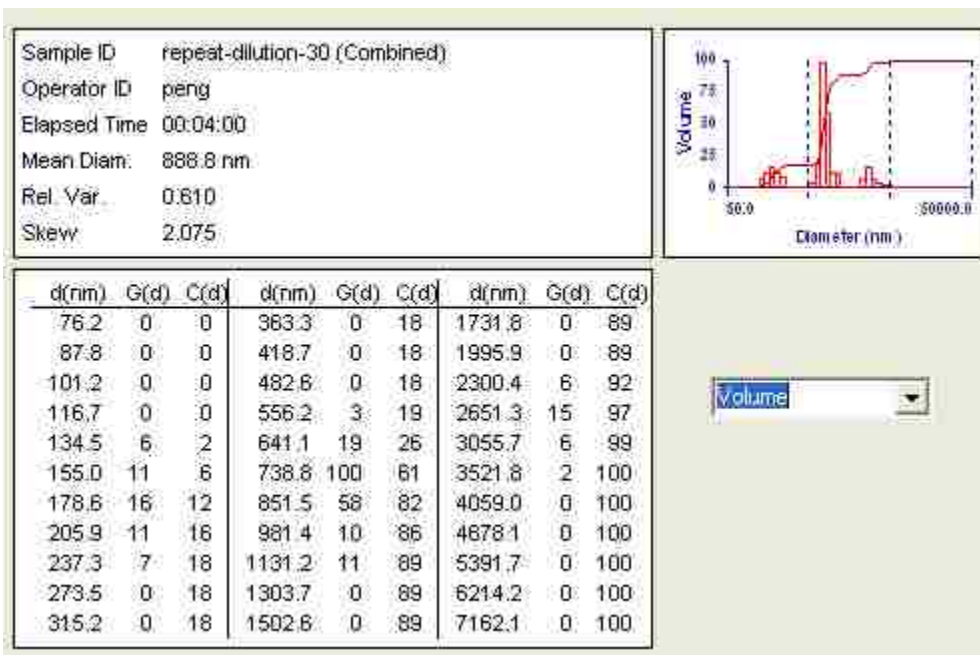


Figure 6.31. Volume based MSD of second batch of secondary emulsion with dilution ratio 1:30. [Table 4.7, row 7]

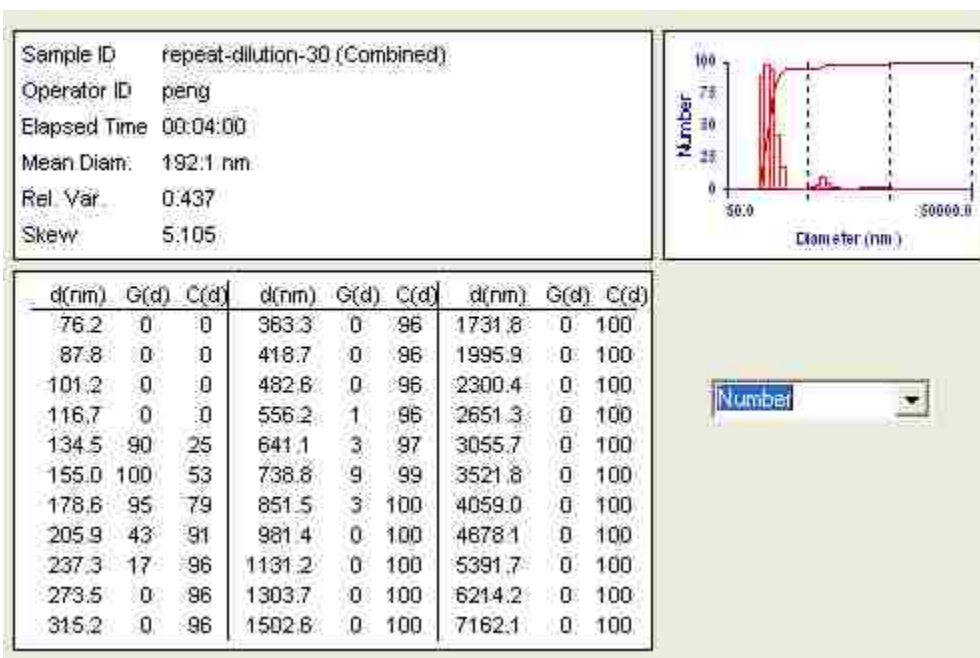


Figure 6.32. Number based MSD of second batch of secondary emulsion with dilution ratio 1:30. [Table 4.7, row 7]

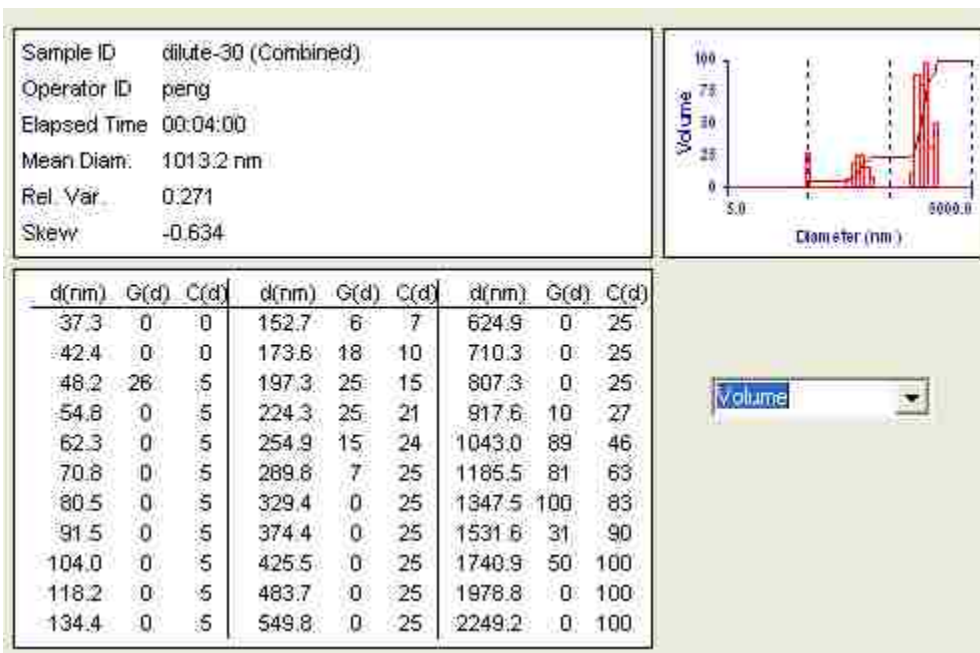


Figure 6.33. Volume based MSD of third batch of secondary emulsion with dilution ratio 1:30. [Table 4.7, row 8]

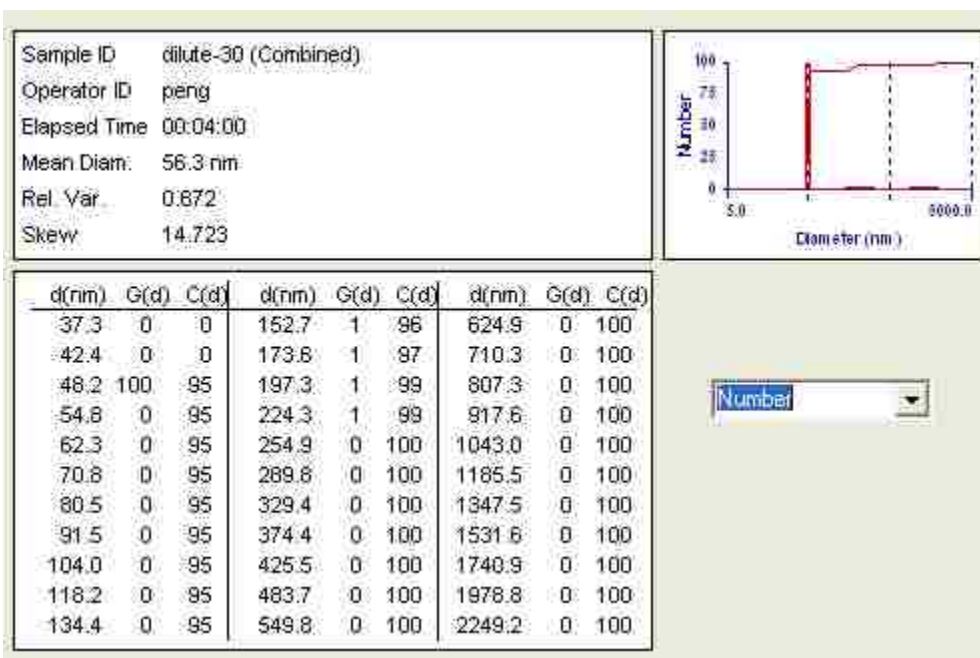


Figure 6.34. Number based MSD of third batch of secondary emulsion with dilution ratio 1:30. [Table 4.7, row 8]

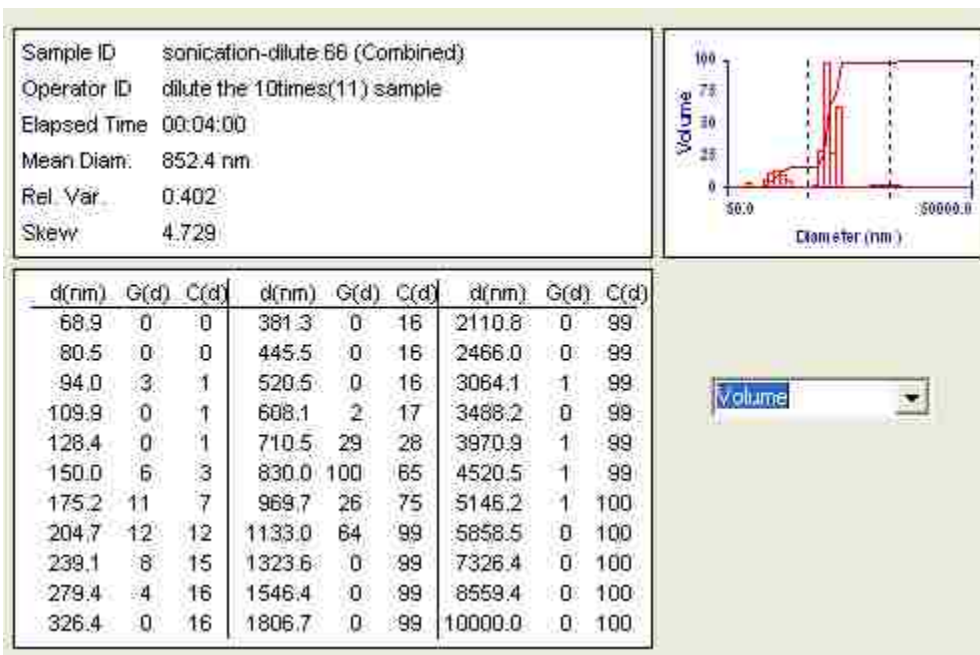


Figure 6.35. Volume based MSD of first batch of secondary emulsion with dilution ratio 1:60. [Table 4.7, row 9]

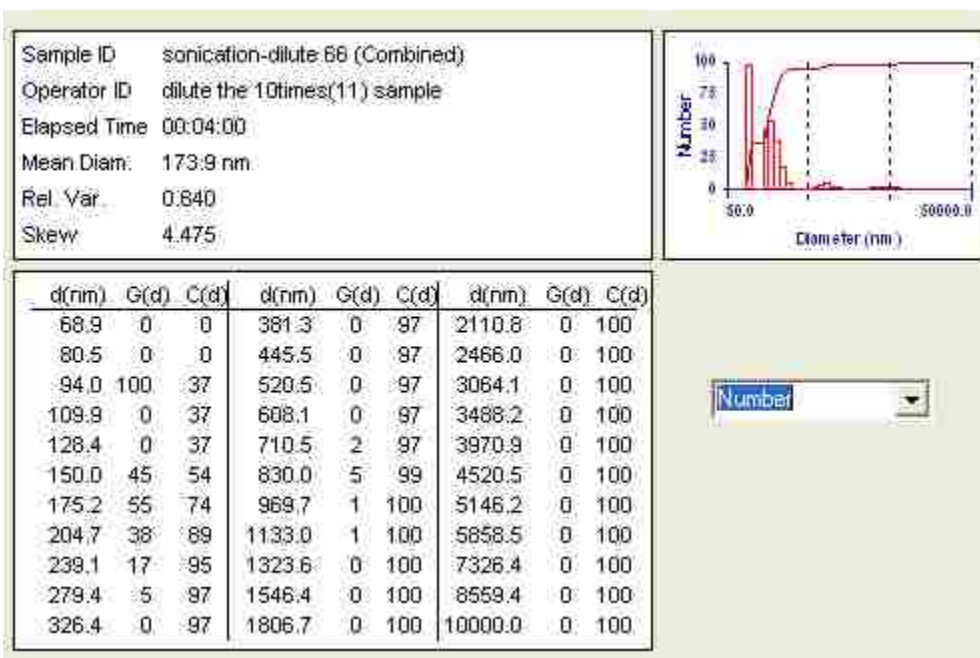


Figure 6.36. Number based MSD of first batch of secondary emulsion with dilution ratio 1:60. [Table 4.7, row 9]

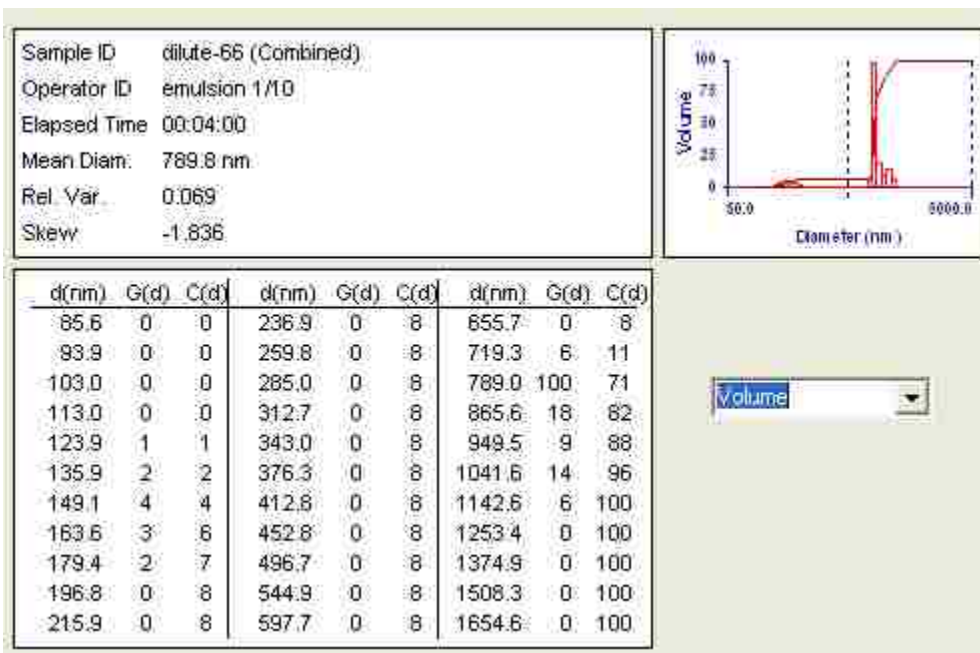


Figure 6.37. Volume based MSD of second batch of secondary emulsion with dilution ratio 1:60. [Table 4.7, row 10]

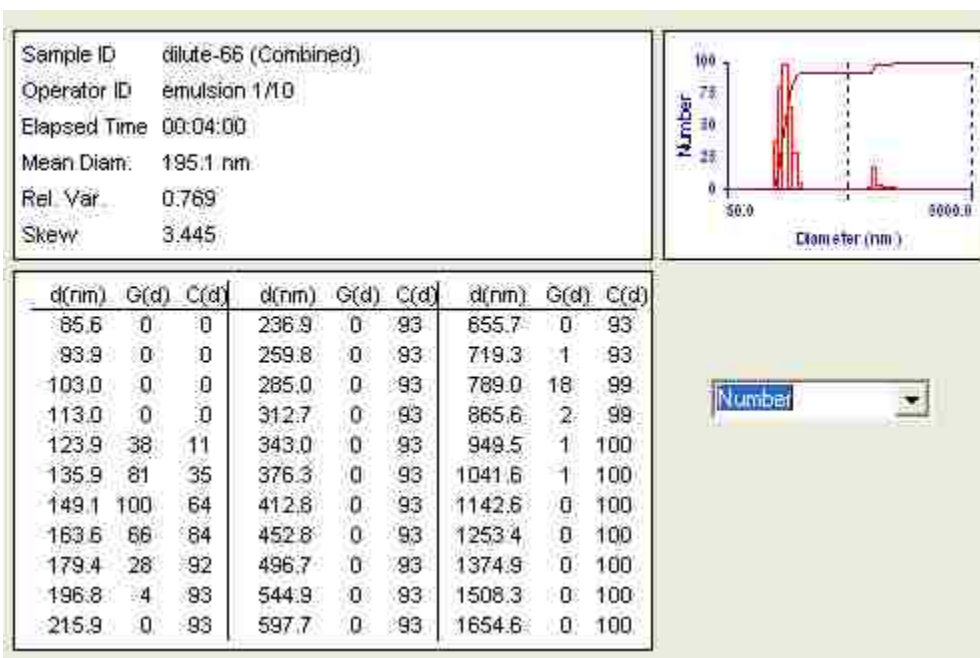


Figure 6.38. Number based MSD of second batch of secondary emulsion with dilution ratio 1:60. [Table 4.7, row 10]

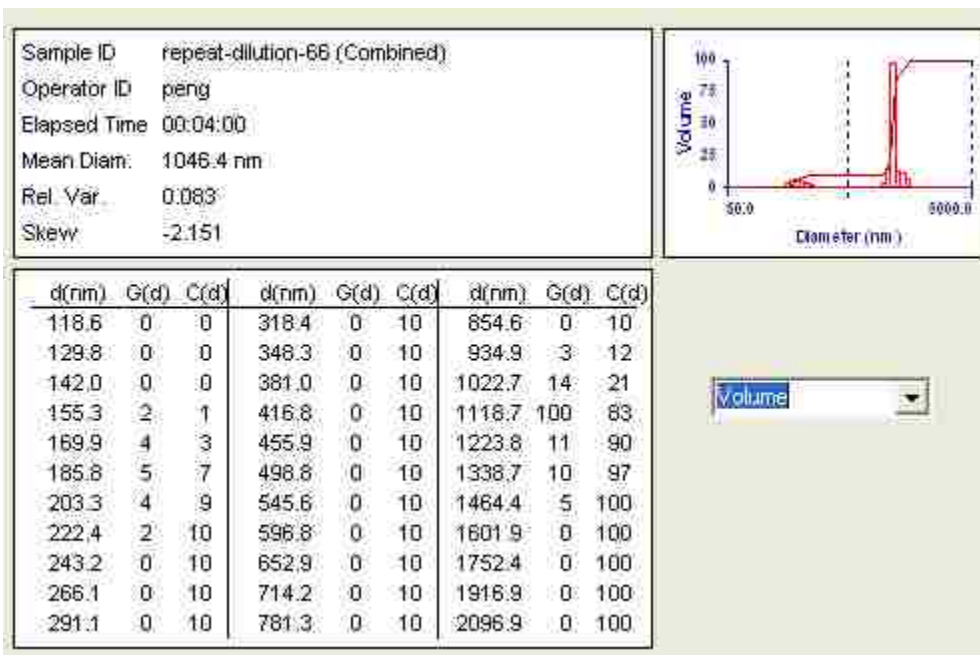


Figure 6.39. Volume based MSD of third batch of secondary emulsion with dilution ratio 1:60. [Table 4.7, row 11]

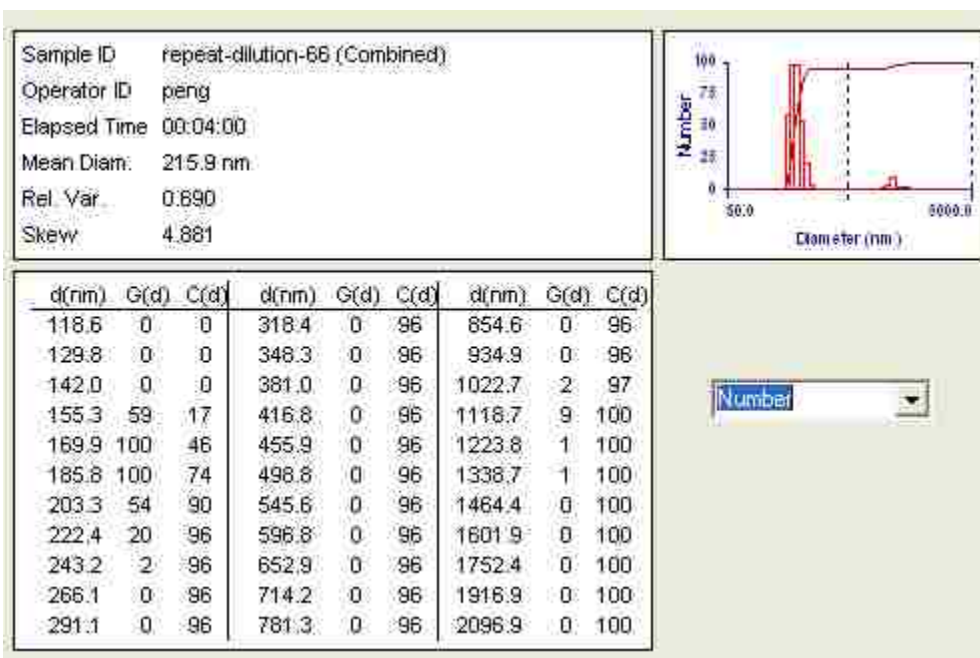


Figure 6.40. Number based MSD of third batch of secondary emulsion with dilution ratio 1:60. [Table 4.7, row 11]

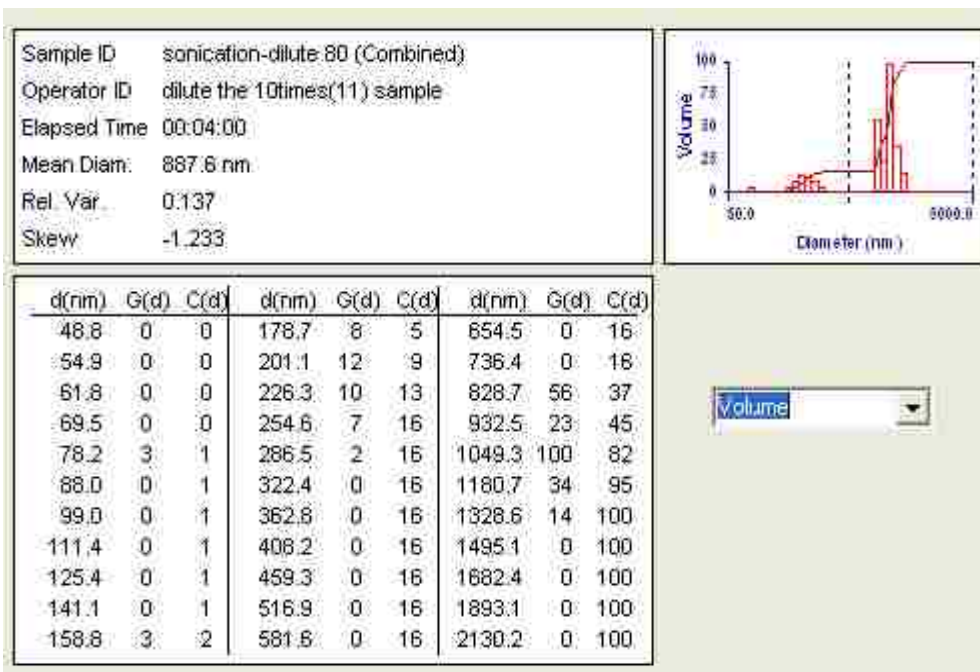


Figure 6.41. Volume based MSD of first batch of secondary emulsion with dilution ratio 1:80. [Table 4.7, row 12]

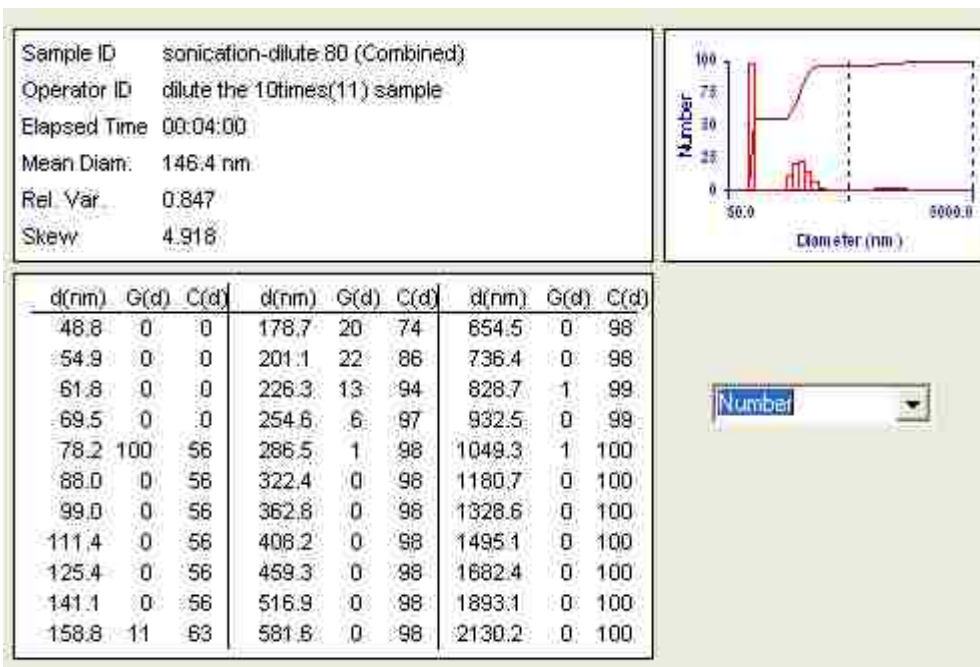


Figure 6.42. Number based MSD of first batch of secondary emulsion with dilution ratio 1:80. [Table 4.7, row 12]

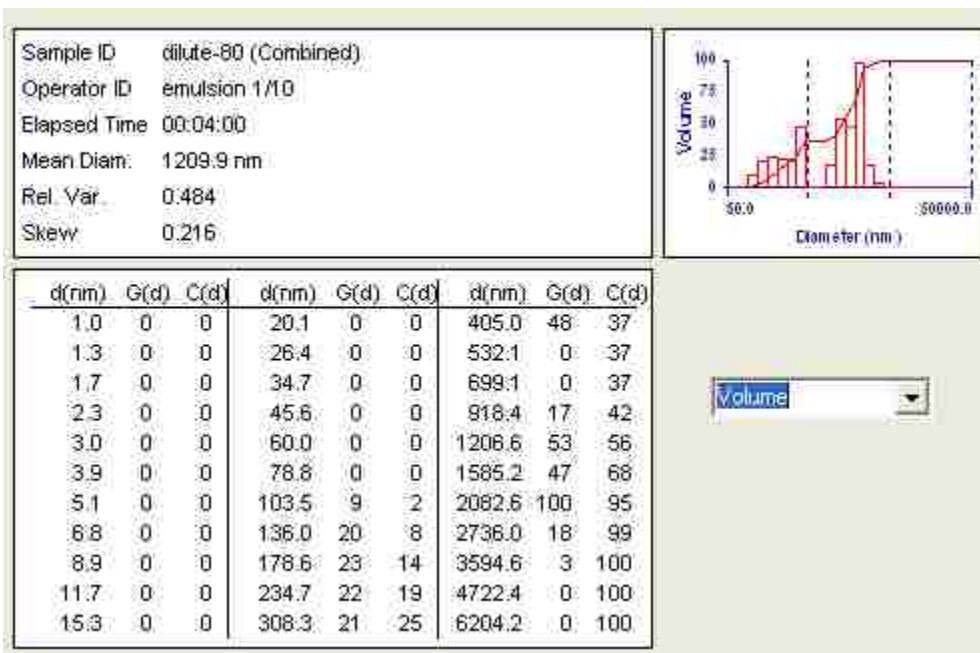


Figure 6.43. Volume based MSD of second batch of secondary emulsion with dilution ratio 1:80. [Table 4.7, row 13]

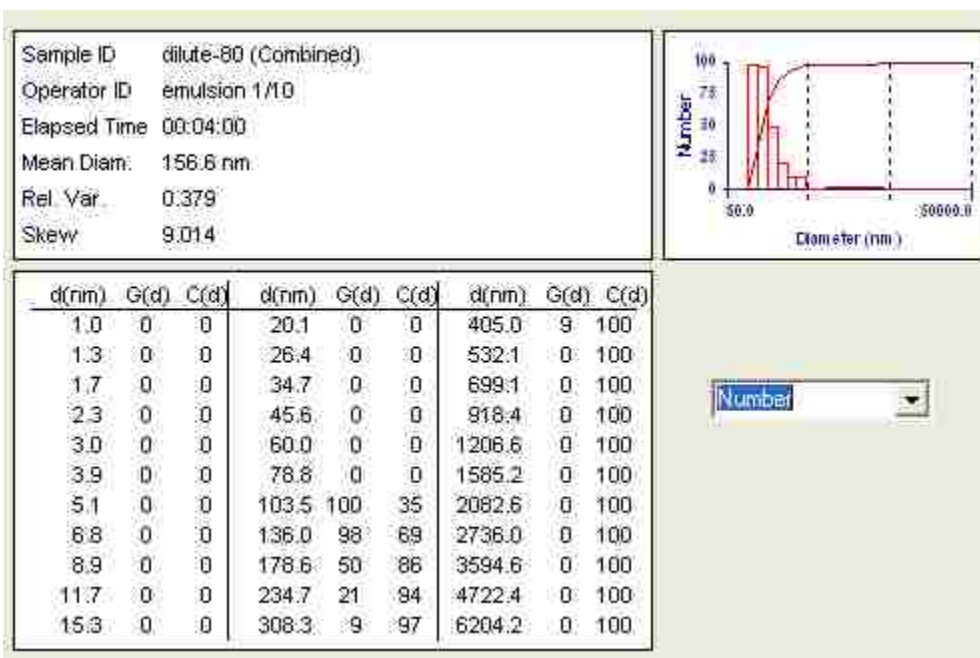


Figure 6.44. Number based MSD of second batch of secondary emulsion with dilution ratio 1:80. [Table 4.7, row 13]

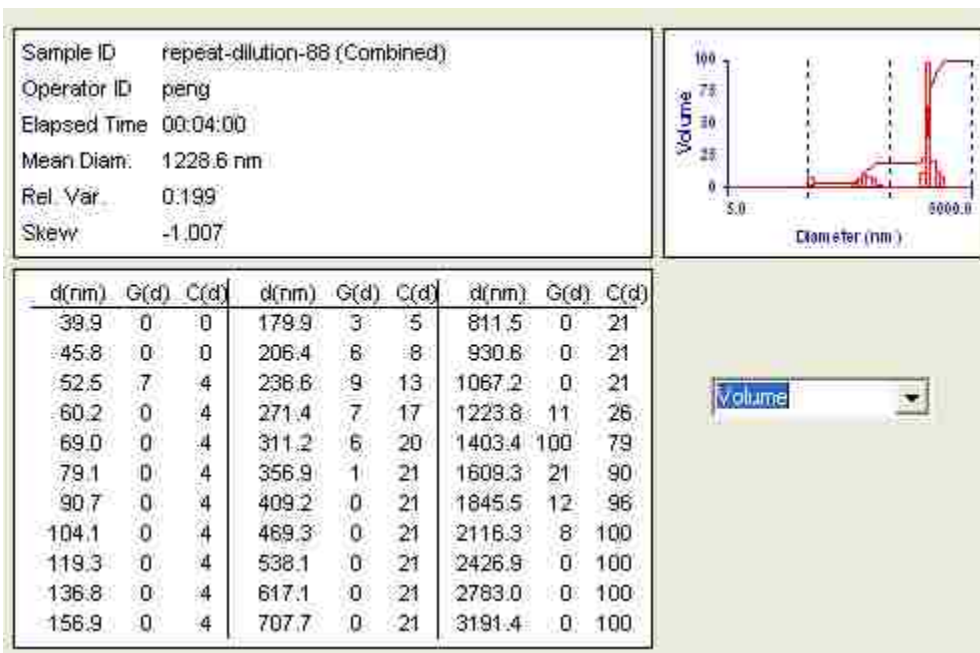


Figure 6.45. Volume based MSD of third batch of secondary emulsion with dilution ratio 1:80. [Table 4.7, row 14]

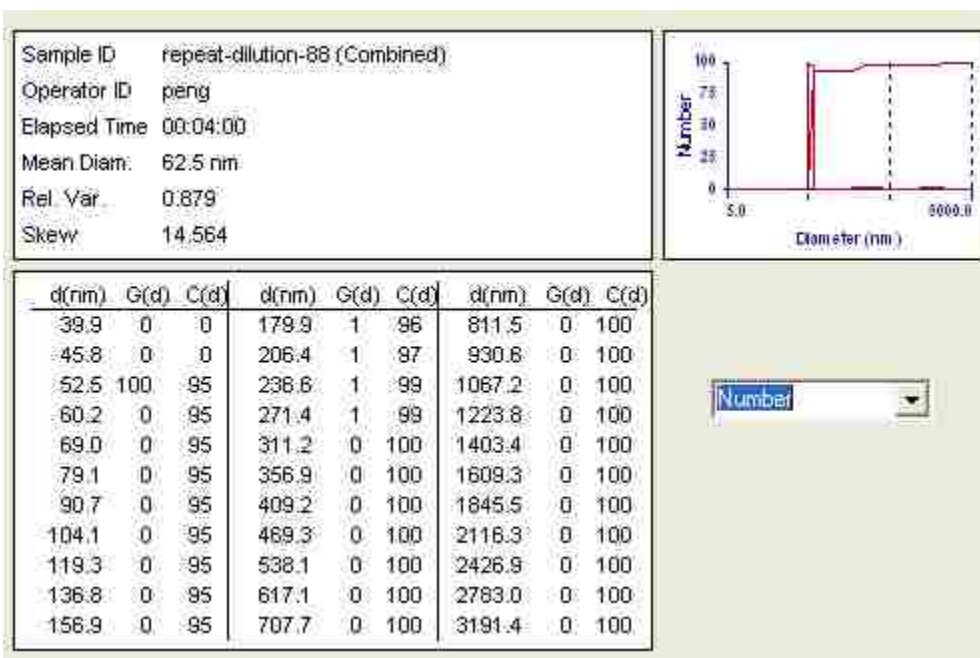


Figure 6.46. Number based MSD of third batch of secondary emulsion with dilution ratio 1:80. [Table 4.7, row 14]

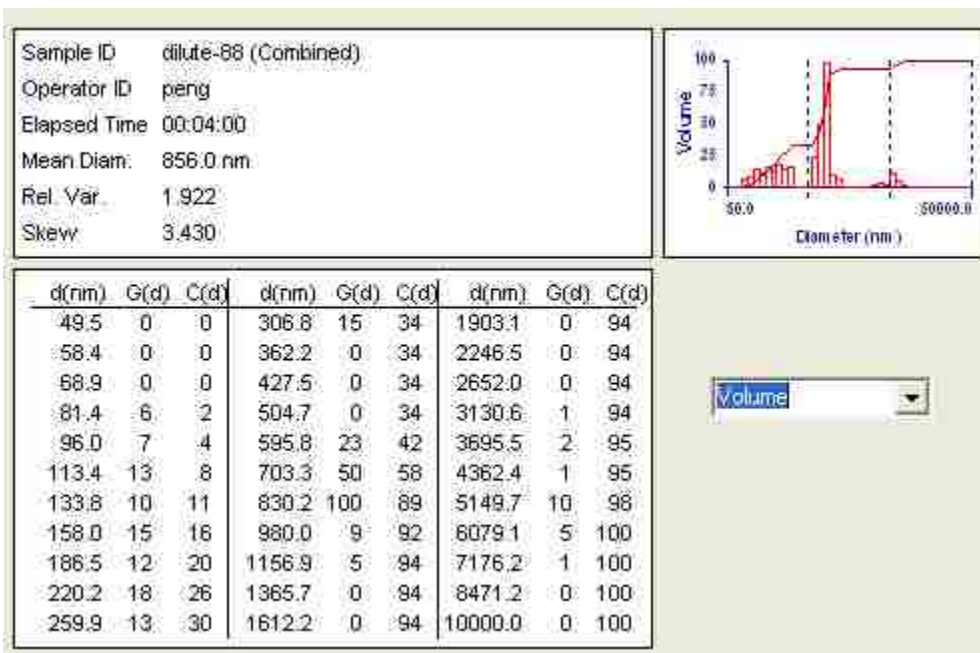


Figure 6.47. Volume based MSD of fourth batch of secondary emulsion with dilution ratio 1:80. [Table 4.7, row 15]

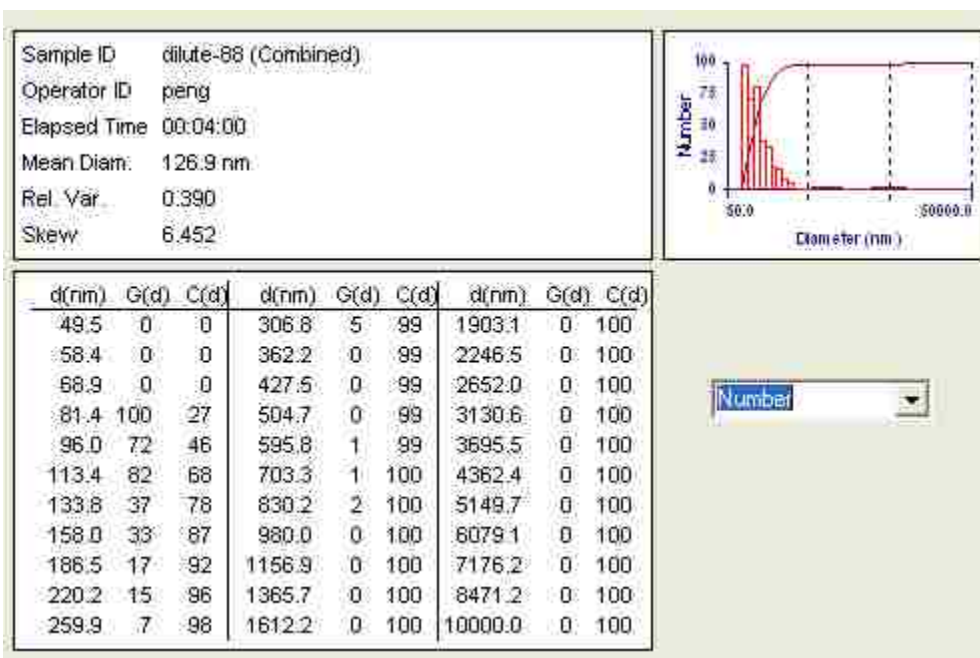


Figure 6.48. Number based MSD of fourth batch of secondary emulsion with dilution ratio 1:80. [Table 4.7, row 15]

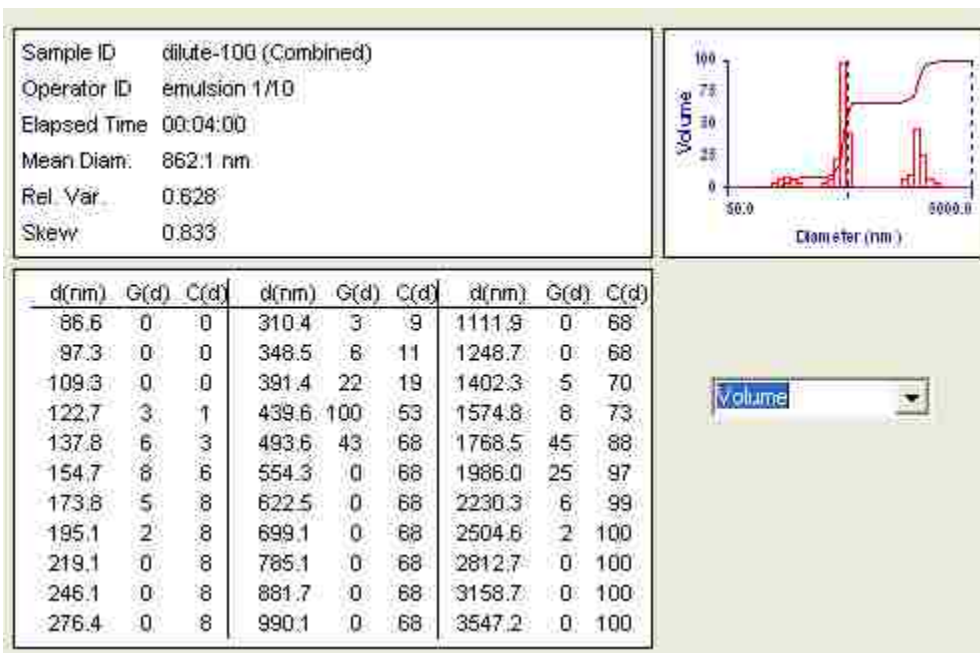


Figure 6.49. Volume based MSD of first batch of secondary emulsion with dilution ratio 1:100. [Table 4.7, row 16]

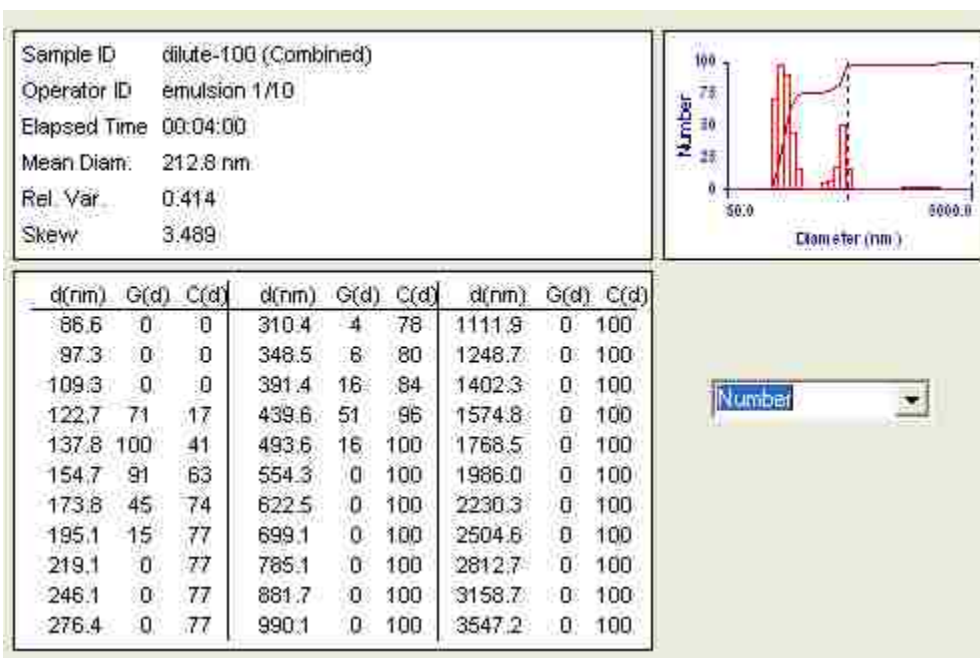


Figure 6.50. Number based MSD of first batch of secondary emulsion with dilution ratio 1:100. [Table 4.7, row 16]

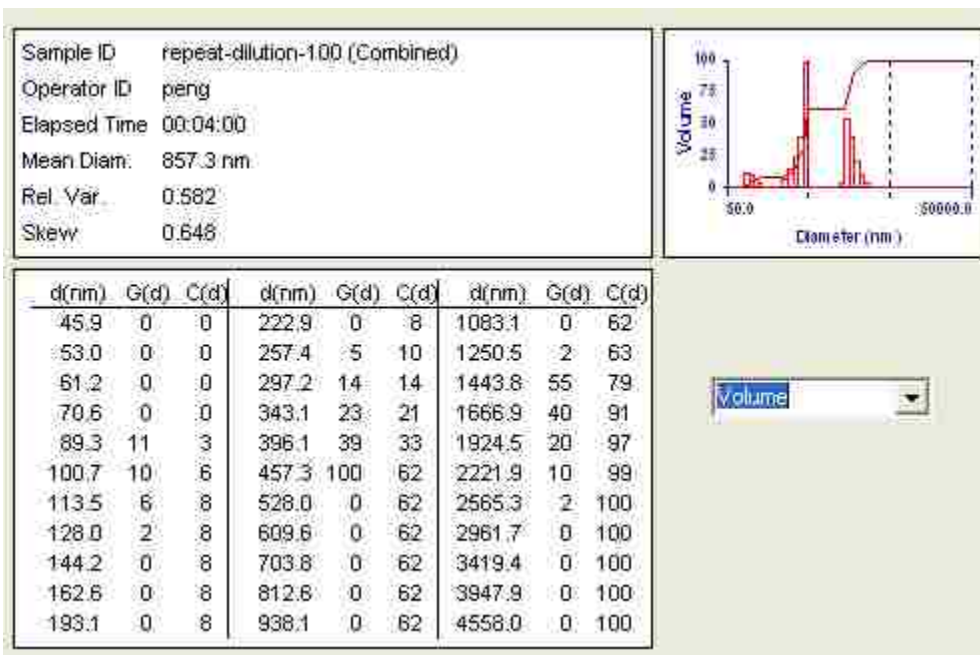


Figure 6.51. Volume based MSD of second batch of secondary emulsion with dilution ratio 1:100. [Table 4.7, row 17]

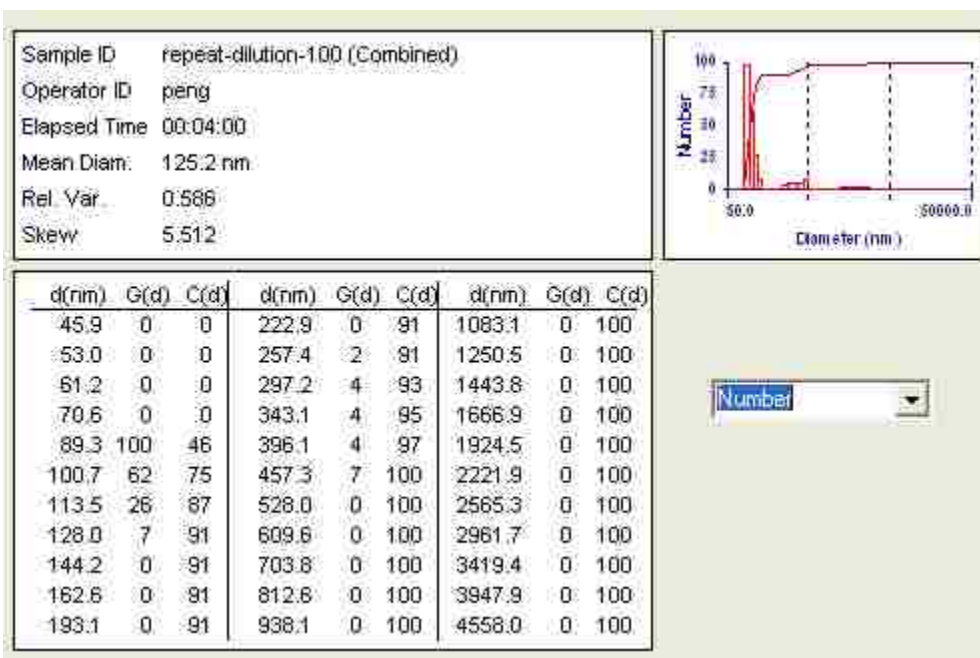


Figure 6.52. Number based MSD of second batch of secondary emulsion with dilution ratio 1:100. [Table 4.7, row 17]

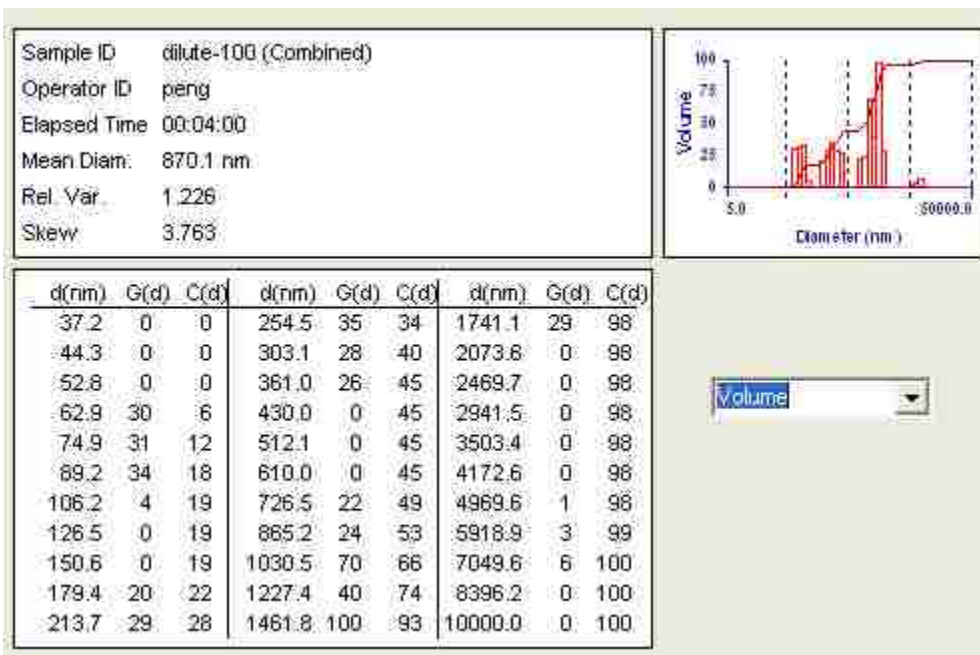


Figure 6.53. Volume based MSD of third batch of secondary emulsion with dilution ratio 1:100. [Table 4.7, row 18]

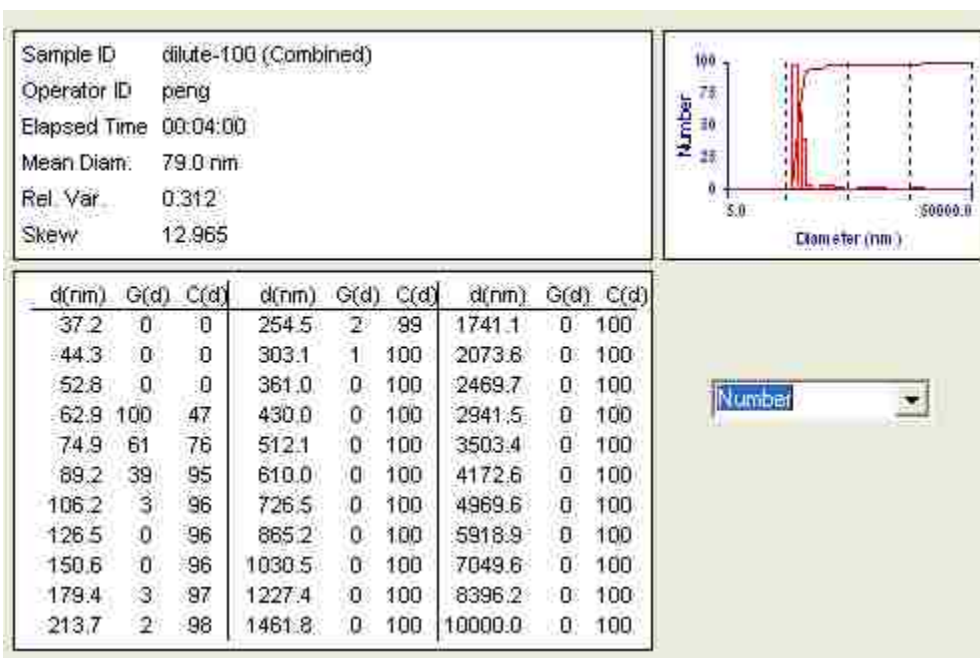


Figure 6.54. Number based MSD of third batch of secondary emulsion with dilution ratio 1:100. [Table 4.7, row 18]

Sonication - static mixer (Table 4.8)

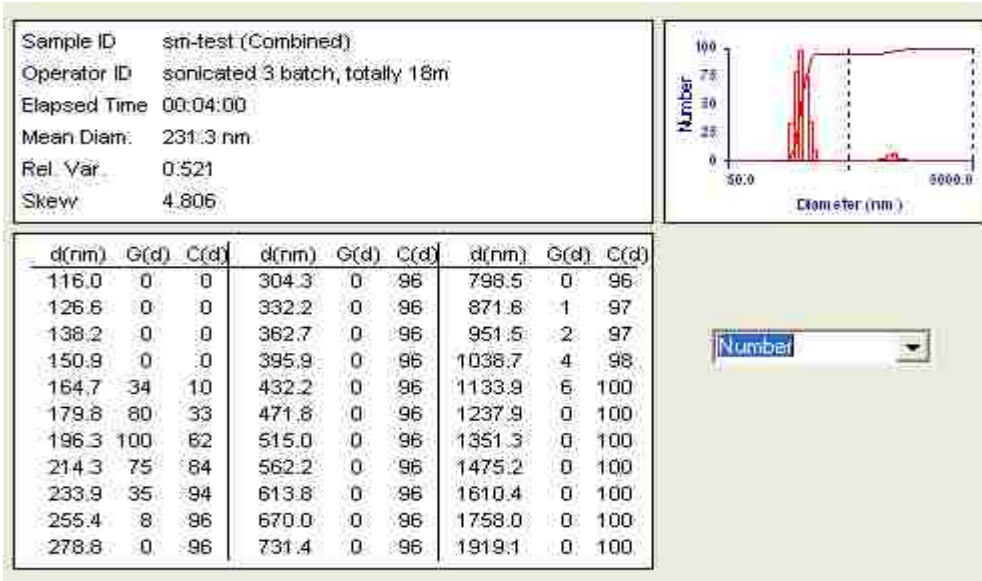


Figure 6.55. Number based MSD of nanoparticles generated by sonication of 1ml organic solution and 5ml aqueous solution resulting in primary emulsion followed by using static mixer at 180ml/min and dilution ratio 1:10 to generate secondary emulsion. [Table 4.8, S.No.1]

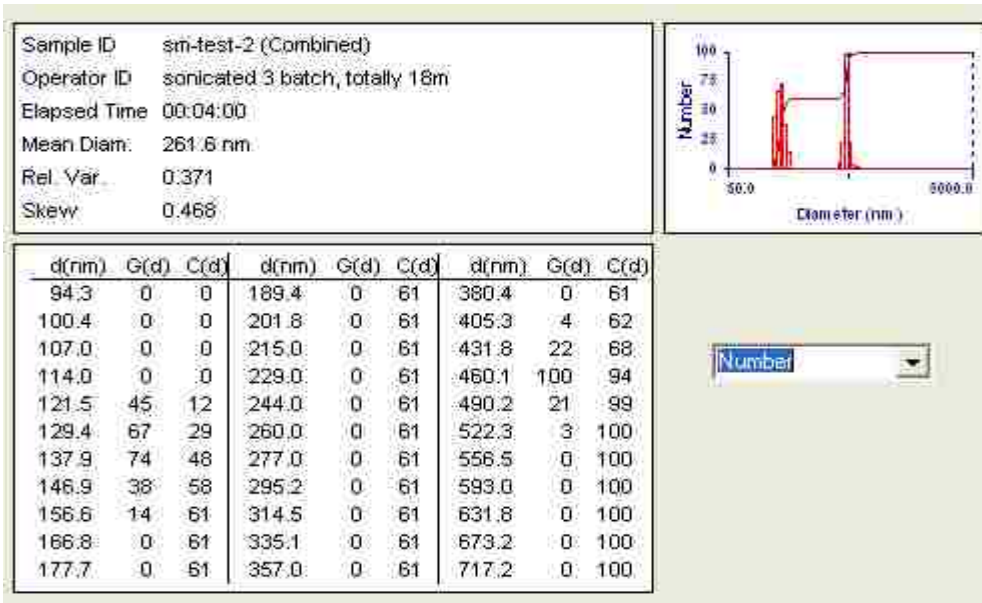


Figure 6.56. Number based MSD of nanoparticles generated by sonication of 1ml organic solution and 5ml aqueous solution resulting in primary emulsion followed by using static mixer at 200ml/min and dilution ratio 1:10 to generate secondary emulsion. [Table 4.8, S.No.2]

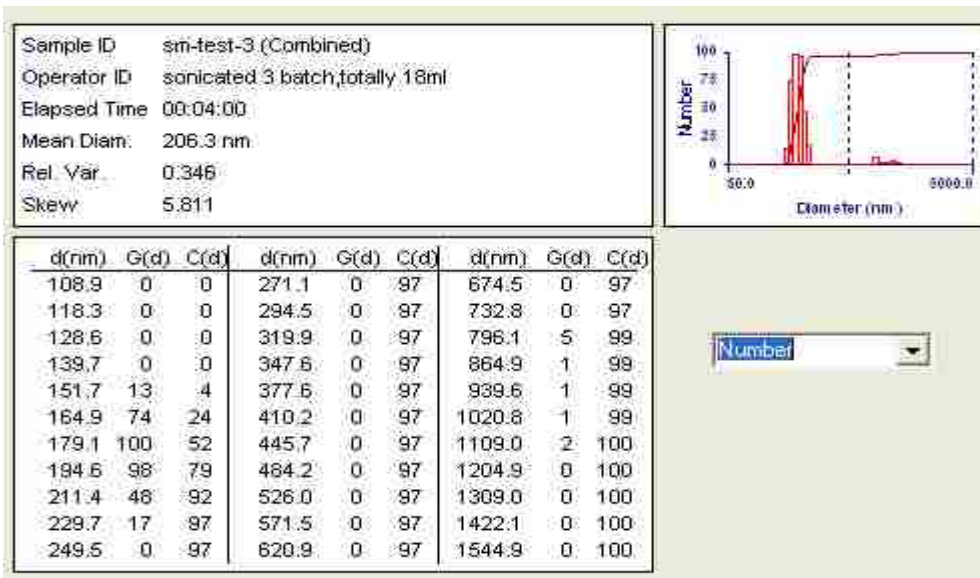


Figure 6.57. Number based MSD of nanoparticles generated by sonication of 1ml organic solution and 5ml aqueous solution resulting in primary emulsion followed by using static mixer at 260ml/min and dilution ratio 1:10 to generate secondary emulsion. [Table 4.8, S.No.3]

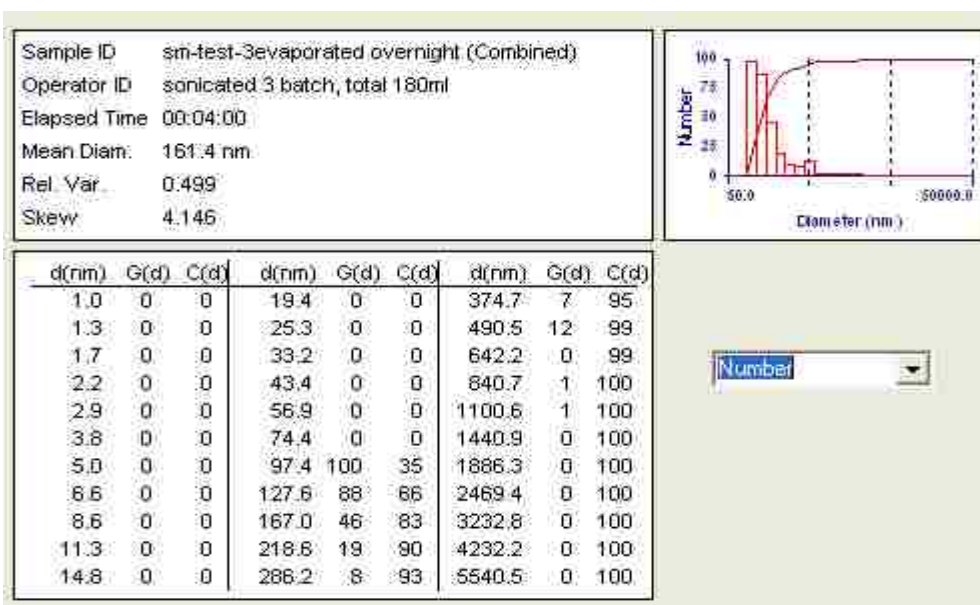


Figure 6.58. Number based MSD of secondary emulsion, after removing EA, generated by sonication of 1ml organic and 5ml aqueous phase resulting in primary emulsion followed by use of static mixer at 260ml/min and dilution ratio 1:10. [Table 4.8, S.No.4]

References

- Allemann, E., R. Gurny, et al. (1992). "Preparation of aqueous polymeric nanodispersions by a reversible salting-out process: influence of process parameters on particle size." Int. J. Pharm. FIELD Full Journal Title:International Journal of Pharmaceutics **87**(1-3): 247-53.
- Anderson, J. M. and M. S. Shive (1997). "Biodegradation and biocompatibility of PLA and PLGA microspheres." Advanced Drug Delivery Reviews **28**(1): 5-24.
- Barratt, G. (2003). "Colloidal drug carriers: Achievements and perspectives." Cellular and Molecular Life Sciences **60**(1): 21-37.
- Barratt, G. M. (2000). "Therapeutic applications of colloidal drug carriers." Pharmaceutical Science & Technology Today **3**(5): 163-171.
- Bennett, G. F. (2005). "Lees' Loss Prevention in the Process Industries: Hazard Identification, Assessment and Control (vol.I) edited by Sam Mannan." Journal of Hazardous Materials **122**(1-2): 188-189.
- Berkman, P. D. and R. V. Calabrese (1988). "Dispersion of viscous liquids by turbulent flow in a static mixer." AIChE J. FIELD Full Journal Title:AIChE Journal **34**(4): 602-9.
- Clancy, J. (1998). Basic Concepts in Immunology: A Student's Survival Guide, McGraw-Hill Professional.
- Dhawan, S., K. Singla Anil, et al. (2004). "Evaluation of mucoadhesive properties of chitosan microspheres prepared by different methods." AAPS PharmSciTech **5**(4): e67.
- Duan, B., L. Wu, et al. (2007). "Hybrid nanofibrous membranes of PLGA/chitosan fabricated via an electrospinning array." Journal of Biomedical Materials Research, Part A **83A**(3): 868-878.
- El-Jaby, U., T. F. L. McKenna, et al. (2007). "Miniemulsification: an analysis of the use of rotor stators as emulsification devices." Macromolecular Symposia **259**(Polymer Reaction Engineering--International Workshop, 2007): 1-9.
- Gao, J. and B. Xu (2009). "Applications of nanomaterials inside cells." Nano Today **4**(1): 37-51.
- Goldberg, M., R. Langer, et al. (2007). "Nanostructured materials for applications in drug delivery and tissue engineering." Journal of Biomaterials Science, Polymer Edition **18**(3): 241-268.
- Gwak, S.-J. and B.-S. Kim (2008). "Poly(lactic-co-glycolic acid) nanosphere as a vehicle for gene delivery to human cord blood-derived mesenchymal stem cells: comparison with polyethylenimine." Biotechnology Letters **30**(7): 1177-1182.
- Hans, M. L. and A. M. Lowman (2002). "Biodegradable nanoparticles for drug delivery and targeting." Current Opinion in Solid State & Materials Science **6**(4): 319-327.
- He, C., S. W. Kim, et al. (2008). "In situ gelling stimuli-sensitive block copolymer hydrogels for drug delivery." Journal of Controlled Release **127**(3): 189-207.
- Italia, J., D. Bhatt, et al. (2007). "PLGA nanoparticles for oral delivery of cyclosporine: Nephrotoxicity and pharmacokinetic studies in comparison to Sandimmune Neoral®." Journal of Controlled Release **119**(2): 197-206.
- Jain, K. K. and Editor (2008). Drug Delivery Systems. [In: Methods Mol. Biol. (Totowa, NJ, U. S.), 2008; 437].

- Jin, T., J. Zhu, et al. (2008). "Preparing polymer-based sustained-release systems without exposing proteins to water-oil or water-air interfaces and cross-linking reagents." Journal of Controlled Release **128**(1): 50-59.
- Kainthan, R. K., M. Gnanamani, et al. (2006). "Blood compatibility of novel water soluble hyperbranched polyglycerol-based multivalent cationic polymers and their interaction with DNA." Biomaterials **27**(31): 5377-5390.
- Kang, S.-W., H.-W. Lim, et al. (2008). "Nanosphere-mediated delivery of vascular endothelial growth factor gene for therapeutic angiogenesis in mouse ischemic limbs." Biomaterials **29**(8): 1109-1117.
- Kumar, M. N. V. R., U. Bakowsky, et al. (2004). "Preparation and characterization of cationic PLGA nanospheres as DNA carriers." Biomaterials **25**(10): 1771-1777.
- Kumar, V., V. Shirke, et al. (2008). "Performance of Kenics static mixer over a wide range of Reynolds number." Chemical Engineering Journal (Amsterdam, Netherlands) **139**(2): 284-295.
- Lee, K. Y. and S. H. Yuk (2007). "Polymeric protein delivery systems." Progress in Polymer Science **32**(7): 669-697.
- Lee, V. H. L. (2001). "Encyclopedia of Controlled Drug Delivery, Volume 1 and 2: Edith Mahiowitz, editor. John Wiley & Sons, Inc., New York, 1999, 1057 pp." Journal of Controlled Release **71**(3): 353-354.
- Lemenand, T., D. Della Valle, et al. (2003). "Droplets formation in turbulent mixing of two immiscible fluids in a new type of static mixer." International Journal of Multiphase Flow **29**(5): 813-840.
- Lewis, R. J. (1999). Sax's Dangerous Properties of Industrial Materials, 10th Edition, 3-Volume Set.
- Limayem Blouza, I., C. Charcosset, et al. (2006). "Preparation and characterization of spirinolactone-loaded nanocapsules for paediatric use." Int J Pharm FIELD Full Journal Title:International journal of pharmaceutics **325**(1-2): 124-31.
- Maa, Y. F. and C. Hsu (1996). "Liquid-liquid emulsification by static mixers for use in microencapsulation." Journal of Microencapsulation **13**(4): 419-433.
- Martin, C. R. and P. Kohli (2003). "The emerging field of nanotube biotechnology." Nat. Rev. Drug Discovery FIELD Full Journal Title:Nature Reviews Drug Discovery **2**(1): 29-37.
- Mather, B. D., K. Viswanathan, et al. (2006). "Michael addition reactions in macromolecular design for emerging technologies." Progress in Polymer Science **31**(5): 487-531.
- Merkli, A., C. Tabatabay, et al. (1998). "Biodegradable polymers for the controlled release of ocular drugs." Progress in Polymer Science **23**(3): 563-580.
- Mi, F.-L., S.-S. Shyu, et al. (2003). "Chitin/PLGA blend microspheres as a biodegradable drug delivery system: a new delivery system for protein." Biomaterials **24**(27): 5023-5036.
- Mittal, G., D. K. Sahana, et al. (2007). "Estradiol loaded PLGA nanoparticles for oral administration: Effect of polymer molecular weight and copolymer composition on release behavior in vitro and in vivo." Journal of Controlled Release **119**(1): 77-85.
- Motwani, S. K., S. Chopra, et al. (2008). "Chitosan-sodium alginate nanoparticles as submicroscopic reservoirs for ocular delivery: Formulation, optimisation and in

- vitro characterisation." European Journal of Pharmaceutics and Biopharmaceutics **68**(3): 513-525.
- Ottenbrite, R. M. and Editor (1999). Frontiers in Biomedical Polymer Applications, Volume 2. (Proceedings of the Second International Symposium, held 12 April 1997, in Eilat, Israel.)
- Ouzineb, K., C. Lord, et al. (2006). "Homogenization devices for the production of miniemulsions." Chemical Engineering Science **61**(9): 2994-3000.
- Peng, C.-L., M.-J. Shieh, et al. "Self-assembled star-shaped chlorin-core poly([var epsilon]-caprolactone)-poly(ethylene glycol) diblock copolymer micelles for dual chemo-photodynamic therapies." Biomaterials **In Press, Corrected Proof**.
- Pitarresi, G., M. A. Casadei, et al. (2007). "Photocrosslinking of dextran and polyaspartamide derivatives: A combination suitable for colon-specific drug delivery." Journal of Controlled Release **119**(3): 328-338.
- Qiu, L. and Y. Bae (2006). "Polymer Architecture and Drug Delivery." Pharmaceutical Research **23**(1): 1-30.
- Qiu, L. Y. and Y. H. Bae (2007). "Self-assembled polyethylenimine-graft-poly([epsilon]-caprolactone) micelles as potential dual carriers of genes and anticancer drugs." Biomaterials **28**(28): 4132-4142.
- Quadros, P. A. and C. M. S. G. Baptista (2003). "Effective interfacial area in agitated liquid-liquid continuous reactors." Chem. Eng. Sci. FIELD Full Journal Title:Chemical Engineering Science **58**(17): 3935-3945.
- Rolland, A. and S. Sullivan (2003). Pharmaceutical Gene Delivery Systems, Informa Healthcare.
- Shanmuganathan, S., N. Shanumugasundaram, et al. (2008). "Preparation and characterization of chitosan microspheres for doxycycline delivery." Carbohydrate Polymers **73**(2): 201-211.
- Solaro, R. (2002). Nanostructured polymeric systems in targeted release of proteic drugs and in tissue engineering.
- Tahara, K., T. Sakai, et al. (2008). "Establishing chitosan coated PLGA nanosphere platform loaded with wide variety of nucleic acid by complexation with cationic compound for gene delivery." International Journal of Pharmaceutics **354**(1-2): 210-216.
- Thakur, R. K., C. Vial, et al. (2003). "Static mixers in the process industries - a review." Chemical Engineering Research and Design **81**(A7): 787-826.
- Vandervoort, J. and A. Ludwig (2002). "Biocompatible stabilizers in the preparation of PLGA nanoparticles: a factorial design study." International Journal of Pharmaceutics **238**(1-2): 77-92.
- Wheatley, M. and R. Langer (1987). "Particles as drug delivery systems." Particulate Science and Technology **5**(1): 53-64.
- Wu, L. and C. S. Brazel (2008). "Modifying the release of proxiphylline from PVA hydrogels using surface crosslinking." International Journal of Pharmaceutics **349**(1-2): 144-151.
- Yang, H. and W. J. Kao (2006). "Dendrimers for pharmaceutical and biomedical applications." J. Biomater. Sci., Polym. Ed. FIELD Full Journal Title:Journal of Biomaterials Science, Polymer Edition **17**(1-2): 3-19.

- Yang, Y.-Y., Y. Wang, et al. (2006). "Polymeric core-shell nanoparticles for therapeutics." Clinical and Experimental Pharmacology and Physiology **33**(5/6): 557-562.
- Yin, L., J. Ding, et al. (2008). "Beneficial properties for insulin absorption using superporous hydrogel containing interpenetrating polymer network as oral delivery vehicles." International Journal of Pharmaceutics **350**(1-2): 220-229.
- Zhou, Y.-M., A. Ishikawa, et al. (2007). "Deposition transfection technology using a DNA complex with a thermoresponsive cationic star polymer." Journal of Controlled Release **123**(3): 239-246.

VITA

o Date and place of birth:

07-28-1985, Rajahmundry, INDIA.

o Educational institutions attended and degrees already awarded:

Jawaharlal Nehru Technological University, Anantapur, INDIA.

Bachelor of Technology in Chemical Engineering.

o Professional positions held:

Research Assistant, Department of Chemical and Materials Engineering, University of Kentucky.

Teaching Assistant, Department of Chemical and Materials Engineering, University of Kentucky.

o Typed name of student on final copy:

Yamuna Reddy Charabudla